HYDROLOGIC RESPONSE TO SPRING SNOWMELT AND EXTREME RAINFALL EVENTS OF DIFFERENT LANDSCAPE ELEMENTS WITHIN A PRAIRIE WETLAND BASIN

A Thesis Submitted to the College of

Graduate Studies and Research

In Partial Fulfillment of the Requirements

For the Degree of Master of Science

In the Department of Soil Science

University of Saskatchewan

Saskatoon

By

Murray A. Lungal

Permission to Use

In presenting this thesis in partial fulfilment of the requirements for a Postgraduate degree from the University of Saskatchewan, I agree that the Libraries of this University may make it freely available for inspection. I further agree that permission for copying of this thesis in any manner, in whole or in part, for scholarly purposes may be granted by the professor or professors who supervised my thesis work or, in their absence, by the Head of the Department or the Dean of the College in which my thesis work was done. It is understood that any copying or publication or use of this thesis or parts thereof for financial gain shall not be allowed without my written permission. It is also understood that due recognition shall be given to me and to the University of Saskatchewan in any scholarly use which may be made of any material in my thesis.

Requests for permission to copy or to make other use of material in this thesis in whole or part should be addressed to:

Head of the Department of Soil Science
University of Saskatchewan
Saskatoon, Saskatchewan (S7N 5A8)

ABSTRACT

Depressions in the prairie pothole region (PPR) are commonly referred to as sloughs and were formed during the most recent glacial retreat, ~10-17 kyrs ago. They are hydrologically isolated, as they are not permanently connected by surface inflow or outflow channels. Extreme thunderstorms are common across the prairies and the hydrologic response of isolated wetlands to intense rainfall events is poorly understood.

The purpose of this study was to compare the response of different landscape/ecological elements of a prairie wetland to snowmelt and extreme rainstorms. Comparisons were completed by investigating the spring snowmelts of 2005 and 2006 and the rainstorm event of June 17 - 18, 2005, in which 103 mm fell at the St. Denis National Wildlife Area (NWA) Saskatchewan, Canada (106°06'W, 52°02'N). The wetland was separated into five landscape positions, the pond center (PC), grassed edge (GE), tree ring (TR), convex upland (CXU), and concave upland (CVU).

Comparison of the rainfall of June 17 – 18, 2005 with the spring snowmelts of 2005 and 2006 indicates that the hydrologic consequences of these different events are similar. Overland flow, substantial ponding in lowlands, and recharge of the groundwater occur in both cases. Analysis of this intense rainfall has provided evidence that common, intense rainstorms are hydrologically equivalent to the annual spring snowmelt, the major source of water for closed catchments in the PPR.

ACKNOWLEDGMENTS

I would like to acknowledge the support and guidance of my supervisor, Dr. Bing Si, and my committee members, Dr. Dan Pennock and Dr. Garth van der Kamp. Their knowledge and direction have been invaluable from the beginning to the completion of this project. Technical and field support was provided extensively by Kirk Elliot, Caden Chalak, Sheala Konecsni, Chadrick Carley, Tom Yates, Hiroyuki Ohiai, Mike Soluhub, and Warren Helgason. Thank you, to the entire staff and students of the department of Soil Science, for your friendship and support.

Very special thanks go to my wife, Leiflynn and to my family for their support and patience throughout this endeavor.

TABLE OF CONTENTS

LIST OF TABLES

Table

LIST OF FIGURES

Figure

CHAPTER 1.0
INTRODUCTION

The prairie pothole region (PPR) extends throughout the southern Canadian Prairies to portions of the mid-western United States. Depressions in these landscapes are commonly referred to as sloughs. They were formed during the most recent glacial retreat, ~10-17 kyrs ago, resulting from ice blocks falling from the retreating glacier. The ice blocks were covered with glacial till, the melting ice block resulted in the inverted topography (Sloan, 1972). They are hydrologically isolated, as they are not permanently connected by surface inflow or outflow channels. Wetlands serve many hydrologic and biologic functions and are highly dependent upon climatic factors. They store precipitation and snowmelt, contribute to groundwater recharge, provide a source of water to the atmosphere, and habitat for biota, from aquatic organisms to nesting habitat for water fowl (LaBaugh, et al., 1998; Price, et al., 2005). Prairie potholes may be significant sources or sinks of greenhouse gases.

The PPR is underlain by glacial till with low hydraulic conductivity at depth. Therefore, surface and soil water interactions with groundwater are dependent upon preferential flow and deep drainage is generally low (Parsons et al., 2004; Price et al., 2005). Regardless, depressions are the major source of groundwater recharge in the Canadian PPR (Hayashi et al., 1998a; Hayashi et al., 1998b; Hayashi et al., 2003). A thorough understanding of the short-term hydrologic interaction of ponded water and groundwater, in particular the results of intense rainfall events, is needed given the increased use of agricultural chemicals and highly variable weather patterns in semi-arid climates.

Wetland research in the PPR has included work in the hydrologic, biological, and greenhouse gas production of wetlands. Hydrologic research has focused on the connection between surface water and groundwater systems and the long-term fate following surface infiltration. Biologically, water fowl populations and nesting habitats have been investigated intensively (LaBaugh et al., 1996). Production or consumption of greenhouse gases, such as carbon dioxide, methane, and nitrous oxide, is a recent realm of study on the prairie agricultural region (Phipps, 2006; Yates, 2006).

The hypothesis is that different landscape/ecological elements respond differently to snowmelt and extreme rainfall events. The objective of this study is to examine how different landscape/ecological elements respond to snowmelt and an extreme rainfall event. Here I define extreme rainfall events as rarely-large rainfall events in a short duration. This objective is completed by determining the hydrologic response of five unique landscape/ecological elements to the spring snowmelts of 2005 and 2006 and the rainstorm event of June 17-18, 2005 at the St. Denis National Wildlife Area (NWA) Saskatchewan, Canada (106°06'W, 52°02'N).

Instrumentation for measuring the hydrologic response of each landscape/ecological element was installed throughout a prairie wetland catchment, both within the basin and the surrounding uplands. Instruments consisted of real-time meteorological, soil water, and groundwater sensors. These sensors, manual measurements, and field observations were used to provide a unique dataset that captured relevant hydrologic measurements for the rainfalls and the spring snowmelts of 2005 and 2006.

I also developed a new soil matric potential sensor, with results presented in Appendix A. Matric potential is a measure of the combined capillary and adsorptive forces of soil particles and is imperative in determining both the direction and magnitude of water flow in unsaturated

soils. The measurement of soil matric potential has been a challenge in semi-arid environments, where matric potential varies over a wide range from 0 MPa, at saturation, to -1.5 MPa, the permanent wilting point of agronomic crops (Hillel, 1998; Kutilek and Nielsen, 1994). Given this challenge, the objective is to develop a soil matric potential sensor capable of functioning through the full spectrum of potentials present in semi-arid environments, 0 MPa to -1.5 MPa. Based on the coiled TDR design of Nissen et al., (1998), a modified TDR probe has been developed and early results indicate the probe functions across the entire range of matric potential values. The results presented are preliminary and require further field verification.

References

Hayashi, M., G. van der Kamp, and D.L. Rudolph. 1998a. Water and solute transfer between a prairie wetland and adjacent uplands, 1. Water balance. Journal of Hydrology 207:42-55.

Hayashi, M., G. van der Kamp, and D.L. Rudolph. 1998b. Water and solute transfer between a prairie wetland and adjacent uplands, 2. Chloride cycle. Journal of Hydrology 207:56-67.

Hayashi, M., G. van der Kamp, and R. Schmidt. 2003. Focused infiltration of snowmelt water in partially frozen soil under small depressions. Journal of Hydrology 270:214-229.

Hillel, D. 1998. Environmental Soil Physics. Academic Press, London.

Kutilek, M., and D.R. Nielsen. 1994. Soil Hydrology. Catena Verlag, Cremlingen-Destedt.

LaBaugh, J.W., T.C. Winter, and D.O. Rosenberry. 1998. Hydrologic functions of prairie wetlands. Great Plains Research 8:17-37.

LaBaugh, J.W., T.C. Winter, R.A. Swanson, D.O. Rosenberry, R.D. Nelson, and N.H. Euliss. 1996. Changes in atmospheric circulation patterns affect mid-continental wetlands sensitive to climate. Limnol. Oceanog 41:864-870.

Nissen, H.H., P. Moldrup, and K. Henrikson. 1998. High-resolution time domain reflectometry coil probe for measuring soil water content. Soil Science Society of America Journal 62:1203-1211.

Parsons, D.F., M. Hayashi, and G. van der Kamp. 2004. Infiltration and solute transport under seasonal wetland: bromide tracer experiments in Saskatoon, Canada. Hydrological Processes 18:2011-2027.

Phipps, K.J. 2006. Spatial and temporal variation in greenhouse gas emissions from two open water prairie wetlands, University of Saskatchewan, Saskatoon.

Price, J.S., B.A. Branfireun, J.M. Waddington, and K.J. Devito. 2005. Advances in Canadian wetland hydrology 1999-2003. Hydrological Processes 19:201-214.

Sloan, C.E. 1972. Ground-water hydrology of prairie potholes in North Dakota. Geological Survey Professional Paper 585-C.

Yates, T. 2006. Spatial and temporal patterns of nitrous oxide and their relationship to soil water and soil properties, University of Saskatchewan, Saskatoon.

CHAPTER 2.0
LITERATURE REVIEW

2.1 Overview

Wetland hydrology in the semi-arid prairie has been extensively studied in the last forty years (Hayashi et al., 1998a; Hayashi et al., 2003; Meyboom, 1966). Extreme precipitation events are generally uncommon, but occur on the prairies due to differential heating of the ground surface and the development of isolated intense storm cells. For example, the city of Saskatoon, within 50 kilometers of the study site, from 1961 – 1990 experienced an average of 19 thunderstorms annually (Environment Canada, 2008). Storms that drop large volumes of water in very short time periods overwhelm hydrologic systems, generate overland flow, ponding in low lying areas, and the rapid infiltration and redistribution of ponded water. The hydrologic consequences of these events are difficult to determine as measuring these events requires extensive, automated, and reliable instrumentation capable of providing measurements on all aspects of the wetland and soil water balance. Currently, little information is available on how these events affect wetland hydrology as they occur intermittently over the landscape, over a short time period, and with little warning.

Soil hydraulic properties, landscape elements, and climate govern the fate of water within the prairie wetland. The same basic physical principles govern soil water movement through the soil and wetland, regardless of the volume of water in the soil system. Soil matric potential and volumetric water content gradients determine the direction, rate, and volume of water flow. Topography, soil texture, and preferential flow

paths cause landscape variability of water fluxes. These physical properties have significant affects on the infiltration capacity of the soil. Infiltration capacity governs the generation of overland flow, which leads to the accumulation of water in low lying wetland depressions.

To examine the impacts of extreme weather events on the hydrology of a prairie wetland the interactions between the soil and water must be completely understood. Therefore, an overview of the major soil hydraulic properties is provided. Additionally, the measurement of soil water and atmospheric inputs is an extremely complex subject. Given this, a discussion of the current technology and its associated deficiency's are presented when required.

2.2 Soil Water Dynamics

Soil water dynamics, as apposed to a static soil water condition is the constant changing state of soil water. Through a combination of inputs, precipitation or irrigation, and losses, drainage and evapotranspiration, soil water properties are constantly changing, giving it a dynamic quality. Essential to understanding this dynamic nature is water potential, described by Gibb's free enthalpy (Feddes et al., 1988; Scott, 2000):

$$\psi_t = \psi_m + \psi_g + \psi_o + \psi_p \qquad (2.1)$$

where ψ_t is the total potential, ψ_m is the matric potential, or the combined capillary and adsorptive forces of soil on the soil water, ψ_g is the gravitational potential, ψ_o is the osmotic potential generated by dissolved solutes, and ψ_p is the pressure potential under saturated conditions. Matric and water pressure potentials are interchanged given unsaturated and saturated conditions, respectively. The matric, water pressure, and gravitational potentials dominate, while the osmotic potential is usually insignificant and often ignored (Zhuo et al., 2004), leaving the following:

$$\psi_t = \psi_m + \psi_g \tag{2.2}$$

or

$$\psi_t = \psi_p + \psi_g \tag{2.3}$$

Basic to all environmental sciences and in particular those focusing on water is the concept of gradients, and the movement of medium and solutes from areas of high potential or concentration to areas of low potential or concentration. This concept, relating to the movement of water was first described by Darcy in 1856 (Youngs, 1988). Where Darcy's Law in one dimension for saturated conditions is (Scott, 2000):

$$q = -K\frac{\Delta H}{\Delta z} \tag{2.4}$$

where K is the hydraulic conductivity, H is the hydraulic head, or water potential, and z is the spatial coordinate. Richard's equation (1931) describes the movement of water under these ideal conditions (Youngs, 1988):

$$\frac{\partial \theta}{\partial t} = div(KgradH) = div(Kgradp) + \frac{\partial K}{\partial z} \tag{2.5}$$

where θ is the volumetric water content, p is the pressure head generated by the soil water, and K is the hydraulic conductivity in three dimensions and time. For unsaturated soils, Darcy's Law is (Scott, 2000):

$$q = -K(\theta_v)\frac{\partial H}{\partial z} \tag{2.6}$$

Unlike Eq. 2.4, hydraulic conductivity is now dependent upon the volumetric water content.

2.3 Soil Water and Matric Potential; Measurements

Fundamental to soil physics and hydrologic studies is the measurement of water within the soil profile. Two significant soil hydraulic variables are volumetric water content and matric potential.

The matric, gravitational and water pressure potentials are extremely important in soil water dynamics, as their interactions govern the movement of soil water. Eqs. 2.2 and 2.3 describe the interaction between these variables. Total water potential is the addition of either the matric and gravitational potentials or the water pressure and gravitational potentials in unsaturated and saturated soil conditions. Matric potential is a measure of the combined capillary and adsorptive forces of soil particles on the soil water and therefore is equal to zero under saturated conditions (Hillel, 1998; Scott, 2000). At saturation, pressure potential is measured with a nest of piezometers, used to determine the pressure head, or the height of the water table above or below a point of interest.

Measuring soil matric potential is a challenge in semi-arid environments, where it varies over a wide range from 0 MPa, at saturation, to -1.5 MPa, the permanent wilting point of agronomic crops (Hillel, 1998; Kutilek and Nielsen, 1994). The most common methods available for measuring soil matric potential are the tensiometer, electrical resistance sensor, psychrometer, and heat dissipation sensor (Reece, 1996; Scanlon et al., 2002) These methods have limited capability (Carlos et al., 2002; Flint et al., 2002; Phene et al., 1971; Reece, 1996; Si et al., 1999). Tensiometers operate through approximately six percent of matric potentials in semi-arid environments (0 to -0.09 MPa) and are limited to the wet end of the spectrum (Reece, 1996). The electrical resistance method uses two electrodes embedded in a porous block. The sensor equilibrates with the soil water solution to measure the electrical conductivity between

the two electrodes. These sensors are exceptionally sensitive to soil salinity and require gypsum to counteract that salinity. These gypsum blocks degrade over time, significantly changing the physical characteristics of the instrument, nullifying the laboratory calibration (Jovanovic and Annandale, 1997). In addition, the range of measurement is limited to -0.09 to -0.5 MPa. Thermocouple psychrometers are suited to very dry soils and do not operate in wet conditions. They are valid from -0.1 MPa to -8 MPa (Agus and Schanz, 2005). These sensors measure the humidity of a porous chamber in equilibrium with the water vapor phase of the surrounding soil. Thermocouple psychrometers measure the total water potential, therefore the matric and osmotic potentials must be separated through a number of rough estimations of the solute concentrations in the soil water (Andraski and Scanlon, 2002). Finally, heat dissipation sensors are the most reliable commercially available technique.

The development of heat dissipation sensors began in 1939 with Shaw and Baver, but took until Phene et al. (1971) to include a porous cup surrounding the heating element and temperature sensor (Fredlund, 1992; Phene et al., 1971). Heat dissipation sensors relate the water content of a porous ceramic cup to matric potential through a laboratory calibration curve. The Campbell Scientific (CS) - 229 sensors have a hypodermic needle, encasing a heating element and thermocouple. This needle is inserted into a porous block. In practice the sensor body is buried or inserted into the soil and the ceramic block is given time to equilibrate with the surrounding soil water. A known and constant energy source is supplied to the heating element. Based on the water content and the high thermal diffusivity of water compared to air, the change in temperature over a set amount of time is directly related to the water content of the sensor body and indirectly to

soil matric potential (Fredlund, 1992; Phene et al., 1971). Unfortunately, calibration is very difficult and time consuming (Flint et al., 2002; Fredlund, 1992; Reece, 1996; Starks, 1999). CS – 229 calibration is required because the construction of the sensor places a heating element and thermocouple within a hypodermic needle. Due to the intricate nature of this process, consistent placement of these two elements cannot be guaranteed and any given sensor may have the thermocouple closer or further away from the heating element, influencing the temperature readings. Secondly, the porous material does not consistently contact the needle and can alter the thermal properties of each sensor. The general method of calibration involves the placement of sensors within packed soil rings, where they undergo a variety of known tensions within a pressure plate (Flint et al., 2002; Fredlund, 1992; Reece, 1996; Starks, 1999). The change in temperature experienced by the sensors at each tension is recorded and a calibration curve is generated. The calibration curve relates the change in temperature to tension, or matric potential. Field measurements of temperature change over a set time are used with the calibration curve to determine matric potential. Heat dissipation sensors are limited in their range, with the CS - 229 sensor detecting matric potentials from -0.01 MPa to -1.0 MPa (Reece, 1996). Again, heat dissipation sensors are the best current available method, but they require a difficult and time consuming calibration and are invalid in extremely wet or dry soils. More research and development needs to occur in this field, please refer to Appendix A for further review of developments in the measurement of matric potential in semi-arid environments.

The second major soil water component is volumetric water content. It is the fraction of a given volume of soil that is occupied by water. Until the recent development of the

multisensor capacitance probe and multiplexed time domain reflectometry, the ability to provide temporally fine data has been time consuming and expensive. Volumetric water content can be collected in variety of ways, including gravimetrics, neutron probe attenuation, time domain reflectometry (TDR), and electrical capacitance. As discussed above, total water potential, including matric, pressure, and gravitational potentials determine the direction of water flows, while changes of volumetric water contents can be used to determine the magnitude of flow. Previous soil water dynamics studies lack real-time data because gravimetrics and neutron probes, the most widely used methods, are by their nature destructive and labour intensive (Paltineanu and Starr, 1997). Determination of gravimetric water contents or neutron probe attenuation requires the researcher to travel to the field and physically collect samples, limiting the temporal scale and the amount of data collected. In addition, gravimetrics is destructive and therefore undesirable. With the development of multiplexed TDR and capacitance probes, real-time data is now readily available. Both of these methods require the use of dataloggers, intensive field installations, and complicated calibrations of capacitance probes, but once that time and effort has been invested the rewards are significant.

TDR and capacitance probes work on the same basic principle. Both methods use the electromagnetic properties of water, soil, and air to determine volumetric water content. The dielectric constant of pure water is 80.4, soil ranges from 3.0 to 7.0, and air is 1.0 (Morgan et al., 1999). The electromagnetic properties of the soil and air are ignored, as the value of the water is much larger. Therefore, measured dielectric constant is solely dependent on the change in water content. An excellent discussion of the TDR and capacitance is provided by Paltineanu and Starr, (1997). TDR is widely accepted and

commonly used in water balance, soil water dynamics studies, and other research (Gomez-Plaza et al., 2001; Jackson and Wallace, 1999; Musters and Bouten, 2000; Si and Kachanoski, 2003; Stahli and Stadler, 1997; van Wesenbeeck and Kachanoski, 1988; Ward et al., 1998). TDR rods can be installed in one of two methods. They are inserted into the soil vertically or a pit dug and the probes inserted horizontally into an open face of the pit. Vertical installation is much less time and labour consuming, but heat conduction and preferential flow paths can be created. Conversely, horizontal placement of the probes solves these problems, but requires the excavation of a pit. The pit digging and refilling destroys the structure and flow paths of the soil, altering the rate and path of soil water movement (Paltineanu and Starr, 1997). The greatest benefit of using TDR is that it does not require calibration, with the exception of soils high in organic content, 2:1 clays, or salinity (Paltineanu and Starr, 1997).

Capacitance probes were developed for determining real-time soil water contents for maximizing water use efficiency in irrigated crops, they are not as widely accepted as TDR, but are gaining popularity in the scientific community. Resistance to the use of capacitance probes is a result of the complicated calibration (Baumhardt et al., 2000; Kelleners et al., 2004a; Kelleners et al., 2004b; Morgan et al., 1999; Starr and Paltineanu, 1998a). The value of real-time volumetric water data has outweighed the difficult calibration and scientists have used capacitance probes in a variety of transport studies (Paltineanu and Starr, 2000; Starr and Paltineanu, 1998b; Starr and Timlin, 2004). The capacitance probe emits an electrical field into the surrounding soil causing the permanent dipoles of the pore water to become aligned. In doing so, the probe is able to

measure the soil's capacitance, used to determine the dielectric constant and in turn the volumetric water content (Paltineanu and Starr, 1997).

A commonly used capacitance probe is the EnviroScan® (Sentek PTY, Ltd., Kent Town, South Australia), which is approximately 2 m long, with capacitance sensors every 10 cm along this length. This system consists of a PVC access tube, capacitance sensors, circuit board, and cap. The installation process includes the formation of an access hole and the insertion of the PVC tube into that hole. A tight fit at this stage is very important, as air spaces between the PVC tubing and the soil profile provide preferential flow conduits or pockets for water or air storage. Given the proper installation, this probe alleviates the issues of the TDR probe mentioned above. There is no pit dug and conductance is kept to a minimum.

Calibration of these sensors is a major concern, as the sensors are influenced by soil type and density (Kelleners et al., 2004b). There is a factory calibration curve based on the scaled frequency in soil (Baumhardt et al., 2000):

$$SF = \frac{(F_a - F_s)}{(F_a - F_w)} \tag{2.7}$$

$$\theta v = (7.792SF - 0.023)^{2.475} \tag{2.8}$$

where F_a is the sensor frequency in air, F_W is the sensor frequency in water, F_S is the sensor frequency in the soil, and θv is the volumetric water content. Baumhardt et al. (2000) in their examination of the factory calibration equation, (Eq. 2.8) concluded that the factory equation is only valid for dry conditions and that a soil specific equation is required. This presents a major problem for the use of capacitance probes, Paltineanu and Starr, (1997) suggest an accurate soil calibration requires the extraction of five undisturbed cores in close proximity to the capacitance access tube. While, Geesing et

al., (2004) found that at least 35 observations of bulk density were required for accurate calibration. These suggestions are not feasible and carrying out these calibration procedures would alter natural flow conditions. Alternatives are the use of a neutron probe or horizontal TDR array to provide benchmark soil water contents to scale capacitance probe measurements. Capacitance probes also experience soil salinity and temperature variation errors. Salinity increases conductance, causing over-estimations of volumetric water content (Baumhardt et al., 2000). Temperature affects are unclear, Baumhardt et al. (2000) report a significant change in volumetric water content with diurnal fluctuations in temperature. In contrast, Paltineanu and Starr, (1997) report that temperature induced errors were insignificant to the operation of the equipment. The greatest limitation of the capacitance probe is its inability to operate in frozen conditions. Measuring matric potential and soil water content present significant problems, but the most reliable, commercially available methods are the CS-229 sensor and the multisensor capacitance system by Sentek Sensor Technologies.

2.4 Factors Controlling Soil Water Potential and Movement

2.4.1 Topography and Soil Texture

Many factors affect the movement of water through the unsaturated zone, including soil texture and landscape position or topography. At first glance the principles guiding the redistribution of water across a landscape are simple, but determining the spatial and temporal arrangement of soil water on the landscape is complex.

Soil texture has the greatest affect on the vertical drainage and retention of soil water. Fine texture soils have a high water holding capacity and require significant tension to break water free from small pores (Bouma and Anderson, 1973; Hanks, 1992; Hillel, 1998). Figure 2.6.1 illustrates that the fine textured clay soil retains significant quantities

of water under tension. In contrast, the sandy soil quickly loses water, even under low tensions.

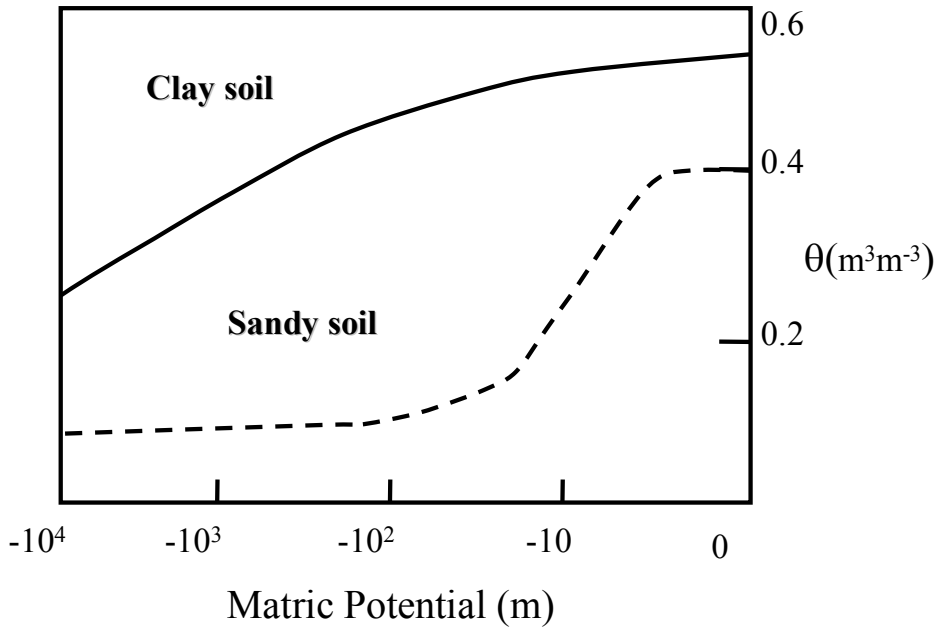

Figure 2.1. Water retention curve and soil texture.

Texture also influences hydraulic conductivity. Under wet conditions, hydraulic conductivity of a fine textured soil is greatly reduced compared to that of a coarse soil. Flow paths within a fine textured soil are more tortuous, reducing flow rates (Bouma and Anderson, 1973). Figure 2.6.2, describes this, as the fine textured clay soil, at low tension, has a lower hydraulic conductivity than the sandy soil. As the soils dry, the clay soil, with superior water retention, maintains higher water content and its hydraulic conductivity exceeds that of the sandy soil. The sandy soil's low water retention causes the soil to dry easily. Once dry, few continuous water filled pore spaces exist, reducing the number of water conducting channels.

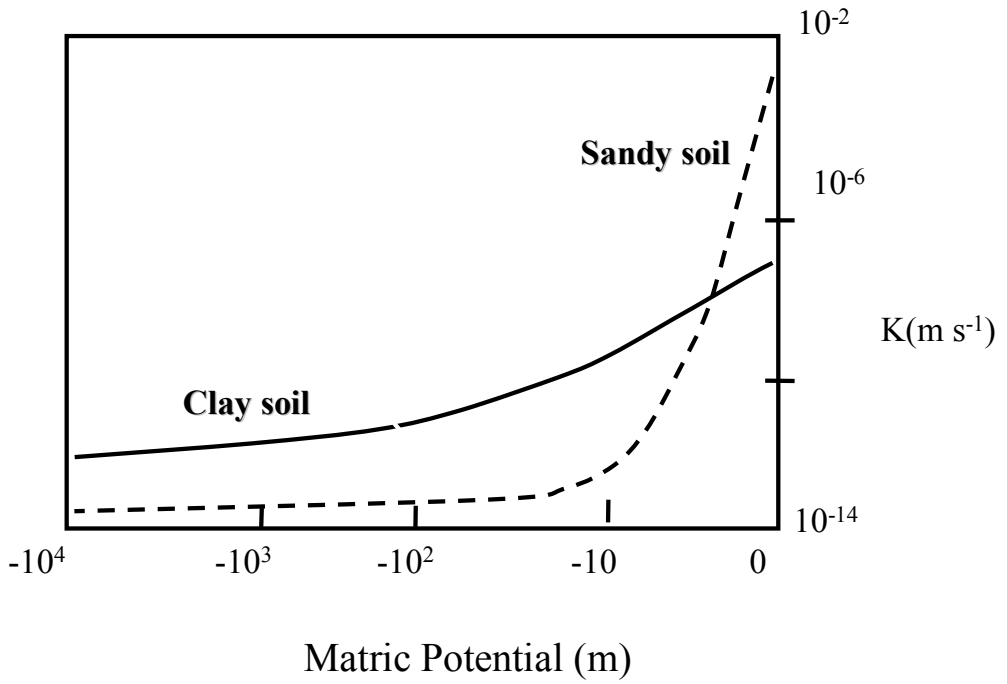

Figure 2.2. Hydraulic conductivity's (K) response to changing soil texture.

The second factor, topography has a significant influence on the spatial arrangement of soil and surface water. Topographic relief does not determine the fate of surface water alone, a variety of factors have a significant influence. These factors are soil moisture conditions, soil texture and structure, terrain indices, including: relative elevation, aspect, and slope curvature, vegetation, and microclimate (Famiglietti et al., 1998; Grayson et al., 1997; Western et al., 2004; Wilson et al., 2004; Wilson et al., 2005). According to Grayson et al. (1997), soil water conditions are the major controlling factor of soil water spatial variability. These researchers have identified two soil water conditions that determine whether soil texture and vegetation or topography is the dominant factor. These conditions are identified as local and nonlocal controls. Nonlocal control describes the situation where the upslope area is controlling the movement of water at a given point and local control is the condition where moisture patterns are controlled by the specific

texture or vegetative characteristics at that given location. The nonlocal condition dominates during periods when precipitation exceeds evapotranspiration, or the soil is likely to be saturated or nearly saturated. Conversely, local controls dominate in the alternative, where evapotranspiration rates exceed precipitation and the soil is unsaturated. If the soil is saturated and the relative topography exceeds 5% (Vidon and Hill, 2004), surface flow or subsurface lateral flow will occur. In this case, upland positions supply water to lowlands and the spatial variability of water is dominated by topography. In unsaturated conditions, lateral flow does not occur (Ridolfi et al., 2003) and soil texture or vegetation will determine the fate of water at any given position. Essentially, the controlling factor is climate. If the climate is predominantly moist, nonlocal controls will dominate and if the region is dry, such as Saskatchewan, local controls will dominate (Wilson et al., 2004). The nonlocal control does not persist in extremely wet conditions, during complete saturation the variability is controlled by soil texture (Bouma and Anderson, 1973; Famiglietti et al., 1998; Hanks, 1992; Hillel, 1998). It appears that one cannot simply state that soil texture or topography determine the spatial redistribution of soil water, instead they are linked and require an integrated analysis. The effect of soil texture and topography on the spatial distribution of soil water and soil water dynamics is straight forward, but the relative importance of the two is site specific and highly dependent upon antecedent soil water conditions.

2.4.2 Preferential Flow

Preferential flow is the movement of water and solutes through the vadose zone that bypasses the soil matrix. The occurrence of preferential flow can greatly alter the rate and volume of water movement through the soil zone. This special case cannot easily be measured or predicted. The matrix is bypassed due to the variability in pore size

distribution, soil density, soil texture, and the presence of cracks, fauna burrows, and decayed root channels (Gerke, 2006; Scott, 2000). Preferential flow can be divided into several categories; macropore flow, unstable flow, and funnel flow. Macropore flow describes the rapid movement of water and solutes through continuous root channels, fauna burrows, cracks in clay rich soils, and natural soil pipes (Hillel, 1998). Unstable flow occurs when water infiltrating a coarse textured soil meets resistance from a hydrophobic source. Hydrophobic sources can include soil textural changes from a fine to coarse texture, air trapped within soil pores, flow involving fluids of variable viscosity or density, or a water repellant soil (Jury and Horton, 2004). This type of preferential flow is often termed "fingering." Funnel flow results from the variation in soil texture or density, where the solute follows the path of least resistance and is funneled through discrete pathways (Gerke, 2006; Jury and Horton, 2004).

The generation of preferential flow is influenced by antecedent soil water content, infiltration rates, and rainfall intensity. Dry initial conditions may result in the dominance of matrix flow, whereas a wet initial condition causes preferential flow to be dominant. Rainfall intensity also has considerable influence. During intense storms preferential flow paths with greater infiltration capacity than the soil matrix, conduct significant volumes of water away from the soil surface. This allows prolonged infiltration and limits the generation of overland flow (Williams et al., 2003).

The greatest challenge is the measurement and modeling of preferential flow. Several laboratory and field methods exist, including the use of conservative chemical tracers, dye tracers, and laboratory core breakthrough curves. Regarding modeling, classic Darcinian flow models cannot predict the rate and depth of soil water preferential flow,

as they assume a single hydraulic conductivity. In response, multiple porosity approaches have been developed, including mobile-immobile transport models and models that integrate both the macropore and matrix flow. A thorough review of these models is provided by Gerke, (2006). Preferential flow can be significant in the movement and fate of water in the PPR. The till and sediments in this region are highly jointed, with lenses of stratified sand, silt, and gravel (Sloan, 1972). Water from intense rainstorms can bypass of the upper matrix portions of the soil and quickly contribute to the groundwater at depth.

2.5 Soil Water Balance

The water balance is a basic concept in hydrologic and soil physics research. The water balance can be completed at a variety of spatial scales from the global scale to a single layer in a soil profile. The same hydrologic processes apply to these and any scale between. The basic concept is that a change in storage, positive or negative, is accounted for by the losses and gains from the system. The soil is the major interface between the atmosphere and the long-term storage in groundwater. Therefore, determination of the soil water balance is essential in determining the fate of water falling on the earth's surface.

Losses include drainage through the soil profile to the groundwater, evapotranspiration, and surface run-off. Inputs include precipitation, snowmelt, upward capillary flow from the groundwater, and run-on from uplands (Hillel, 1998; McCoy et al., 2006). The hydrologic processes occurring are highly variable, daily, seasonally, and annually. In the long run, soil storage is generally zero and gains to the system are lost through the growing season. In the short term, changes in storage are frequent and are positive or negative. In a semi-arid environment, a negative storage term is caused by

evapotranspiration demands exceeding rainfall or snowmelt. Alternatively, a positive storage term can result from an intense rainfall event that overwhelms the normally dry system.

Many criticisms of the soil water balance exist. Soil water balances are small scale studies as they measure limited areal extent, this if the greatest drawback of the soil water balance approach. Scaling point, soil water data to an areal study is extremely difficult and requires many mathematical computations and assumptions. The soil water balance requires estimations of deep drainage and evapotranspiration and does not take into account vegetative interception (Wilson et al., 2001). Regardless, the small scale is practical and computationally feasible. The major processes assessed by a soil water balance are precipitation, infiltration, evapotranspiration, and drainage. All of these are discussed further in the following.

2.5.1 Precipitation: Measurement

The Saskatoon, Saskatchewan 30 year average total precipitation is approximately 350 mm with 24 % (1971 – 2000) as snowfall (Environment Canada, 2008). Spring snowmelt infiltration is substantially reduced by the frozen state of soil (Gray et al., 1985; Gray et al., 2001). Therefore, the largest input to a Canadian prairie wetland is spring snowmelt. Snowmelt infiltration studies are very difficult to complete, as most soil water measurement techniques do not function in partially frozen soils. Key to determining the soil water balance is estimating the rate and volume of precipitation. There are many different instruments for measuring rainfall and all have limitations and errors associated with them.

Direct precipitation is normally measured at a single point. Many different types of precipitation gauges are available, from a tin bucket to sophisticated automated systems.

The development of automated systems is valuable in field studies, as they eliminate the need for personnel to constantly monitor gauges. Although they are an improvement, all automated gauges have their own specific problems leading to under-catch, over-catch, and delays in response. Wind has the greatest influence on precipitation gauges installed above the ground's surface. The presence of the gauge causes eddies that generate fast moving air currents above the gauge orifice. These air currents blow raindrops and snowflakes past the gauge opening and a portion of the precipitation is not measured. This error is the most common and serious, accounting losses of 2 - 15% of rainfall and up to 80% for snowfall (Dingman, 2002; Sevruk, 1996; Yang et al., 1998). As mentioned, there are many different types of gauges and all have their own unique problems.

The oldest and most common gauge is the simple collecting device, requiring an observer to record and empty the gauge with each precipitation event. These gauges are the simplest and provide good quality back-up data for field work, but are inaccurate due to observer error (Dingman, 2002). Observer dependent gauges are prone to collection error and cannot gather temporally fine-scale data. Automated systems have solved the time-scale and observer errors, but have a range of other drawbacks.

The most common automated gauge is the tipping bucket (TB). TB gauges are relatively inexpensive and easy to obtain and install. The TB gauge consists of a collection vessel, funnel, and two tipping buckets. The tipping buckets are of a known and equal volume and are attached to each other at a fulcrum. As one bucket fills, from the funnel, it rotates on the fulcrum and places the other bucket under the outlet of the funnel. The TB gauge is connected to a datalogger that measures a switch closure with

each tip of the bucket (Habib et al., 2001; Campbell Scientific, 2003). As mentioned, the major downfall of the TB gauge is wind induced under-catch. Other TB gauge errors are related to bucket size, if the amount of precipitation falling is too little to cause the bucket to tip, the gauge will not register any precipitation. This accounts for a small portion of error, as commercially available TB gauges have resolutions of 0.1, 0.254, or 0.5 mm. Therefore, very little precipitation is missed. If manufacturers were to attempt to correct this issue and make the buckets smaller, extreme events are likely to overwhelm the gauge and the switch closures would not occur fast enough. A temporal lag would result or the rainfall could overwhelm the collection vessel and spill over onto the ground, under-estimating the rainfall. These bucket size limitations cause the TB gauge to be imprecise at small time scales, such as 1 - 5 minutes. Over a larger time scales, such as 1 hour, these errors are negligible (Ciach, 2003; Habib et al., 2001). Other errors are technological in nature. Field equipment is often powered by batteries prone to losing power or communication errors between the datalogger and instrument may result in the loss of data (Dingman, 2002). These errors cannot be predicted, but with careful preparation and proper installation and maintenance, they are easily mitigated.

The other common automated gauge is the weighing type gauge. These gauges collect a sample of precipitation into a bucket and then measure the change in weight. Some of these gauges are modified for snowfall measurement and the bucket is partially filled with antifreeze to melt incoming snow (Geonor T-200B). These gauges have many advantages over others, they provide fine resolutions, both temporally and volumetrically, require less energy to operate, and limit evaporative losses (Sevruk and Chvila, 2005). Weighing gauges are still subject to wind induced errors and their own

unique problems. They under-predict precipitation, compared to a common observer recorded gauge, and they have difficulty measuring small events (Sevruk and Chvila, 2005). Wind induced errors have not been solved by weighing gauges, but the most recent technique, the optical gauge, may be a significant advancement.

Optical gauges are the newest technology available. These gauges use an infrared light emitting diode, which measures the disturbance of light when particles of precipitation travel between the emitter and a light sensitive sensor (Dingman, 2002; Lundberg and Johansson, 1994). These optical instruments are not readily available and the present precipitation measurement techniques provide a reasonable estimate of actual precipitation. The common TB gauge is sufficiently accurate for the development of the soil water balance in the prairie environment.

2.5.2 Infiltration

Infiltration into the soil profile is of interest in many fields, from irrigation specialists to contaminant hydrogeologists. Infiltration into the soil surface is the central process in the soil water balance, a soils ability to infiltrate water determines the fate of that water. Water that does not infiltrate is lost down-slope through overland flow or evaporates directly from the surface. The major concepts of soil infiltration are infiltration capacity and cumulative infiltration. A soil's infiltration capacity, or infiltrability, is dependent upon the hydraulic conductivity of the soil surface. Surface hydraulic conductivity is affected by antecedent soil water content, soil texture, structure, and the type of clay present. Generally, the infiltrability of a soil is high during the early stages of water application and decreases till it reaches the steady-state infiltration rate, or the soil's saturated hydraulic conductivity. Once this occurs, the rate of infiltration is no longer

supply-controlled and the hydraulic properties of the soil profile now control the infiltration rate and redistribution of water (Hillel, 1998; Scott, 2000).

Cumulative infiltration is simply the total amount of water that has infiltrated the soil to a given depth or over a given time period, calculated in the following manner;

$$I = \int_0^{z_f} \Delta\theta dz \qquad (2.9)$$

$$I = \int_{t_1}^{t_2} i(t)dt \qquad (2.10)$$

where, z_f is the depth of the wetting front, $\Delta\theta$ is the change in water content over that depth, and t_1 and t_2 are the initial and final times of infiltration (Scott, 2000). Determining the cumulative infiltration is valuable if overland or surface ponding may occur. For example, if the cumulative infiltration is significantly less than a precipitation event, there is an excess amount of water in the system. That water will either run-off, given the appropriate topographic relief, or pool and evaporate into the atmosphere. McCoy et al., (2006) used the changes in volumetric water content over time to determine the soil water budget and the proportion of overland flow to determine the effects of different tillage techniques on infiltration. Both of these variables are determined by the physical characteristics of the soil and the nature of the precipitation event. Those physical and meteorlogic factors are discussed in detail in the following sections.

2.5.2.1 Factors Affecting Infiltration

Determining and estimating the rates of infiltration into a soil has been of major concern for nearly a century. The Green and Ampt infiltration model proposed in 1911 was the first model to solve this problem (Jury and Horton, 2004). Many soil and environmental factors affect the infiltrability of a soil. Some of these factors are related

to the soil, such as the antecedent soil water content, the soil texture, structure, and type of clay present in the soil. Other factors relate to the environmental or land use conditions, such as the rainfall intensity, presence of a frost layer, slope, vegetative cover, and agricultural influences (Dingman, 2002; Hillel, 1998; Scott, 2000; Williams et al., 1998).

The antecedent soil water condition is the major factor determining the fate of water falling onto a soil. Wet antecedent conditions greatly reduce the infiltrability of a soil. An already saturated soil will saturate early in the event and the rate of infiltration is greatly reduced as the soil reaches steady-state (Hillel, 1998). A dry soil surface with wet conditions below may still have reduced infiltrability. Wet profiles are unlikely to have sufficient suction gradient to pull water into the soil from the surface (Williams et al., 1998). Alternatively, dry soils, both at surface and depth can accept great quantities of water before saturation is reached and water at the surface layer can easily move within the profile. The affects of soil texture were discussed in the previous section. In general, a coarse textured soil has a higher hydraulic conductivity and allows greater volumes of water to infiltrate than a fine textured soil. Soil structure and the presence of preferential flow paths can greatly decrease or increase the rate of infiltration. Again, preferential flow is discussed in the previous section. The type of clay present in the soil is a major concern. Soils with shrink and swell clays tend to have high rates of infiltration during the onset of rainfall. Eventually, the clays swell and seal the cracks at the surface, greatly reducing infiltration rates. Considerable topographic relief reduces the time available for infiltration and overland flow is more likely (Williams et al., 1998). Additionally, agriculture affects infiltration through many processes, including compaction due to

machinery and grazing livestock, and tillage effects. Heavy grazing decreases the surface saturated hydraulic conductivity by up to 35% by compaction and reduced vegetative cover, (Fiedler et al., 2002). The physical properties of the soil are important, but if no water is supplied, no infiltration occurs.

The rate and duration of rainfall or irrigation application ultimately determines the proportion of rainfall infiltration. Extreme events can overwhelm the infiltration capacity of the soil and cause either ponding and/or overland flow (Williams et al., 1998). Overland flow developed in this manner is termed Hortonian Overland Flow (Ritter et al., 2002). Furthermore, intense rainfall events are characterized by large raindrops. These large drops cause rain-splash that seals surface pores, decreasing infiltrability (Dingman, 2002).

The thermal state of the soil has major consequences regarding the infiltration during the spring snowmelt. Frozen soil infiltration is separated into three distinct categories, unlimited, limited, and restricted (Gray et al., 1985; Gray et al., 2001). The unlimited case occurs when the soil accepts all available water. This occurs when soils have low water contents, a coarse texture, an organic mat, or many preferential flow paths. Limited infiltration occurs when a portion, but not all available water infiltrates. Conditions in the snow pack and soil diminish the infiltrability of the soil, but infiltration into the soil matrix still occurs. Restricted infiltration occurs when there is no snowmelt infiltration. In this case there is significant spring run-off and evaporation of ponded water into the atmosphere. Infiltration cannot occur due to the presence of ice lenses or when a frozen soil is saturated or nearly saturated. Ice lenses form on the soil surface from snow melting and refreezing during the winter. Infiltration into frozen soils is a

complex subject and the details are beyond the scope of this research. For a complete review refer to Gray et al. (2001).

2.5.3 Evapotranspiration

Evapotranspiration is the greatest source of water loss from soils in the semi-arid prairie environment. Understanding and estimating evapotranspiration is important for predicting climate change, evaluating the amount of freshwater available for consumption, groundwater recharge, irrigation, and crop production.

Evapotranspiration is the combination of evaporation from the earth's surface and transpiration from plants. The two processes are nearly impossible to separate in field based research. Therefore, they are almost always combined into one term. The basic understanding of evapotranspiration is imbedded in Fick's first law. It is dependent upon wind speed, resistance to transport, and the magnitude of the vapour gradient between the surface and the atmosphere (Dingman, 2002). The movement of water molecules from the soil or plant surface requires a water vapour gradient between the soil or plant interior and the atmosphere. Two simple ways to consider humidity are vapour density and vapour pressure. Vapour density is a measure of the mass of water molecules present in a volume of air and vapour pressure is the partial pressure exerted by those molecules. If the air is drier than the soil, water molecules will diffuse into the atmosphere. Provided an unlimited source of water, the air will eventually reach saturation and equilibrium occurs between the rate of molecular diffusion between the soil and atmosphere and vice versa. A parcel of air in this state has reached saturation vapour density or pressure. The air cannot hold anymore moisture. Temperature greatly affects the saturation vapour pressure or density. Warmer conditions allow greater amounts of water to be held before saturation is reached. If a turbulent force; wind, is present it is nearly impossible to reach

equilibrium, as newly moistened air is driven away from the surface and replaced with dry atmospheric conditions (Oke, 1987).

The two processes are not easily separated, but are still two separate processes. The simpler, evaporation, occurs provided a sufficient vapour gradient and energy to cause the phase change, from a liquid or solid into water vapour. Water molecules from the surface of a soil, water body, or even from a plant will passively diffuse into the atmosphere, provided a vapour gradient. Alternatively, transpiration is actively controlled by plants. Transpiration still occurs by the same basic principles, but given dry conditions a plant can generate a significant resistance to water loss. Plants have the ability to open and close stomata, the opening into or out of the plant leaf. Photosynthesis requires a supply of carbon dioxide gas from the atmosphere. Plants open their stomata in an attempt to capture carbon dioxide and as a result allow water molecules to diffuse of from the saturated interior of the leaf to the dry atmosphere. The rate of water loss from the interior of the leaf is twice the rate of carbon dioxide diffusion into the leaf. Therefore, during dry conditions the plant will close its stomata, and diffusion of both gases ceases. Closed stomata generate considerable resistance to molecular diffusion and in highly vegetated landscapes can greatly decrease the overall rate of evapotranspiration (Smith and Smith, 2001). Both processes occur based on the basic principles of diffusion and turbulent transfer, but plants can actively limit the loss of water to the atmosphere. There are several different methods for estimating evapotranspiration. These include the energy balance, water balance, mass-transfer, and eddy-correlation approaches. As mentioned, none of these methods can separate the evaporation and transpiration components. This is generally of little consequence

because water molecules which are evaporated or transpired have the same fate-either way they are lost to the atmosphere.

2.5.4 Drainage

The second loss term from the soil water balance is drainage from the soil zone to the zone of saturation. It is generally accepted that deep drainage in the semi-arid to arid environments is extremely small. In a long-term drainage study, Dyck et al., (2003) examined the movement of a conservative tracer (chloride) and calculated the long-term drainage under natural conditions. They found that the rate of movement was greatly reduced at depth. Four years after application, the bulk of the chloride had moved to a depth of 1.34 m. Thirty years after application, the bulk of the tracer had only moved another 0.34 m. These authors report a drainage velocity of 11 mm yr^{-1} for the rooting zone and 3 mm yr^{-1} below. It is apparent that the majority of water draining through the soil zone is returned to the atmosphere, likely through uptake and plant transpiration. If large volumes of soil water were feeding the groundwater, the chloride tracer would have continued to move to greater depths in the long term.

The vegetative community has a great control over drainage through the soil profile. In a study of desert vegetative communities, Walvoord and Phillips (2004) found that deep drainage occurred only on sites with woody vegetation. The authors do not propose that this is the only factor affecting deep drainage, but contend that this may be good indicator to determine the locations of drainage to the groundwater system. Topographic relief also has a significant effect upon soil water drainage. Water that is unable to infiltrate into upland soils or infiltrated water moved by through-flow will inevitably find its way to the lowest landscape position. These topographic depressions become the primary locations of infiltration and drainage from the rooting zone (Hayashi et al.,

1998a; Hayashi et al., 1998b; Hayashi et al., 2003). A detailed discussion of the impacts and fate of this depression focused infiltration and drainage is provided in the following section on wetland hydrology.

Measuring the components of the soil water balance is relatively easy. Assessing the inputs and outputs from the system may require several estimations, but overall the soil water balance is practical and computationally simple.

2.6 Wetland Hydrology; Prairie Pothole Region

Depressions within the PPR are commonly referred to as sloughs and were formed during the most recent glacial retreat, ~10-17 kyrs ago. They result from the melting of ice blocks dropped by the retreating glacier. These ice blocks were buried under till and following melting, the till settled and the inverted topography was formed (Sloan, 1972). They are hydrologically isolated, as they are not permanently connected by surface inflow or outflow channels. The climate of the region is dry and on an annual basis evapotranspiration exceeds precipitation. These depressions serve many hydrologic and biological functions and are highly dependent upon climatic factors. They store precipitation and snowmelt that recharges groundwater and provides habitat for biota, from aquatic organisms to nesting habitat for water fowl (LaBaugh et al., 1998; Price et al., 2005).

Soils in these regions have low hydraulic conductivities at depth, owing to high clay content and the glacial history of the region. Therefore, interactions with groundwater are generally dependent upon preferential flow and deep drainage to groundwater is low (Parsons et al., 2004; Price et al., 2005). These depressions play a major role in prairie

hydrology and are the main source of surface water infiltration in the prairie pothole region (Hayashi et al., 1998a; Hayashi et al., 1998b; Hayashi et al., 2003).

2.6.1 Precipitation, Snowmelt, and Run-off

The Canadian Prairies are characterized by a cold semi-arid climate. The thirty year mean annual temperature in Saskatoon, Saskatchewan is 2 ^{o}C, with a minimum monthly mean for January of -17.5 ^{o}C, and a maximum monthly mean of 18.6 ^{o}C for the month of July. Snowfall accounts for approximately 24% of precipitation (Environment Canada, 2008). As a result of limited spring upland infiltration snowmelt is the major water source for ponding in wetland basins. The other major contributor is direct precipitation on the ponded water surface.

As previously discussed, during snowmelt, soils are frozen and upland infiltration rates are significantly reduced. This results in the transfer of 30 - 60% of upland snowmelt water to the pond center (Hayashi et al., 1998a). Snow surveys are commonly used to measure the depth and density of snow in a catchment. These surveys are laden with errors and do not take into account sublimation and evaporation of the snow-pack.

Direct rainfall is the other input into the pond. The methods and the associated errors of measuring rainfall were previously discussed. Examining the pond water level during a storm may work as a field scale rain gauge, with the rise in the pond level equaling the rainfall accumulation. Therefore, if the pond depth increase exceeds the rainfall accumulation, overland flow from the current event or throughflow from water that previously infiltrated upland soils. Overland flow is very difficult to measure, but has been reported in the past. Meyboom (1966) reported an event of ~50 mm, causing a dry wetland to fill and shallow pond center piezometers to rise between 0.3 - 0.6 m (1 - 2 ft.). Shallow upland piezometers did not respond to this event, indicating limited infiltration

in the uplands and possible overland flow to the depression. Hayashi et al., (1998a) reported that on July 4, 1996 a rainfall event of 54 mm generated a pond response of approximately 210 mm, obviously due to overland flow. These events are rare, and it is unusual that they are measured. Thorough understanding of the hydrologic effects of these events is nonexistent.

2.6.2 Infiltration and Evapotranspiration in the pond

Following pond development, water is lost in one of two ways, infiltration or evapotranspiration. The major physical processes governing infiltration rates and infiltration capacity were previously discussed; please refer to those sections for greater detail. Infiltration of ponded water accounts for the majority of loss from the pond. Researchers report that infiltration through the pond center accounts for 47 – 80 % of losses from wetland ponds (Hayashi et al., 1998a; Hayashi et al., 1998b; Parsons et al., 2004). Parsons et al. (2004), reports that infiltration rates are variable throughout the summer, accounting for 47 % of loss in May and 67 % in June – July. Variable transpiration rates of wetland and pond-edge vegetation are believed to be responsible for the seasonal variation. Surface conditions of wetlands are dominated by thick porous organic horizons. In an in-depth study of surface hydraulic properties of a small Saskatchewan wetland, Stoof (2004) measured the porosity and hydraulic conductivity of a variety of landscape elements. Conductivities reported for the pond center are two orders of magnitude larger than upland positions. These results are supported by Bodhinayake and Si (2004), who determined that land use and vegetation have major implications on soil hydraulic properties and therefore surface infiltration rates. These researchers found that grasslands, both native and brome, had significantly higher saturated and unsaturated hydraulic conductivity and water conducting macro-porosity

than nearby cultivated land. With regard to the infiltration of ephemeral wetlands, the high rates of infiltration and porosity reported by Stoof (2004) are misleading. Once steady-state is reached, infiltration rates are controlled by mineral soils at depth, which have much lower porosities and hydraulic conductivities than the surface layers (Hayashi et al., 2003). Therefore, mineral soils control the rate of pond water infiltration, not the surface.

Evapotranspiration accounts for the remainder of ponded water loss. Again, this occurs through two different processes, the direct evaporation from the water surface and transpiration by vegetation. Direct evaporation from the pond is controlled by atmospheric demands. Atmospheric conditions are extremely variable from wetland to wetland on the same site and vary daily, seasonally, and annually for a single wetland. Open water evaporat^{io}n was measured with the pan method by Hayashi et al. (1998a). They reported evaporative rates of 3.1 ± 0.7 mm d^{-1}. While Parsons et al. (2004) reported 1.9 mm d^{-1} in May and 2.2 mm d^{-1} in June - July on the same wetland, but for a different year. Transpiration is highly variable and just as in the case of evaporation is dependent upon the daily, seasonal, and annual climatic conditions. Specifically, transpiration is variable throughout the day, where rates of evapotranspiration show a "step-like" pattern. Rates are high in the afternoon, during the time of highest demand by the atmosphere, and level off throughout the night (Hayashi et al., 1998a). Vegetation on the pond center and uplands consume water that has infiltrated through the pond basin. Upland vegetation aids in the lateral movement of water from under the wetland to uplands. This lateral process is discussed in detail in a later section.

2.6.3 Groundwater Recharge and Flow

Interactions between surface and groundwater are used to define the hydrologic function of wetlands. Wetlands are considered to be sites of recharge, discharge, or both. Recharge wetlands are characterized by the movement of water and solutes in an outward direction. Discharge wetlands are often saline and have the reverse situation, where groundwater supplies water to the surface of the wetland and solutes remain following evaporation of ponded water (LaBaugh et al., 1998). The direction of flow may change from year to year and throughout the growing season, but there is an overall dominant flow direction that characterizes every wetland. Rates of groundwater recharge are required for determining contaminant transport in agricultural regions, where the use of fertilizers and pesticides has increased dramatically. Wetlands are the major location of recharge in knob and kettle landscapes and therefore understanding the rates of basin centered infiltration and redistribution is extremely important. These rates are generally low and are dependent upon the jointed and fractured nature of the glacial till. Flow of groundwater and perched water tables is controlled by the jointed nature of the deposits and lenses of stratified sand, silt, and gravel (Sloan, 1972). Parsons et al. (2004), in a conservative bromide tracer pond study, detected bromide in piezometers at several meters below the pond within weeks of tracer application. Preferential flow likely occurred along coarse textured lenses or joints within the till. Estimates of annual groundwater recharge range from 2 – 6 mm yr^{-1} (Hayashi et al., 1998a; Hayashi et al., 1998b). Local shallow water tables receive greater amounts of annual recharge, up to 45 mm yr^{-1} (Parsons et al., 2004). On an annual basis the majority of this local recharge is lost to evapotranspiration by upland vegetation. The effect of extreme precipitation events on groundwater recharge is not clearly understood. Significant rainfall events can

cause preferential flow to depth in a very short time-scale, resulting in high rates of recharge in a short time period (days to weeks). These events may be offset by dry or normal seasons where very little to no recharge occurs, causing the measured low long-term recharge rates. Both regional and local groundwater flows are seasons. Vegetation, both wetland and upland, play a major role in determining seasonal flow directions. During the winter and early spring groundwater moves in a downward direction due to gravitational forces. Following the spring snowmelt, low infiltrability results in overland flow and the formation of a pond in the lowlands. Upland groundwater is depleted in the early spring, due to the downward winter flows, and little upland snowmelt recharge occurs. Ponded water is generally at higher potential than the surrounding upland groundwater, resulting in the lateral movement of water from the pond center to the water table under the uplands. Once vegetation is active, there is a reversal of flow, in which vegetation on the edges of wetlands cause a cone of depression and groundwater from below the pond center and uplands feed transpiration demands. Winter flow conditions return with the senescence of vegetative communities (Meyboom, 1966). Groundwater flow is not only variable on a seasonal basis. It is also variable on an hourly time-scale. Wetland fringe vegetation actively transpires through the day causing a draw-down of adjacent groundwater. Throughout the night, these plants are inactive and this depression is filled by groundwater of greater potential from the pond center and uplands (Meyboom, 1967; Sloan, 1972). Overall, the rates of recharge in semi-arid environments are very low and the hydrologic cycle is dominated by the dry atmosphere.

2.6.4 Lateral Water Movement and Upland Evapotranspiration

Hayashi et al., (1998a; 1998b) in a combined water balance and solute transfer study provided an excellent prairie wetland water balance. According to these researchers, 75 -

80% of ponded water infiltrates into the soil. This high proportion is attributed to suction created by vegetation from the pond and adjacent upland. Following infiltration to the soil and parent material underlying the pond, the water and solutes are transferred laterally to uplands surrounding the wetland. Water redistribution from below the pond center to the surrounding upland is driven by both the mound effects of the pond and by suction from upland vegetation. Hydraulic conductivities of the glacial till decrease with depth. Till above the commonly observed oxidation zone are several orders of magnitude higher than sediments below this zone (Meyboom, 1967). As a result, infiltrated water is evapotranspired into the atmosphere by adjacent upland vegetation.

Hayashi et al., (1998a; 1998b) discovered elevated chloride concentrations in upland soils and in doing so, identified the location of the greatest rates of evapotranspiration. The authors state that 25% of ponded water is lost to the atmosphere, through evapotranspiration, with greater losses during the afternoon. If infiltration is partially governed by the biological requirements of adjacent upland vegetation, then more than 25% of the water within the wetland is eventually lost to the atmosphere. In addition, summer precipitation events were consumed by an upward gradient in the vadose zone, with the further loss of this water through evapotranspiration. Evapotranspiration is the dominant factor in the prairie pothole environment, with an estimate of only 1% of annual precipitation contributing to recharge. Annual water balance studies have provided a substantial amount of information regarding the annual fate of water within a prairie wetland, but the short-term hydrologic effects on a wetland are not considered.

2.7 References

Agus, S.S., and T. Schanz. 2005. Comparison of four methods for measuring total suction. Vadose Zone Journal 4:1087-1095.

Andraski, B.J., and B.R. Scanlon. 2002. Thermocouple Psychrometry, p. 609-642, *In* J. H. Dane and G. C. Topp, eds. Methods of Soil Analysis, Part 4, Physical Methods, Vol. SSSA Book Ser. 5. SSSA, Madison, WI.

Baumhardt, R.L., R.J. Lascano, and S.R. Evett. 2000. Soil material, temperature, and salinity effects on calibration of multisensor capacitance probes. Soil Science Society of America Journal 64:1940-1946.

Bodhinayake, W., and B. Si. 2004. Near-saturated surface soil hydraulic properties under different land uses in the St. Denis National Wildlife Area, Saskatchewan, Canada. Hydrological Processes 18:2835 - 2850.

Bouma, J., and J.L. Anderson. 1973. Relationships between soil structure characteristics and hydraulic conductivity, p. 77-105, *In* R. R. Bruce, et al., eds. Field Soil Water Regime, Vol. 5. Soil Science Society of America Inc., Madison, Wisconsin.

Campbell Scientific. 2003. Manual: TE525 Tipping Bucket Rain Gauge, Edmonton.

Carlos, M.P., J.W. Hopmans, A. Macedo, L.H. Bassoi, and D. Wildenschild. 2002. Soil water retention measurements using a combined tensiometer-coiled time domain reflectometry probe. Soil Science Society of America Journal 66:1752-1759.

Ciach, G.J. 2003. Local random errors in tipping-bucket rain gauge measurements. Journal of Atmospheric and Oceanic Technology 20:752-759.

Dingman, S.L. 2002. Physical Hydrology. 2nd ed. Prentice Hall, Upper Saddle River, NJ.

Dyck, M.F., R.G. Kachanoski, and E. de Jong. 2003. Long-term movement of a chloride tracer under transient, semi-arid conditions. Soil Science Society of America Journal 67:471-477.

Environment Canada. 2008. Canadian climate normals [Online] http://www.climate.weatheroffice.ec.gc.ca/climate_normals/index_e.html (Verified May 27 2008).

Famiglietti, J.S., J.W. Rudnicki, and M. Rodell. 1998. Variability in surface moisture content along a hillslope transect: Rattlesnake Hill, Texas. Journal of Hydrology 210:259-281.

Feddes, R.A., P. Kabat, P.J.T.V. Bakel, J.J.B. Bronswijk, and J. Halbertsma. 1988. Modeling soil water dynamics in the unsaturated zone-state of the art. Journal of Hydrology 100:69-111.

Fiedler, F.R., G.W. Frasier, J.A. Ramirez, and L.R. Ahuja. 2002. Hydrologic Response of Grasslands: Effects of Grazing, Interactive Infiltration, and Scale. Journal of Hydraulic Engineering 7:293-301.

Flint, A.L., G.S. Campbell, K.M. Ellett, and C. Calissendorff. 2002. Calibration and temperature correction of heat dissipation matric potential sensors. Soil Science Society of America Journal 66:1439-1445.

Fredlund, D.G. 1992. Background, theory, and research related to the use of thermal conductivity sensors for matric suction measurement. Soil Science Society of America Journal SSSA Special Publication Number 30:249-261.

Geesing, D., M. Bachmaier, and U. Schmidhalter. 2004. Field calibration of soil water probe in heterogeneous fields. Australian Journal of Soil Research 42:289-299.

Gerke, H.H. 2006. Review Article: Preferential flow descriptions for structured soils. Journal of Plant Nutrition and Soil Science 169:382-400.

Gomez-Plaza, A., M. Martinez-Mena, J. Albaladejo, and V.M. Castillo. 2001. Factors regulating spatial distribution of soil water content in small semiarid catchments. Journal of Hydrology 253:211-226.

Gray, D.M., P.G. Landine, and R.J. Granger. 1985. Simulating infiltration into frozen prairie soils in streamflow models. Canadian Journal of Earth Sciences 22:464-474.

Gray, D.M., B. Toth, L. Zhao, J.W. Pomeroy, and R.J. Granger. 2001. Estimating areal snowmelt infiltration into frozen soils. Hydrogeology Processes 15:3095-3111.

Grayson, R.B., A.W. Western, and F.H.S. Chiew. 1997. Preferred states in spatial soil moisture patterns: Local and nonlocal controls. Water Resources Research 33:2897-2908.

Habib, E., W.F. Krajewski, and A. Kruger. 2001. Sampling errors of tipping-bucket rain gauge measurements. Journal of Hydraulic Engineering 6:159-166.

Hanks, R.J. 1992. Applied Soil Physics: Soil Water and Temperature Applications.

Hayashi, M., G. van der Kamp, and D.L. Rudolph. 1998a. Water and solute transfer between a prairie wetland and adjacent uplands, 1. Water balance. Journal of Hydrology 207:42-55.

Hayashi, M., G. van der Kamp, and D.L. Rudolph. 1998b. Water and solute transfer between a prairie wetland and adjacent uplands, 2. Chloride cycle. Journal of Hydrology 207:56-67.

Hayashi, M., G. van der Kamp, and R. Schmidt. 2003. Focused infiltration of snowmelt water in partially frozen soil under small depressions. Journal of Hydrology 270:214-229.

Hillel, D. 1998. Environmental Soil Physics Academic Press, London.

Jackson, N.A., and J.S. Wallace. 1999. Analysis of soil water dynamics in an agroforestry system based on detailed soil water records from time-domain reflectometry. Hydrology & Earth System Sciences 3:517-527.

Jovanovic, N.Z., and J.G. Annandale. 1997. A laboratory evaluation of Watermark electrical resistance and Campbell Scientific 229 heat dissipation matric potential sensors. Water SA 23:227-232.

Jury, W.A., and R. Horton. 2004. Soil Physics. 6th ed. John Wiley & Sons Inc., Hoboken, NJ.

Kelleners, T.J., R.W.O. Soppe, J.E. Ayars, and T.H. Skaggs. 2004a. Calibration of capacitance probe sensors in a saline silty clay soil. Soil Science Society of America Journal 68:770-778.

Kelleners, T.J., R.W.O. Soppe, D.A. Robinson, M.G. Schaap, J.E. Ayars, and T.H. Skaggs. 2004b. Calibration of capacitance probe sensors using electric circuit theory. Soil Science Society of America Journal 68:430-439.

Kutilek, M., and D.R. Nielsen. 1994. Soil Hydrology Catena Verlag, Cremlingen-Destedt.

LaBaugh, J.W., T.C. Winter, and D.O. Rosenberry. 1998. Hydrologic functions of prairie wetlands. Great Plains Research 8:17-37.

Lundberg, A., and R.M. Johansson. 1994. Optical precipitation gauge - determination of precipitation type and intensity by light attenuation technique. Nordic Hydrology 25:359-370.

McCoy, A.J., G. Parkin, C. Wagner-Riddle, J. Warland, J. Lauzon, P. von Bertoldi, D. Fallow, and S. Jayasundara. 2006. Using Automated Soil Water Content Measurements to estimate Soil Water Budgets. Canadian Journal of Soil Science 86:47-56.

Meyboom, P. 1966. Unsteady groundwater flow near a willow ring in hummocky moraine. Journal of Hydrology 4:38-62.

Meyboom, P. 1967. Mass-transfer studies to determine the groundwater regime of permanent lakes in hummocky moraine of Western Canada. Journal of Hydrology 5:117-142.

Morgan, K.T., L.R. Parsons, T.A. Wheaton, D.J. Pitts, and T.A. Obreza. 1999. Field calibration of a capacitance water content probe in fine sand soils. Soil Science Society of America Journal 63:987-989.

Musters, P.A.D., and W. Bouten. 2000. A method for identifying optimum strategies of measuring soil water contents for calibrating a root water uptake model. Journal of Hydrology 227:273-286.

Oke, T.R. 1987. Boundary Layer Climates. 2nd ed. Routledge, New York.

Paltineanu, I.C., and J.L. Starr. 1997. Real-time soil water dynamics using multisensor capacitance probes: laboratory calibration. Soil Science Society of America Journal 61:1576-1585.

Paltineanu, I.C., and J.L. Starr. 2000. Preferential water flow through corn canopy and soil water dynamics across rows. Soil Science Society of America Journal 64:44-54.

Parsons, D.F., M. Hayashi, and G. van der Kamp. 2004. Infiltration and solute transport under seasonal wetland: bromide tracer experiments in Saskatoon, Canada. Hydrological Processes 18:2011-2027.

Phene, C.J., G.J. Hoffman, and S.L. Rawlins. 1971. Measuring soil matric potential in situ by sensing heat dissipation within a porous body: I. theory and sensor construction. Soil Science Society of America Proc 35:27-32.

Price, J.S., B.A. Branfireun, J.M. Waddington, and K.J. Devito. 2005. Advances in Canadian wetland hydrology 1999-2003. Hydrological Processes 19:201-214.

Reece, C.F. 1996. Evaluation of a line heat dissipation sensor for measuring soil matric potential. Soil Science Society of America Journal 60:1022-1028.

Ridolfi, L., P. D'Odorico, A. Porporato, and I. Rodriquez-Iturbe. 2003. Stochastic soil moisture dynamics along a hillslope. Journal of Hydrology 272:264-275.

Ritter, D.F., R.C. Kochel, and J.R. Miller. 2002. Process Geomorphology. 4th ed. McGraw Hill, Boston.

Scanlon, B.R., B.J. Andraski, and J. Bilskie. 2002. Miscellaneous methods for measuring matric or water potential, p. 643-670, *In* J. H. Dane and G. C. Topp, eds. Methods of soil analysis, Part 4, Physical Methods, Vol. SSSA Book Ser. 5. SSSA, Madison, WI.

Scott, H.D. 2000. Soil physics; agricultural and environmental applications Iowa State University Press, Ames.

Sevruk, B. 1996. Adjustment of tipping-bucket precipitation gauge measurements. Atmospheric Research 42:237-246.

Sevruk, B., and B. Chvila. 2005. Error sources of precipitation measurement using electronic weight systems. Atmospheric Research 77:39-47.

Si, B., and R.G. Kachanoski. 2003. Measurement of local soil water flux during field solute transport experiment. Soil Science Society of America Journal 67:730-736.

Si, B., R.G. Kachanoski, F. Zhang, G.W. Parkin, and D.E. Elrick. 1999. Measurement of hydraulic properties during constant flux infiltration: field average. Soil Science Society of America Journal 63:793-799.

Sloan, C.E. 1972. Ground-water hydrology of prairie potholes in North Dakota. Geological Survey Professional Paper 585-C.

Smith, R.L., and T.M. Smith. 2001. Ecology and Field Biology. 6th ed. Benjamin Cummings, Toronto.

Stahli, M., and D. Stadler. 1997. Measurement of water and solute dynamics in freezing soil columns with time domain reflectometry. Journal of Hydrology 195:352-369.

Starks, P.J. 1999. A general heat dissipation sensor calibration equation and estimation of soil water content. Soil Science 164:655-661.

Starr, J.L., and I.C. Paltineanu. 1998a. Real-time soil water dynamics over large areas using multisensor capacitance probes and monitoring system. Soil & Tillage Research 47:43-49.

Starr, J.L., and I.C. Paltineanu. 1998b. Soil water dynamics using multisensor capacitance probes in nontraffic interrows of corn. Soil Science Society of America Journal 62:114-122.

Starr, J.L., and D.J. Timlin. 2004. Using high-resolution soil moisture data to assess soil water dynamics in the vadose zone. Vadose Zone Journal 3:926-935.

Stoof, C. 2004. Soil hydraulic properties of landscape elements in a cultivated hummocky till in Southern Saskatchewan, Canada, Wageningen University, Wageningen.

van Wesenbeeck, I.J., and R.G. Kachanoski. 1988. Spatial and temporal distribution of soil water in the tilled layer under a corn crop. Soil Science Society of America Journal 52:363-368.

Vidon, P.G.F., and A.R. Hill. 2004. Landscape controls on the hydrology of stream riparian zones. Journal of Hydrology 292:210-228.

Walvoord, M.A., and F.M. Phillips. 2004. Identifying areas of basin-floor recharge in the Trans-Pecos region and the link to vegetation. Journal of Hydrology 292:59-74.

Ward, P.R., F.X. Dunin, S.F. Micin, and D.R. Williamson. 1998. Evaluating drainage responses in duplex soils in a Mediterranean environment. Australian Journal of Soil Research 36:509-523.

Western, A.W., S. Zhou, R.B. Grayson, T.A. McMahon, G. Bloschl, and D.J. Wilson. 2004. Spatial correlation of soil moisture in small catchments and its relationship to dominant spatial hydrological processes. Journal of Hydrology 286:113-134.

Williams, A.G., J.F. Dowd, D. Scholefield, N.M. Holden, and L.K. Deeks. 2003. Preferential Flow Variability in a Well-Structured Soil. Soil Science Society of America Journal 67:1272-1281.

Williams, J.R., Y. Ouyang, and J.S. Chen. 1998. Estimation of Infiltration Rate in Vadose Zone: Application of Selected Mathematical Models Vol. 2 EPA/600/R-97/128b. United States Environmental Protection Agency, Ada, OK.

Wilson, D.J., A.W. Western, and R.B. Grayson. 2004. Identifying and quantifying sources of variability in temporal and spatial soil moisture observations. Water Resources Research 40:W02507.

Wilson, D.J., A.W. Western, and R.B. Grayson. 2005. A terrain and data-based method for generating the spatial distribution of soil moisture. Advances in Water Resources 28:43-54.

Wilson, K.B., P.J. Hanson, P.J. Mulholland, D.D. Baldocchi, and S.D. Wullschleger. 2001. A comparison of methods for determining forest evapotranspiration and its components: sap-flow, soil water budget, eddy covariance and catchment water balance. Agricultural and Forest Meteorology 106:153-168.

Yang, D., B.E. Goodison, J.R. Metcalfe, V.S. Golubev, R. Bates, T. Pangburn, and C.L. Hanson. 1998. Accuracy of NWS 8" standard nonrecording precipitation gauge: results and application of WMO intercomparison. Journal of Atmospheric and Oceanic Technology 15.

Youngs, E.G. 1988. Soil physics and hydrology. Journal of Hydrology 100:411-431.

Zhuo, X., L. Wan, B. Fang, W.B. Cao, S.J. Wu, F.S. Hu, and W.D. Feng. 2004. Soil moisture potential and water content in the unsaturated zone within the arid Ejina Oasis in Northwest China. Environmental Geology 46:831-839.

CHAPTER 3.0
HYDROLOGIC RESPONSE TO SPRING SNOWMELT AND EXTREME RAINFALL EVENTS OF DIFFERENT LANDSCAPE ELEMENTS WITHIN A PRAIRIE WETLAND BASIN

3.1 Introduction

Understanding the effects of intense rainfalls within the prairie pothole region (PPR) is integral to determine contaminant transport potential within wetland depressions. The PPR covers extensive portions of North America, including the southern Canadian Prairies and portions of the Mid-Western United States. Depressions in these landscapes are commonly referred to as sloughs. They were formed during the most recent glacial retreat, approximately 10-17 kyrs ago, from melting ice blocks dropped by the retreating glacier (Sloan, 1972). Most importantly, these depressions are hydrologically isolated, as they are not permanently connected by surface inflow or outflow channels. As a result, prairie pothole depressions are the dominant source of groundwater recharge in the Canadian PPR (Hayashi et al., 1998a; Hayashi et al., 1998b; Hayashi et al., 2003).

The regional climate is characterized by long cold winters and hot, dry summers. Snowfall accounts for 24% of the 30-year average (1971 – 2000) precipitation reported at the Saskatoon International Airport (Environment Canada, 2008). Snowmelt is the predominant water source for these wetland basins. During snowmelt, soils are frozen, thereby reducing upland infiltration and increasing the movement of snowmelt water to depressions. The second contributor to ponding within wetland depressions is summer rainfall. During a typical rainfall, direct precipitation is the sole contributor to the wetland. Relatively unknown in the prairies, overland flow, may play a greater role than

previously thought. Overland flow is difficult to measure, but has been reported in previous prairie wetland studies (Hayashi et al., 1998a; Meyboom, 1966). Overland flow is dependent upon several factors, including the infiltration capacity of the soil, rate or volume of rainfall, and topography. If the rate of rainfall exceeds the soil's infiltration capacity and there is adequate topographic relief overland flow will occur. Antecedent water content, soil texture, structure, such as the presence of preferential flow paths, and the type of clay present concurrently determine a soil's infiltrability and direction of water redistribution within the profile. Generally, the infiltration capacity of a soil is high during the early stages of water application and decreases until it reaches steady state, or the soil's saturated hydraulic conductivity. Prior to reaching steady state, infiltration and redistribution is supply-controlled, but under steady state conditions the hydraulic properties of the soil control infiltration and redistribution (Hillel, 1998; Scott, 2000). Prairie overland flow events are rare, but can occur and may play a major role in the hydrologic function and cycle of prairie wetlands.

Overland flow results in the rapid movement of water, solutes, and sediments to lowland depressions. Rapid groundwater recharge and contamination could result from depressional ponding. At depth, glacial till on the Canadian Prairies has low hydraulic conductivity, resulting in low rates of groundwater recharge. Flow of groundwater is controlled by the jointed nature of the glacial till and the presence of lenses of stratified sand, silt, and gravel (Sloan, 1972). In a long-term conservative tracer (chloride) study in Saskatchewan, Dyck et al., (2003) determined the tracer infiltrated to a depth of 1.34 m four years after application. Thirty years after application, the tracer moved another 0.34 m. These authors report a drainage velocity of 11 mm yr^{-1} for the rooting zone and 3 mm

yr^{-1} below. Therefore, over the long-term there appears to be little connection between the soil water and groundwater. Alternatively, in locations with significant jointing or preferential flow paths the interactions can be significant. Parsons et al. (2004), using a bromide tracer, working at the St. Denis National Wildlife Area (NWA) Saskatchewan, Canada within wetland S109, found bromide present in piezometers beneath S109 at several meters depth within weeks of application of the tracer to the ponded water. Therefore, significant rainfall events could cause preferential flow to depth in short periods given the appropriate geologic stratigraphy. Preferential flow results in high rates of recharge in days to weeks, which long-term studies fail to capture. The majority of previous research has studied the annual water budget of prairie wetlands, effectively ignoring short-term events.

The hypothesis is that different landscape/ecological elements respond differently to snowmelt and extreme rainfall events. The objective of this chapter is to examine how different landscape/ecological elements respond to snowmelt and an extreme rainfall event. This objective is completed by tracking the hydrologic response of five unique landscape/ecological elements to the spring snowmelts of 2005 and 2006 and the rainstorm event of June 17-18, 2005 at the St. Denis National Wildlife Area (NWA) Saskatchewan, Canada (106°06'W, 52°02'N).

3.2 Materials and Methods

3.2.1 Field Site

The field study took place at the St. Denis National Wildlife Area (NWA) Saskatchewan, Canada (106°06'W, 52°02'N), focusing on a single wetland, S118 (Figures 3.1 and 3.2). The upland surrounding the wetland was recently (summer 2004) seeded to a mixed grass permanent cover. S118 is ~1400 m^2, with a total catchment basin of 11

000 m^2. Based on the low salinity of the pond sediments, measured indirectly by time domain reflectometry (TDR probes), S118 is a recharge wetland.

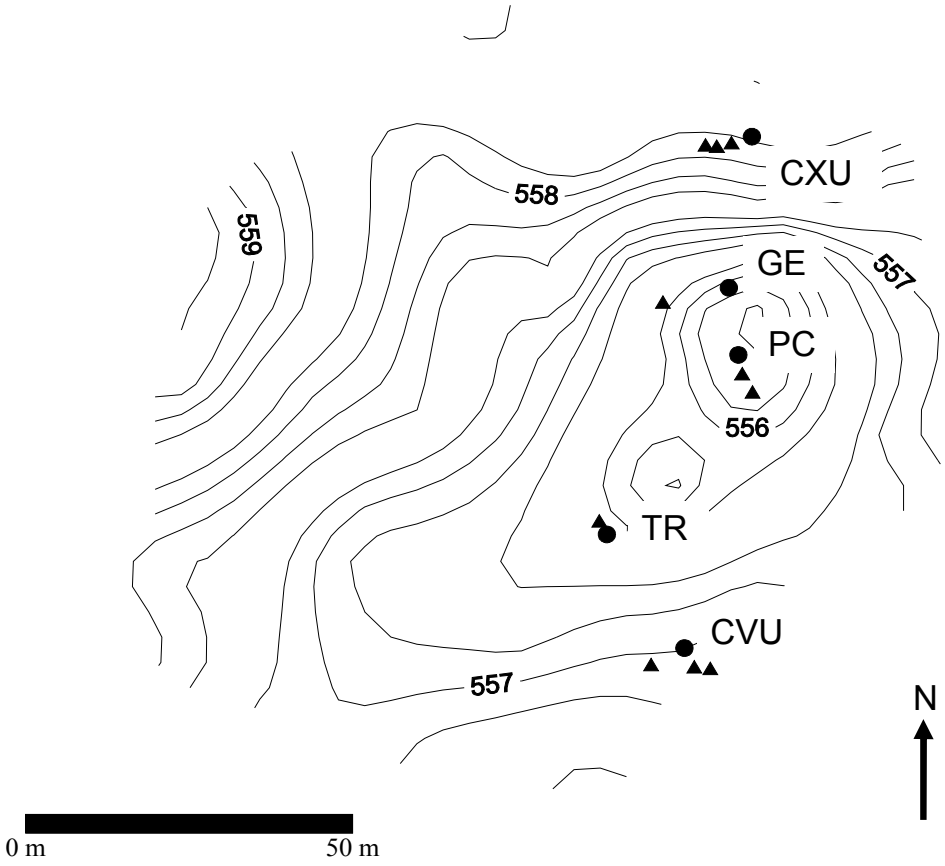

Figure 3.1. Topographic map of the study site. Land elements include Convex Upland (CXU), Grassed Edge (GE), Pond Center (PC), Tree Ring (TR), and Concave Upland (CVU). The locations of the meteorological and soil instruments are represented by the solid circles, while the locations of the piezometers are represented by the solid triangles.

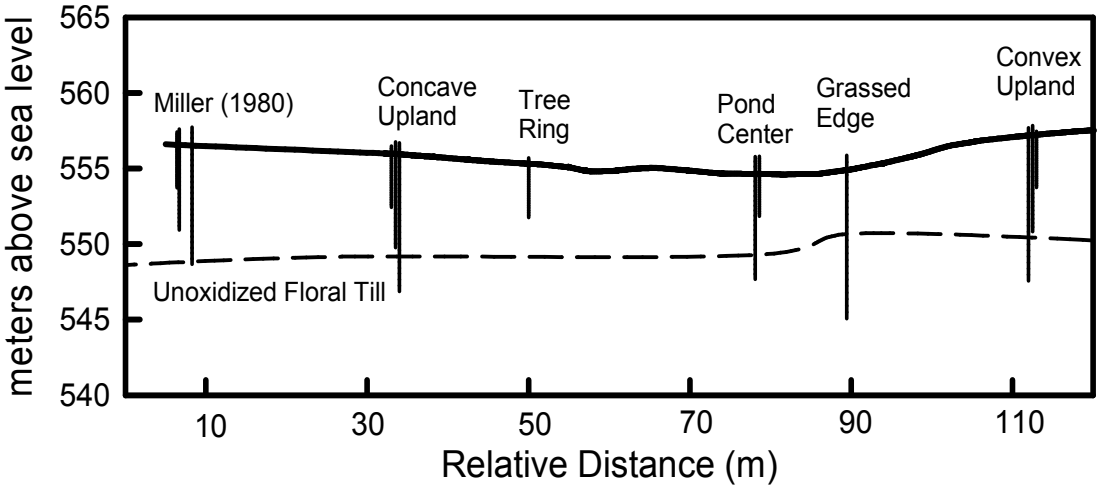

Figure 3.2. Cross-section of S118, presenting the distance between stations and the relative elevation of each piezometer, including three of four piezometers installed by Miller in 1980. The fourth Miller piezometer is not included as available location data is incomplete.

Overall, the site is typical of the rolling topography of the PPR. The area is characterized by a semi-arid continental climate. Based on the 30 year averages at the Saskatoon Airport from 1971-2000 (Environment Canada, 2008), the temperatures for five months of the year are below the freezing mark. The mean annual precipitation is approximately 365 mm with 97.5 mm as snowfall. Spring snowmelt is the dominant water source for wetland depressions, with 30 – 60% of upland snowmelt running off into the wetlands (Hayashi et al., 1998a), determined at S109. S109 is located approximately 100 meters southwest of S118. Rainfall on the site is variable and summer storms are relatively uncommon. Over the 30-year mean for the Saskatoon International Airport (1971 – 2000) approximately 1 day per summer (June – September) receives a rainfall that exceeds 25 mm (Environment Canada, 2008).

The soils are highly variable in both texture and genesis. The variability in soil development and texture lies in the glacial history and redistribution of water over the rolling landscape (Miller et al., 1985). The study site was divided into five distinctive

landscape elements, including pond centre (PC), grassed edge (GE), tree ring (TR), and two uplands, which were classified based on micro-topography, a concave upland (CVU) and convex upland (CXU). The soil of the five landscape elements were classified in the following manner and are described in detail in Table B1 of Appendix B. The PC and GE are subject to annual inundation in the spring, resulting Gleysolic soil development. The PC soil is classified as an Orthic Humic Gleysol, resulting from the alternating reducing and oxidizing state of the soil and the development of a thick Ah-horizon (0.50 m). The GE is classified as a Humic Luvic Gleysol, due to the alternating oxidizing and reducing conditions, but this profile has a distinct accumulation of clay from 0.65 – 1.20 m. Bedard-Haughn et al., (2006) identified that wetlands on this site, including S118, commonly have buried finely textured sediment tongues from past erosional events. TR soils, owing to the presence of woody vegetation and seasonal inundation have been classified as an Orthic Dark Grey Chernozem. In the past, this wetland was cultivated for crop production. Prior to the settlement of the Canadian prairies wild fires commonly destroyed woody vegetation, leading to the grassland Chernozemic soil formation. The uplands surrounding the wetland were used in agricultural production until 2004. They were home to similar vegetative communities throughout history. Due to differences in slope, relative elevation, micro-topography, and ultimately water redistribution, different soils have formed at each upland location. The CVU developed a Gleyed Calcareous Dark Brown Chernozem. The soil is a productive grassland soil, but the slight gleying indicates that this location was historically inundated by water from S118. Alternatively, the CXU at a higher elevation, greater slope, and therefore reduced plant productivity,

has resulted in poor soil development and the classification of the soil as an Orthic Regosol. All soils found within S118 are consistent with Miller et al., (1985).

In an intensive study of S118, Stoof, (2004) used both a tension and double ring infiltrometer to determine the variability of surface porosity and saturated hydraulic conductivity of landscape elements. In terms of porosity, the highly organic pond elements have the highest mean total porosity and macroporosity, while the upland positions, with much greater mineral elements and greater anthropogenic influence, have considerably lower porosities. When looking at the micro and mesoporosities, there is a smaller variation, with the majority of the landscape elements at approximately 40%, the pond center is again slightly higher, at > 50%. Regarding saturated hydraulic conductivity, as expected the pond elements, including the PC, GE, and TR have conductivities two orders of magnitude larger than those of the uplands. For example, the conductivity determined with a double ring infiltrometer for an upland position is $5.3x10^{-6}$ m s^{-1}, while in the PC is $1.0x10^{-4}$ m s^{-1}. Therefore, lowlands have considerably higher surficial infiltrability. In addition, the shape, or micro-topography, of cultivated landscape was found to be an important factor in soil development and potential infiltrability. Concave cultivated elements were identified as having thicker A-horizons, higher porosity, field saturated hydraulic conductivity, and surface residue than convex cultivated elements. These findings indicate concave cultivated soils retain greater volumes of water, are more productive. As a result, of this increase in organic matter root channels develop greater infiltrability than the convex upland elements.

Tills below the vadose zone are high in clay content and are jointed and fractured to ~6 m, the zone of oxidation (Hayashi et al., 1998a; Miller et al., 1985). The site is

underlain by the Battleford Till Formation, 5 – 15 m deep, which overlies the Floral Till Formation. Miller et al., (1985) thoroughly describes the site's geologic stratigraphy. The zone of oxidation is important regarding the movement of groundwater. Hydraulic conductivity of the upper 6 m of sediment is several orders of magnitude larger than below the zone of oxidation (Hayashi et al., 1998a; Hayashi et al., 1998b; Hayashi et al., 2003; Miller et al., 1985).

A brief survey of the vegetation within S118 was completed on July 25, 2005 to determine the dominant species at each landscape position. The upland positions were seeded in the summer of 2004 with the following: tall wheatgrass (*Agropyron elongatum*), intermediate wheatgrass (*Agropyron intermedium*), meadow bromegrass (*Bromus biebersteinii*), dahurian wild ryegrass (*Elymus dauricus*), creeping red fescue (*Festuca rubra*), sainfoin (*Onobrychis viciifolia*), Canadian wild rye (*Elymus canadensi*), slender wheatgrass (*Agropyron trachycaulum*), and alfalfa (*Medicago sativa*). In addition to the seeded species, several weed species were also found within the upland positions. These included, sow thistle (*Sonchus arvensis*), foxtail barley (*Hortium jerbatum*), canada thistle (*Cirsium arvense*), and an unidentified vetch species. The TR was dominated by trembling aspen (*populus tremuloides*), the largest tree and willow (*Salix discolor*), the most abundant. In addition to the tree species, the floor of the TR was covered with brome grass (*Bromus Sp*), along with quack grass (*Agropyron repens*), and several *Salix Sp*. The dominant vegetation of the GE was quack grass and a small amount of brome grass. In addition, there was a small amount of water smartweed (*Rumex amphibium*), from the PC. PC vegetation is highly dependent on the pond levels. On July 25, water was ponded and the dominant species were water smartweed,

Ranunculs Sp, and *Carex atherodes*. These species thrive while the pond is flooded, but decline once surface water recedes. On August 28, following the drainage of the pond, the PC and GE had very similar vegetative communities.

3.2.2 Field Methods

3.2.2.1 Precipitation, Pond Depth, and Volume

Precipitation at the site was monitored approximately 200 m to the north-west of S118. Two tipping bucket (TB) rain gauges were connected to separate dataloggers, recording hourly precipitation values. The measurements from each of the gauges were averaged together to reduce measurement error and eliminate extraneous values.

Pond depth was measured using a SR-50 Sonic Ranging Sensor produced by Campbell Scientific. The SR-50 was attached to a solid wooden post within the PC and was connected directly to a datalogger. The accuracy of the sensor is ± 1 cm, with a resolution of 0.1 mm. Travel velocity of the ultrasonic pulse is temperature dependent and corrections were made automatically on site. A thermistor housed within a gill shield recorded the air temperature. These air temperatures were used in the thermal correction. Converting the depth of water to a volume was completed using an equation developed from the catchment digital elevation model (DEM). The equation is as follows (Pennock, personal communication).

$$Volume = 958Depth^2 - 175Depth \tag{3.1}$$

Depth and volume for Eq. 3.1 are reported in meters and cubic meters. The equation is invalid for depths < 0.184 m. This is not a concern as there is relatively little water in the wetland at depths below 0.20 m and these volumes are inconsequential in the overall water balance of the wetland basin.

3.2.2.2 Vadose Zone

Volumetric water content was monitored using both TDR and capacitance sensors. The EnviroScan® (Sentek PTY, Ltd., Kent Town, South Australia) capacitance probes were installed using a Giddings Punch and sampling tube in late summer of 2004. These sensors provide real-time water content measurements and allow examination of soil water dynamics in very short time periods. A core was punched to approximately 2 m and the samples were broken into 0.10 m samples for gravimetric water and textural analysis using standard hydrometer methodology. Following the removal of the core, the Enviroscan access tube was inserted in the hole and the center of the tube cleaned of debris. The sampling core was smaller diameter than the access tube of the capacitance sensors, ensuring a tight fit and consistent contact between the outside of the tube and soil. Each of the sensors on the rail of the Enviroscan system measures a volume of soil, 0.10 m in length with a radius of 0.10 m surrounding the access tube. CXU and TR sensors were placed along the probe rail every 0.10 m for the upper meter and every 0.20 m below one meter. CVU sensors were located every 0.10 m to a depth of 0.60 m and every 0.20 m for the remainder. Data for missing depths was interpolated based on measurements above and below the missing depth. The PC and GE had recently drained of water from the spring snowmelt at the time of the rainfall event. Probes were not returned to these positions before the rainfall induced inundation of the pond. Therefore, there are no water content measurements for PC and GE during the rainfall of June 17 – 18, 2005. All capacitance sensor measurements were recorded hourly by dataloggers. These measurements are highly dependent upon soil density and texture (Geesing et al., 2004; Paltineanu and Starr, 1997). Therefore, they were scaled to real volumetric water contents using manual TDR measurements.

TDR is widely accepted and commonly used in water balance, soil water dynamics studies, and other research (Gomez-Plaza et al., 2001; Jackson and Wallace, 1999; Musters and Bouten, 2000; Si and Kachanoski, 2003; Stahli and Stadler, 1997; van Wesenbeeck and Kachanoski, 1988). TDR probes were installed horizontally at depths of 0.05, 0.15, 0.30, 0.50, 0.70, 0.85, 1.05, 1.25, 1.50, and 1.85 m in a soil pit in close proximity to the capacitance probe, providing a robust method of calibration. Manual measurements of the TDR arrays were done using a Tektronix 1502 - B cable tester on a semi-biweekly basis during the growing seasons of 2005 and 2006. TDR and capacitance sensor measurements were pooled and linear regression was used to develop an equation to scale raw capacitance readings to volumetric water content determined with the TDR probes. A unique equation was required for each capacitance sensor. Unfortunately, high salinity levels prevented the function of CXU volumetric water content sensors past a depth of 0.85 m. No laboratory analysis was completed to confirm salinity, but below 0.85 m the TDR wave measured with the Tektronix 1502 - B cable tester had no reflection, indicating the presence of excessive soil salts. Excessive upland soil salts were also found on the site by previous researchers (Hayashi et al., 1998b; Berthold et al., 2004). Due to the high soil salinity, analysis of the CXU required a water retention curve to provide analysis below 0.5 m. The water retention curve derived from the CXU volumetric water content and matric potential measurements at 0.3 m depth. The water retention curve is described in Eq. 3.2.

$$\theta = b + (0.43 - b)(1 + (\alpha\psi 1000)^n)^{(-1+1/n)} \tag{3.2}$$

where, θ is the predicted volumetric water content, ψ is the measured matric potential, and α, b, and n are fitting parameters equal to 6.27×10^{-3}, 0.0, and 1.205, respectively.

Rainfall and snowmelt infiltration and redistribution was calculated using the soil water balance approach for each 0.10 m segment within the instrumented 2.0 m profile. In this manner, water infiltrating and moving through the soil profile was tracked over time and depth. Cumulative infiltration was calculated using Eqs. 3.3 and 3.4 to determine the proportion of available water entering the soil and the depth of redistribution at each landscape location.

$$I = \int_0^{z_f} \Delta\theta dz \tag{3.3}$$

$$I = \int_{t_1}^{t_2} i(t) dt \tag{3.4}$$

where, z_f is the depth of the wetting front, $\Delta\theta$ is the change in water content over that depth, and t_1 and t_2 are the initial and final times of infiltration (Scott, 2000). The cumulative infiltration was compared to the cumulative precipitation rainfall event to determine the location and magnitude of overland flow. This method assumes one-dimensional flow, meaning that run-on and lateral flow are minimal or non-existent, and rainfall was uniform across the catchment.

Soil matric potential was monitored bi-hourly at each location using eight CS-229 heat dissipation sensors. These sensors were installed at depths of 0.05, 0.15, 0.30, 0.50, 0.85, 1.05, 1.50, and 1.85 m into the uphill face of the pit used for TDR installation. Due to the delicate nature of the ceramic, holes were drilled into the face of the pit to provide a point of installation.

Matric potential sensor calibration was completed in a manner similar to Starks, (1999). Calibration involved a general calibration equation with a tension table and

pressure plate apparatus. Five of the forty probes installed were packed into an 80 cm^3 soil core and the change in temperature over 30 seconds was measured at the following tensions: 0, -0.002, -0.003, -0.005, -0.007, -0.008, -0.0085, -0.01, -0.3, -0.5, -0.8, and -1.5 MPa. Data from these five sensors was pooled and plotted to determine the relationship between the normalized change in temperature over 30 seconds and matric potential. The data was curve fit, with an R^2 value of 0.90. This procedure was used to develop the following equation:

$$\ln(-\psi) = -7.6983 + 9.1282\left(\frac{\Delta T30}{\Delta T_{Dry}}\right) \tag{3.5}$$

Field matric potential is calculated for each of the sensors using the above equation.

To monitor freeze and thaw cycles on the site, soil temperature probes were installed at 0.15, 0.30, 0.50, and 0.70 m. All vadose zone instrumentation, with the exception of the TDR probes, was monitored with CR10X dataloggers. Frequent trips were made to the field to download data and to ensure the proper operation of the equipment.

3.2.2.3 Snow Survey

Snow surveys were competed in late winter 2005 and 2006, prior to the initiation of snowmelt. A 69 mm diameter aluminum snow survey tube was used to collect samples at a representative number of locations. Additional depth measurements were determined using an aluminum meter stick. Snow water equivalent (SWE) was determined in the field based on the snow density calculated from the mass and volume of snow collected at each of the sample sites. The 2005 survey was carried out in conjunction with another research project on the same field site. The data from this adjacent research is available for statistical purposes only. The 2006 survey focused solely on wetland S118.

The 2005 survey was completed on March 4 (day of year (DOY) 63). This survey was limited for wetland S118 as only five sampling points were completed, one at each of the instrumented locations. Statistical relationships are derived from the adjacent research where 235 depth measurements and 118 snow samples were taken. In 2006, the snow survey measurement density was greatly increased within wetland S118. Two hundred snow depths were measured within wetland S118's catch basin. Snow density was based on a single measurement at each of the instrumented locations on March 29, 2006 (DOY 88). The 2005 snow survey results are highly variable with large standard deviations. The majority of these measurements were taken from two transects crossing a variety of landscape elements. The coarse classification of this into upland and wetland is likely the cause of the large variability in the data. Alternatively, the 2006 survey data is separated into four landscape positions, representative of a relatively small area.

3.2.2.4 Snowmelt Infiltration

Snowmelt infiltration was determined by integrating the cumulative infiltration, using Eq. 3.3 from the fall of 2004 and 2005, and the spring of 2005 and 2006. This method assumes minimal losses of soil water and negligible snowmelt infiltration during the winter season. Soil temperature sensors, installed at depths stated above, were used to determine the depth and time of soil thawing. Variability in soil density, texture, and water content causes distinct thermal properties, resulting in soils freezing and thawing at different rates. Therefore, soil volumetric water content measurements were taken on different dates at each landscape position.

Snowmelt infiltration for the two snowmelt seasons on the CXU was determined using volumetric water content measurements from November 12, 2004 (DOY 317) compared to April 12, 2005 (DOY 102) and November 7, 2005 (DOY 311) compared to April 14,

2006 (DOY 104). Water content measurement dates for the CVU included November 22, 2004 (DOY 327) compared to April 7, 2005 (DOY 97) and November 25, 2005 (DOY 329) compared to April 14, 2006 (DOY 104). Volumetric water content readings were collected to the depth where volumetric water content was unchanged. Soil temperature sensors were used to ensure that soils thawed on all spring dates and the depth of water infiltration was verified by the matric potential CS-229 sensors. In addition, spring water content measurement dates were confirmed by visual inspection of snowmelt with photographs taken. Due to the inundation of the lower elevations, snowmelt infiltration of TR, PC, and GE landscape positions could not be determined.

3.2.2.5 Groundwater

Groundwater within wetland S118's catchment was monitored with piezometers at each landscape position. Piezometers were installed in the fall of 2004. 3, 6, and 9 m piezometers were installed at the CVU site and a 9 m piezometer was installed at the GE site. The remainder of the piezometers, 3, 6, and 9 m on the CXU and 4 m in the TR, were installed in the fall of 2005. All drilling was completed with a 0.10 m diameter solid stem auger. PVC pipe with a 0.052 m inside diameter was used for the instrument casing. Screen length was 1.0 meter, with 1.4 m sand pack. The remainder of the hole was backfilled with bentonite chips. Piezometers in the PC were installed by previous researchers at depths of 4 and 8 m. Installation procedures are described by Miller et al. (1985). Drilling was completed with a 0.152 m diameter auger, silica sand was placed around the intakes screens and bentonite pellets and clay was used to backfill the hole above the screen. All piezometers were measured manually at intervals of one week to one month. During the rainfall of June 17 – 18, 2005, piezometers were not installed at the TR and CXU locations. On these dates, the TR capacitance probe determined that the

soils were saturated 1.2 m from the ground surface. This is likely the depth to the water table as the PC piezometers, at a similar elevation, indicated the water was just below surface.

During the fall and winter of 2005, slug tests were completed on all of the groundwater instruments. The results are detailed in Table 3.1. Tests were carried out using a solid slug submerged into a static piezometer. Following the introduction of the slug, the head drawdown and time were measured and recorded using a pressure transducer connected to a datalogger. Pressure transducer measurements were taken

Table 3.1. Results of Slug Tests, carried out during the winter of 2005 - 2006.

Landscape Position	Piezometer Depth (m)	K_s (m s^{-1})	Lag Time (hrs)
Convex Upland	6	1.74×10^{-8}	12.50
	9	1.60×10^{-9}	135.45
Grassed Edge	9	1.37×10^{-7}	1.58
Pond Center	8	3.58×10^{-7}	0.60
Tree Ring	4	3.09×10^{-6}	0.07
Concave Upland	6	2.40×10^{-6}	0.09
	9	1.54×10^{-9}	140.85

at 30 second intervals and averaged over two minutes. Saturated hydraulic conductivities were calculated using the Hvorslev (1951) time lag methodology Saturated hydraulic conductivity of the shallow piezometers (4 - 6 m), screened within the oxidized till, ranged between 10^{-6} m s^{-1} to 10^{-8} m s^{-1}, while the deeper piezometers (8 - 9 m), screened within the unoxidized till, provided conductivity values in the range of $10^{-7} – 10^{-9}$ m s^{-1}. These values are similar to those found by other researchers working on the site (Hayashi et al., 1998a; Hayashi et al., 1998b; Miller et al., 1985). The lag time presented in Table

3.1, indicates that the oxidized till measured with the shallow piezometers will react quickly to changes in pore water pressure, from minutes to hours. In contrast, the deep upland instruments within unoxidized till require more than 5 days to react to potential increases or decreases in water levels surrounding the instrument.

3.3 Results and Discussion

3.3.1 Wetland Response due to Snowmelt

3.3.1.1 Snowmelt 2005

Snowmelt began in late March of 2005. The first recorded mean daily air temperature above freezing was on March 28, 2005 (DOY 87). The pond reached its maximum depth ten days later, indicative of a rapid snowmelt. Upland soils remained frozen (data not shown) throughout the melt period, reducing the infiltrability of these soils and increasing runoff to the pond.

The results of the 2005 snow survey are presented in Table 3.2. Too few data were within the catch basin of S118 to perform any statistical analysis. Fortunately, the 2005 snow survey was completed in conjunction with another on-site snow survey in a much larger field where S118 is located. The additional data point SWE standard deviation is applied to the S118 data to provide an indication of the variability in the snow survey results. This additional data was coarsely grouped into upland and wetland data. The upland SWE standard deviation of the field is applied to the S118's CXU and SU, while the wetland data standard deviation of the field snow survey is representative of S118's GE, PC, and TR. This provides a mean SWE for the uplands within S118 of 48.93 mm with a standard deviation of 23.1 mm. The SWE in the wetland landscape

Table 3.2. Results of 2005 Snow Survey of the Catch Basin of S118.

Landscape Position	No. Sample Points	Mean Depth (cm)	Density (g cm^{-3})	Snow Water Equivalent (SWE) (mm)	SWE – Standard Deviation
*Upland	171	31.6	0.229	72.36	23.1
*Wetland	64	40.4	0.227	91.71	32.4
Uplands	2	21	0.233	48.93	N/A
Grassed Edge (GE)	1	70	0.354	247.8	N/A
Pond Center (PC)	1	32	0.181	57.92	N/A
Tree Ring (TR)	1	36	0.242	87.12	N/A

* Data collected for other research in a much large area (much larger than S118) in the field and therefore had a much larger standard deviation than snow survey of 2006 for S118 only. The upland and wetland snow data were used exclusively for statistical analysis in the 2005 snow survey

positions were substantially higher. The measured SWE for the GE was 247.8 mm, the PC was 57.92 mm, and the TR was 87.12 mm. The wetland, 32.4 mm, standard deviation is applied to these three lowland locations. The coarse classification of the data for statistical analysis into upland and wetland of the large field survey is likely the cause of the large variability in the data. The data provided was too coarse to be refined any further.

Eq. 3.1 was used to estimate the snowmelt water captured within S118 from the spring snowmelt. The maximum estimated pond volume is approximately 535 m^3 on April 7, 2005 (DOY 97). Air temperatures were used in conjunction with PC SR-50 depth measurements to ensure that the pond was no longer frozen. Figure 3.3 shows the response of the pond to direct snowmelt from the TR, GE, and PC and runoff from the surrounding uplands.

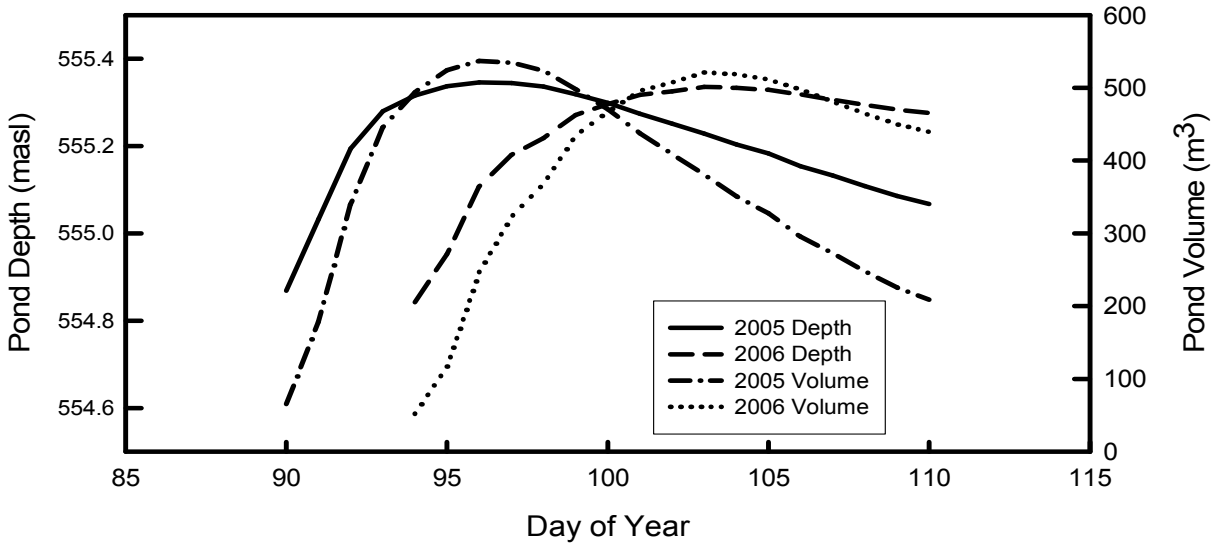

Figure 3.3. Pond volume and depth of snowmelt for 2005 and 2006.

Upland snowmelt infiltration was measured by the cumulative increase in volumetric water content, using Eq. 3.3 to a depth of 0.60 meter. Soil water content profiles for the CVU from November 22, 2004 (DOY 327) and April 7, 2005 (DOY 97) and November 12, 2004 (DOY 317) and April 12, 2005 (DOY 102) for the CXU are presented in Figure 3.4. Cumulative infiltration from snowmelt in spring 2005 was ~56 mm for the CVU site and ~ 47 mm for the CXU site. Snowmelt is the greatest single contributor to ponding and as a result is the greatest contributor to seasonal and long-term groundwater recharge (Hayashi et al., 1998a). Piezometers respond quickly in the PC as the spring water table is close to the surface and instrument lag times are relatively small (Table 3.1). GE and PC reach their maximum potentials on May 19 (DOY 139) and May 3 (DOY 123), respectively. Figure 3.5 a) and b) illustrates that GE-9 was not directly connected to pond water level, while the piezometric surface of the PC is the pond itself. This may

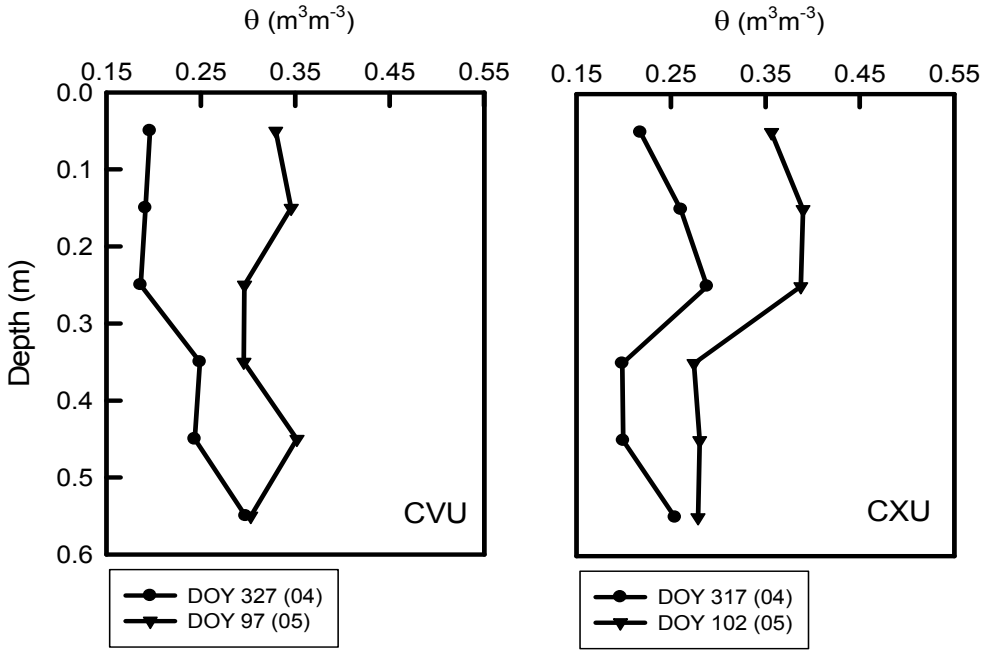

Figure 3.4. Upland soil water profiles for fall of 2004 compared to spring 2005.

indicate the presence of a mounded water table, where the water table within the basin is at a greater potential than the surrounding areas of higher elevation. The shallow PC-4 piezometer drops 0.5 m by June 15 (DOY 166). In contrast, PC-8 and GE-9 fluctuate very little until May 19 (DOY 139). PC-4 is embedded in the oxidized till, while the deep piezometers in both the PC and GE are screened in the un-oxidized layers with considerably lower saturated hydraulic conductivities, as described in Table 3.1. Regarding the upland water table, spring 2005 found CVU-3 dry until mid-summer, July 5 (DOY 186). The deeper installations, CVU-6 and CVU-9, gained potential early in the spring and were sustained by the lateral movement of water from the mounded water table. Lateral movement from focused pond center infiltration is typical of these wetlands during the spring and early summer (Miller et al., 1985).

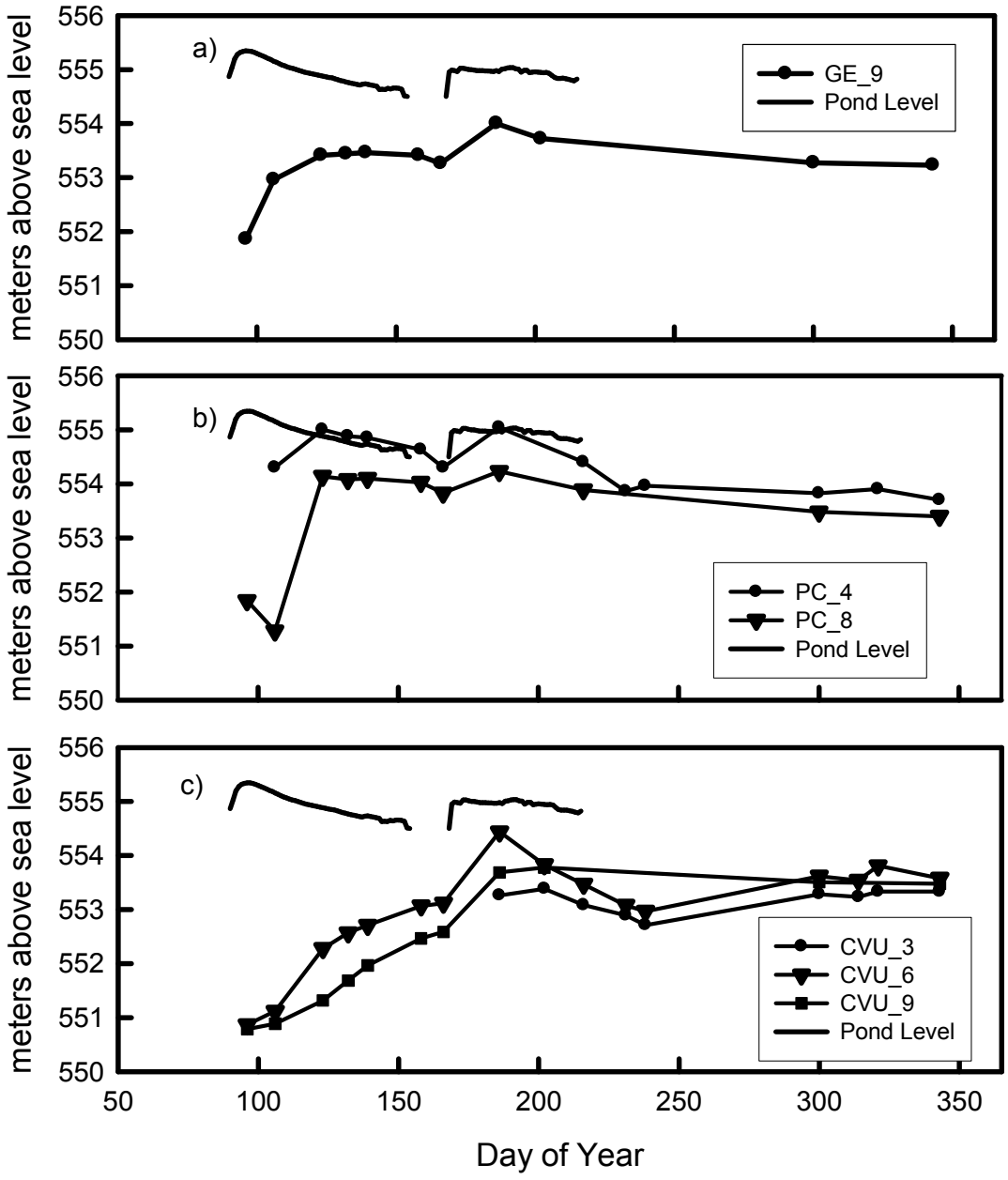

Figure 3.5. Groundwater levels for 2005. a) Grassed Edge (GE), b) Pond center (PC), and c) Concave Upland (CVU). June 15 corresponds to DOY 166 and July 5 corresponds to DOY 186.

3.3.1.2 Snowmelt 2006

Spring snowmelt in 2006 began in early April. The first recorded mean daily air temperature above zero degrees Celsius was on April 2, 2006 (DOY 94). Just as in 2005, upland soils were frozen throughout the snowmelt period (data not shown). Therefore, upland infiltration was reduced and overland flow to the pond occurred. The PC SR-50 depth gauge measured the depth of water within the pond and Eq. 3.1 was used to convert water depths to pond volumes. The maximum estimated pond volume from snowmelt is approximately 520 m^3 on April 13, 2006 (DOY 103). Air temperatures were used in conjunction with PC SR-50 depth measurements to ensure that the pond was no longer frozen. Figure 3.3 illustrates the response of the pond to direct snowmelt from the PC, TR, and GE and upland snowmelt runoff.

The result of the 2006 snow survey is presented in Table 3.3. Sampling density was increased substantially from the 2005 survey to ensure that statistical relationships could be drawn from the S118 specific snow survey data. In late winter of 2006, the SWE for the uplands was 94.41 mm with a standard deviation of 3.29 mm. The measured SWE for the GE was 190.07 mm with a 7.04 mm standard deviation. The PC SWE was 183.87 mm with a 5.86 mm standard deviation, and the TR SWE was 24.53 mm with a 4.86 mm standard deviation. The S118 landscape position standard deviations are substantially lower than the general site standard deviations used in the 2005 survey. The 2005 statistical relationships are drawn from the entire site with multiple wetlands and uplands. In contrast, the 2006 statistics are drawn from data that is solely representative of S118.

Table 3.3. Results of 2006 Snow Survey.

Landscape Position	No. Sample Points	Mean Depth (cm)	Density (g cm^{-3})	Snow Water Equivalent (SWE) (mm)	SWE – Standard Deviation
Upland	95	39.8	0.271	94.41	3.29
Grassed Edge (GE)	16	50.2	0.379	190.07	7.04
Pond Center (PC)	55	53.8	0.342	183.87	5.86
Tree Ring (TR)	34	56.8	0.432	24.53	4.86

Upland (including CXUs and CVUs) snowmelt infiltration was calculated by determining the increase in volumetric water content from the fall of 2005 to the spring of 2006, using Eq. 3.3 to a depth of 0.50 meter. Volumetric water content measurements were completed with capacitance probes at both upland landscape positions. Soil water content profiles are described in Figure 3.6. CXU water content measurements from November 7, 2005 (DOY 311) were compared to April 14, 2006 (DOY 104). Water content measurements dates for the CVU included November 25, 2005 (DOY 329) compared to April 14, 2006 (DOY 104). 2006 snowmelt infiltration is estimated at approximately 36 mm and 41 mm on the CXU and CVU, respectively. The 2006 cumulative infiltration was reduced from 2005, even though the maximum spring pond levels were nearly equivalent.

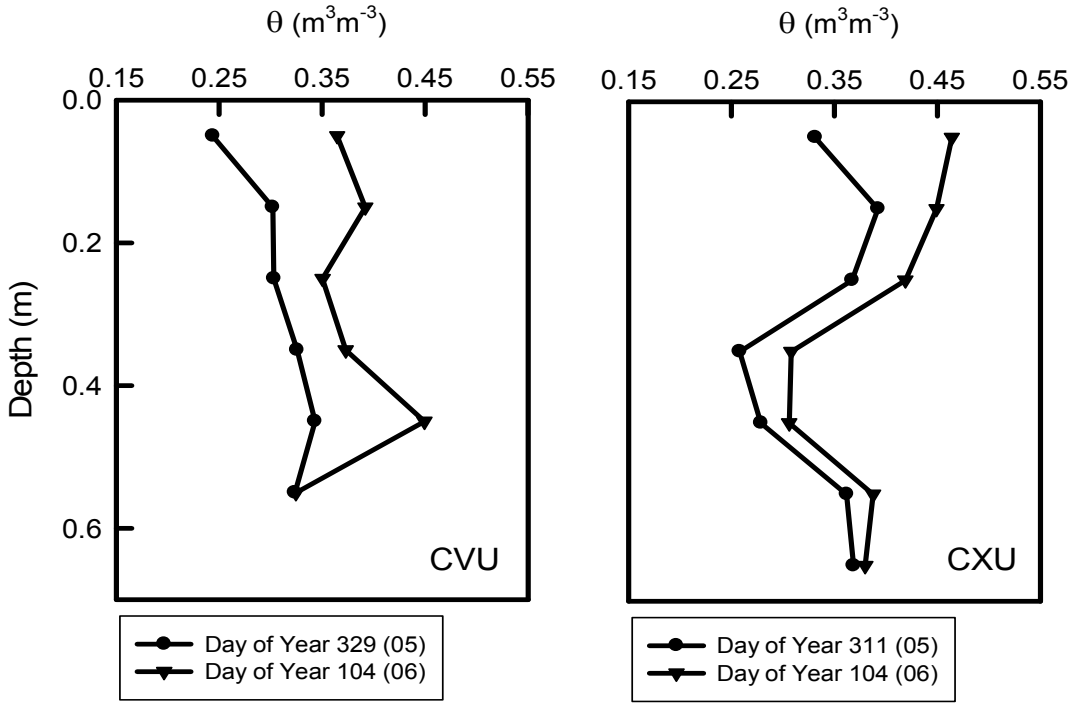

Figure 3.6. Upland soil water profiles for fall 2005 compared spring 2006.

Groundwater response during the growing season of 2006 is described by Figure 3.7. Piezometers within the PC and TR are directly connected to the pond rise and fall. They respond to snowmelt very rapidly, reaching their seasonal maximums shortly after the completion of snowmelt. Shallow piezometers, PC-4 and TR-4, were measured at their maximum values on April 19 (DOY 109) and were equipotential to the ponded surface water on April 28 (DOY 118). PC-4 water level dropped at 9.93 mm d^{-1} nearly the same rate as the pond, at 7.87 mm d^{-1} throughout the pond inundation, April 28 (DOY 118) – July 30 (DOY 211). TR-4 dropped at a rate of 3.76 mm d^{-1} until surface waters drained from the treed area on June 2 (DOY 153), nearly identical to the ponded water drop at 3.36 mm d^{-1}. Following draining of water from the TR, TR-4 water levels dropped at 26.9 mm d^{-1} from June 2 (DOY 153) – July 30 (DOY 211), more than twice as

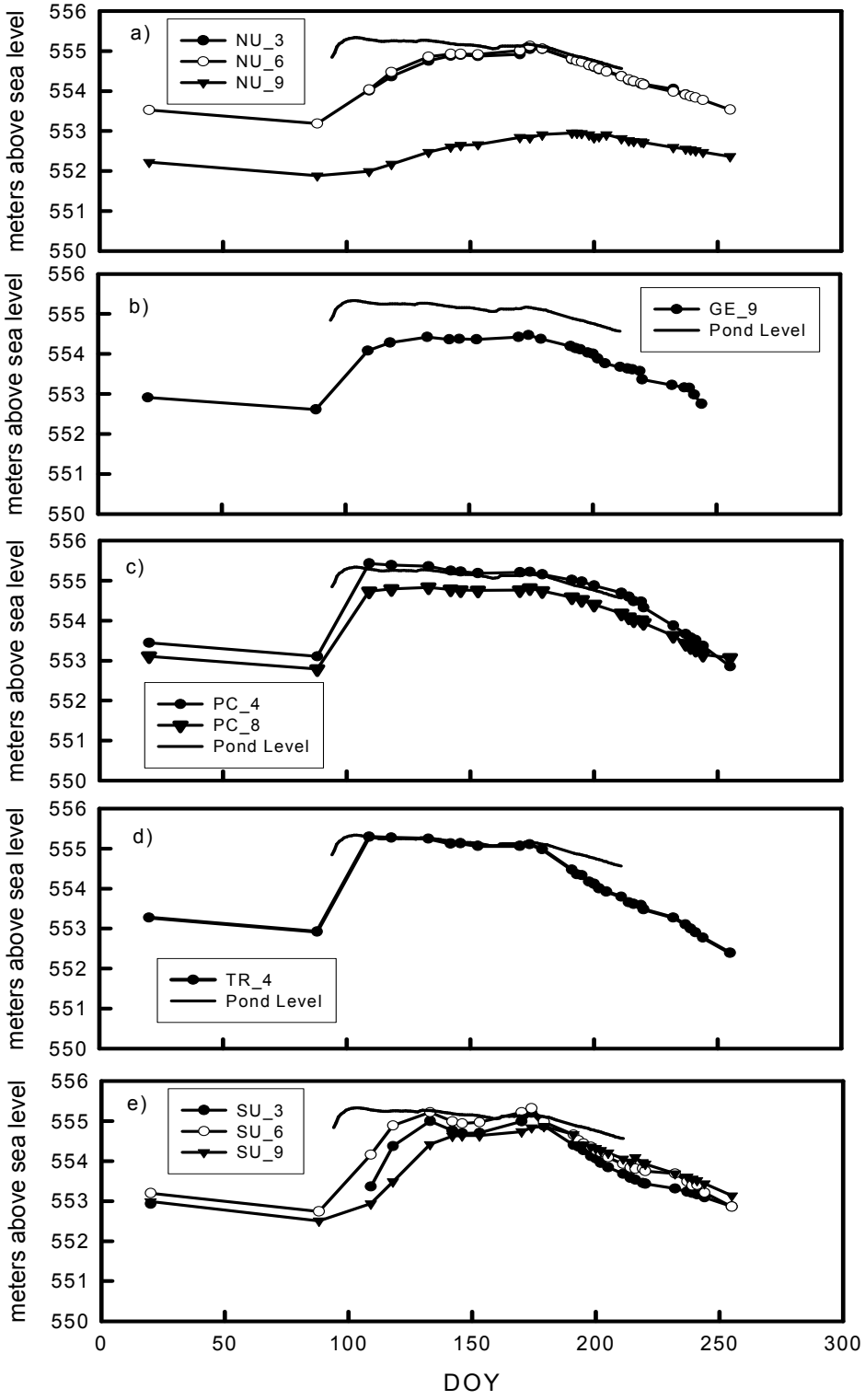

Figure 3.7. Groundwater levels for 2006. a) Convex Upland (CXU), b) Grassed Edge (GE), c) Pond Center (PC), d) Tree Ring (TR), and e) Concave Upland (CVU).

fast as the 11.06 mm d^{-1} decline of the pond. The rapid decrease of TR water levels coincides with increasing rates of evapotranspiration of under-story grass and trees.

GE-9 piezometer measurements are not directly linked to the pond water levels, although the rise and fall of the pond surface and GE-9 water level have the same general trends. Upland groundwater response lags behind the lowlands, just as in 2005. CXU piezometers reach their maximum values on the following: CXU-3 and CXU-6 on June 23 (DOY 174), and CXU-9 on July 10 (DOY 191). While the CVU ground water reaches its highest potential on May 13 (DOY 133) for CVU-3 and CVU-6 and June 28 (DOY 179) for CVU-9. These late rises in the upland piezometric surface supports the theory of lateral flow from the mounded water table beneath the pond, meaning the increases in the upland water table are moving laterally from below the wetland. Potentially, very little of the water infiltrating into the upland soils is reaching the water table and is instead consumed by evapotranspiration prior to reaching the zone of saturation.

3.3.2 Wetland Response due to Typical Rainfall Events

Understanding the significance of the June 17 – 18 (DOY 168 - 169), 2005 event requires an examination of the response of S118 to all rainfalls measured in 2005 and 2006. There were nearly 50 and 25 rainfall events in 2005 and 2006 with average accumulations of 8.7 and 7.7 mm, respectively. The average rate of rainfall was 0.9 and 0.5 mm h^{-1} for 2005 and 2006. Maximum event accumulation, excluding the event of June 17 - 18 (DOY 168 - 169), 2005, was 57 mm in 2005 and 46 mm in 2006. Therefore, the June 17 – 18, 2005 (102.6 mm) event is substantially larger than the normal on-site rainfall.

3.3.2.1 Typical Rainfall Events 2005

Rainfall events from the growing season of 2005, March 31 (DOY 90) – October 27 (DOY 300), are presented in Figure 3.8. Volumetric water content throughout those periods from the CXU, TR, and CVU are also presented. Depths of 0.0 – 0.1 and 0.4 – 0.5 m are presented for the CXU, as salinity below a depth of 0.85 m prevents analysis of the entire profile. TR 2005, depths of 0.0 – 0.1, 0.4 – 0.5, 0.9 – 1.0, and 1.4 – 1.5 m are presented. CVU measurements at depths of 0.0 – 0.1, 0.4 – 0.5, 0.9 – 1.0, 1.4 – 1.5, and 1.9 – 2.0 m are shown. Gaps in the volumetric water content data signify flooding and the removal of the sensor system or technical problems.

The pond is affected very little by the majority of rainfalls. Although not presented with rainfall data, the pond water level of 2005 is presented in Figure 3.5. Two substantial rises in the pond water level are a result of the spring snowmelt and the rainfall event of June 17 – 18, 2005.

Vadose zone responses to the rainfalls of the 2005 are described in Figure 3.8 a), b), and c). The upper 0.1 m of soil, in all landscape positions is the most responsive, volumetric water content has the greatest variability. Surface layers are the direct connection with the soil and atmosphere and are highly dynamic. Surface variability in the TR soil is subdued compared to the uplands. The thick foliage of the TR shades the floor, reducing turbulent transfer of water vapour from the soil surface and intercepts rainfall. This reduces the rates of evaporation and infiltration, and limits soil moisture variability of the TR soil.

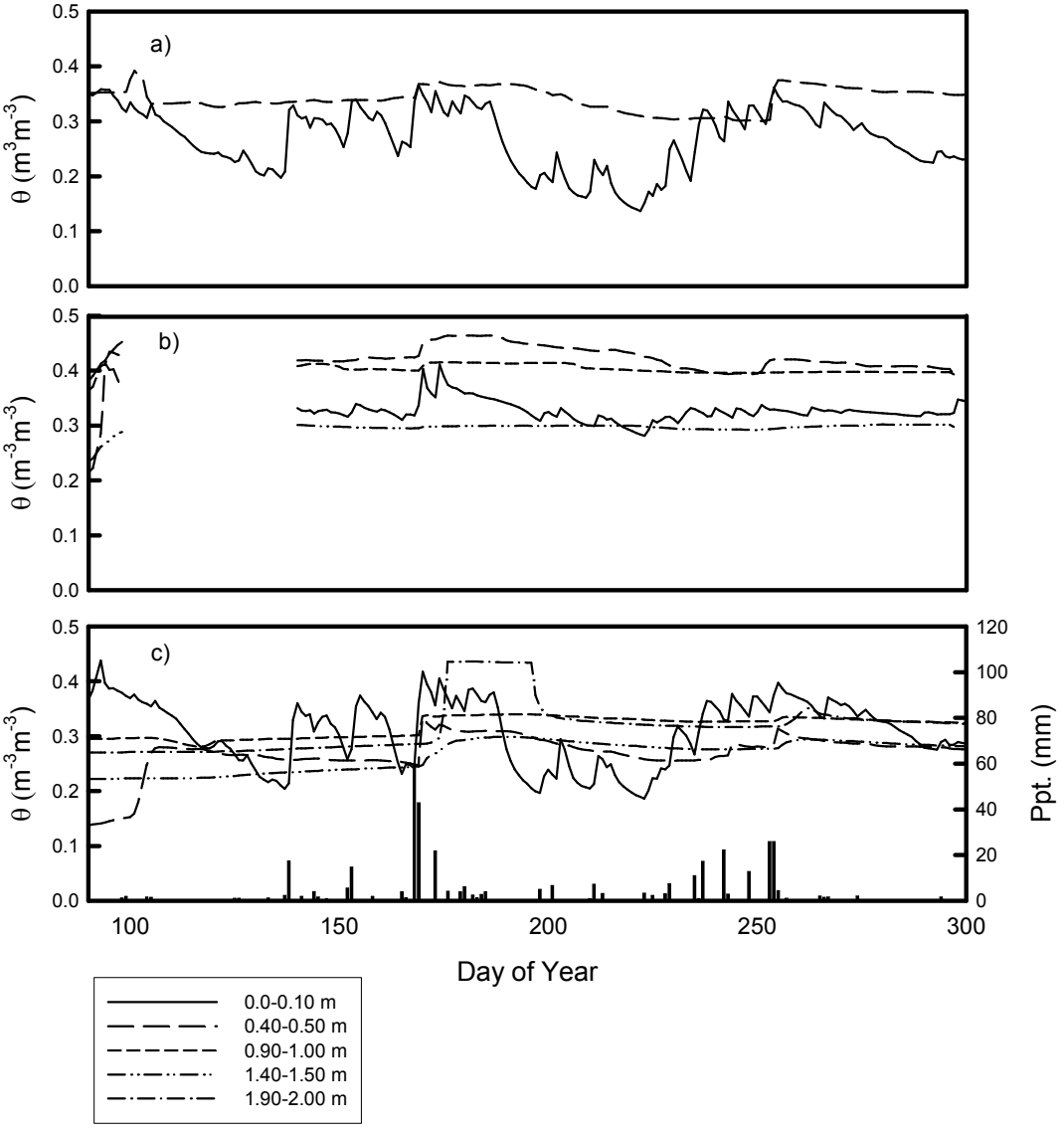

Figure 3.8. Rainfall and volumetric water content for the 2005 growing season. a) Convex Upland (CXU), b) Tree Ring (TR), and c) Concave Upland (CVU).

The largest soil response of 2005 occurred following the rainfall event of June 17 – 18, 2005 (DOY 168 – 169). This event is presented in detail in Section 3.3.3 and will not be discussed here. In contrast, the remaining rainfall events have very little influence over the soil water profiles below 0.5 m. Water from typical rainfalls evapotranspired and has little to no influence on the ground water underlying the wetland basin and pond.

3.3.2.2 Typical Rainfall Events 2006

Rainfall events from the growing season of 2006, March 31 (DOY 90) – September 7 (DOY 250) are presented in Figure 3.9. Volumetric water content throughout those periods from the CXU, TR, and CVU are also presented. Measurement depths did not change from 2005 for the CVU. A sensor was added to the TR site from 1.9 – 2.0 m. The CXU 0.4 – 0.5 m sensor was damaged over the winter and the 0.3 – 0.4 m sensor is presented instead. Again, gaps in the volumetric water content data signify flooding and the removal of the sensor system or technical problems. Pond water levels are presented in Figure 3.7. Just as in 2005, typical rainfalls have very little effect on the pond water levels. Instead, they help to maintain the water level through the 2006 growing season. The greatest influence on water levels in 2006 was the spring snowmelt.

Due to the above average rainfall of 2005 and the substantial snowpack of the 2005/2006 winter, volumetric water contents, throughout the catchment, are higher in spring of 2006 as compared to the same period in 2005. The majority of rainfalls in 2006 did not influence water levels below 0.5 m. The exception is an extended wet period from June 9 – 19, 2006 (DOY 160 – 170) that provided adequate rainfall for infiltration and redistribution to depth within the CVU profile. During this time, the TR remained inundated from the spring snowmelt and sensors were absent. TR enviroscan sensors were returned to the field on June 23, 2006 (DOY 174). Antecedent water contents were high on the CXU at 0.3 – 0.4 m and there was little response to this 10 day wet period.

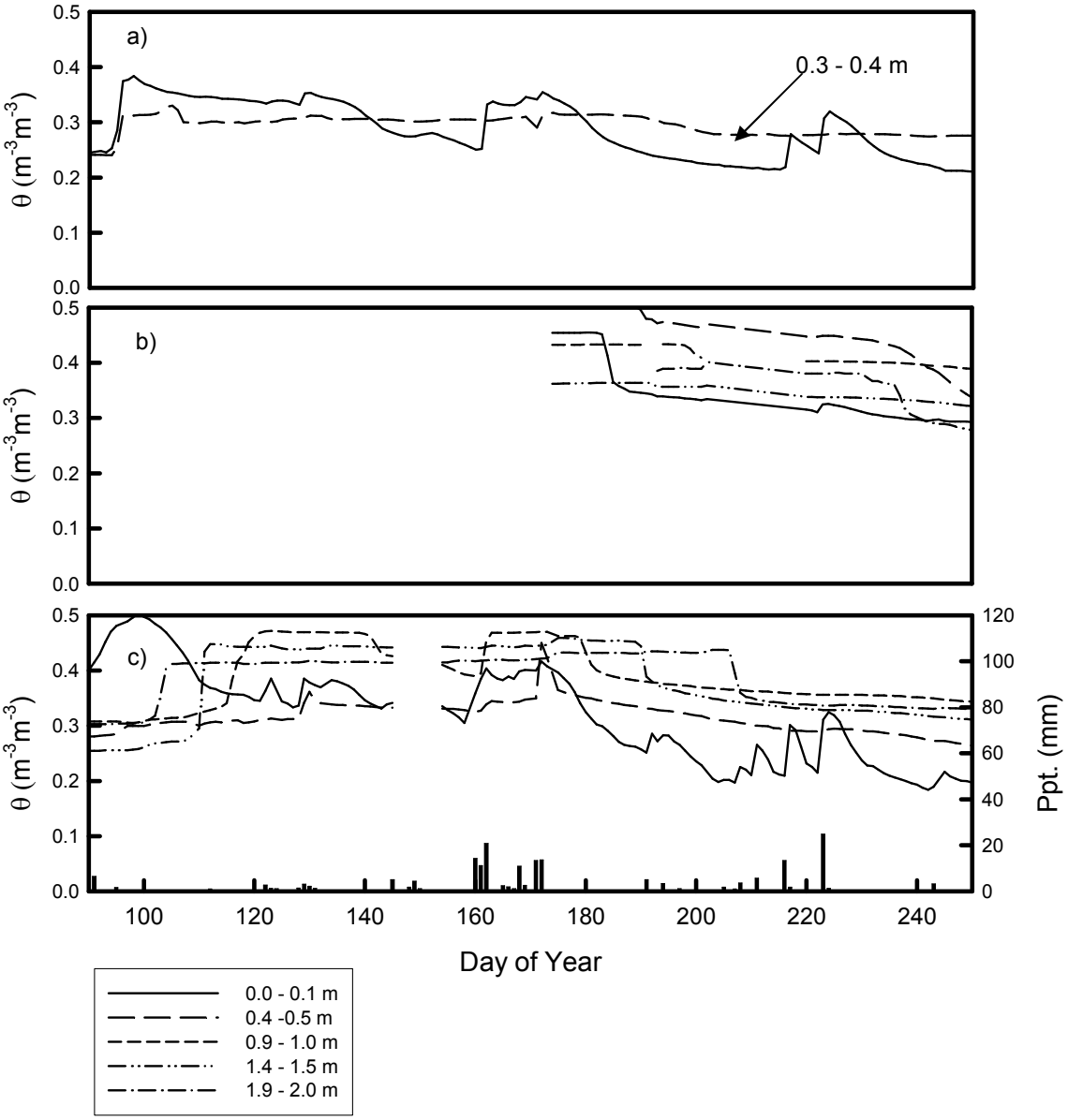

Figure 3.9. Rainfall and volumetric water content for the 2006 growing season. a) Convex Upland (CXU), b) Tree Ring (TR), and c) Concave Upland (CVU). The CXU 0.4 – 0.5 m was damaged over the winter of 2005/2006, therefore the 0.3 – 0.4 m depth is provided.

Overall, the soils at each landscape position respond in the same manner as they did in 2005. The TR soil profile responds minimally to rainfall events, as the low relative elevation and nearly saturated soils limit the detection of infiltration and redistribution. The CVU profile responds to all events, as it is a location of high infiltration and

redistribution through the soil profile. Intense rainfalls, such as June 17 – 18, 2005, and wet periods, such as June 9 – 19, 2006, result in redistribution throughout the entire profile, Figures 3.8 c) and 3.9 c). The CXU, due to salinity, is difficult to analyze over the growing season, but can be examined in the short-term by focusing on the upper portions of the profile.

Average rainfalls on the site are easily infiltrated into each of the landscape positions, with the majority of redistribution limited to the upper 0.5 m. Exceptions are the very intense storms and extended wet periods. Water from the common events appears to be consumed by evaporative demands prior to exceeding depths of 0.5 m. The land use change in 2004 from a cultivated land to permanent grass cover could substantially change the hydraulic properties of the CXU. Bodhinayake and Si, (2004) found that permanent grasslands have significantly higher rates of near surface saturated and unsaturated hydraulic conductivity than cultivated fields. Overtime, through plant root growth and decay the number of continuous macropores on the CXU will increase infiltration and redistribution to depth and reduce the amount of upland water reaching the wetland, supported by van der Kamp et al., (2003) findings on the St. Denis National Wildlife Area.

3.3.3 The Precipitation Event of June 17 and 18th

The record single day rainfall for the month of June at the Saskatoon Airport is 96.6 mm on June 24, 1983 (Environment Canada, 2008). The rainfall event of June 17 – 18 (DOY 168 – 169), 2005 had an accumulated rainfall of 102.6 mm over 25 hours. This does not break the record as it occurred in two separate portions over two days. The first portion began at 5:00 on June 17 (DOY 168) and carried on for four hours with an accumulated rainfall of 28.5 mm. The second portion of the event started at 21:00 that

same day and continued for eight hours with an accumulated rainfall of 74 mm. The highest rate recorded was 19.7 mm h^{-1} at 3:00, June 18 (DOY 169). According to Gray, (1973) there is a two-year return period for this hourly rainfall intensity. The hourly rainfall is shown in Figure 3.10. The initial rainfall wet the upper layers of the soil and later rainfall overwhelmed the system, generating overland, throughflow, and preferential flow within S118's catchment.

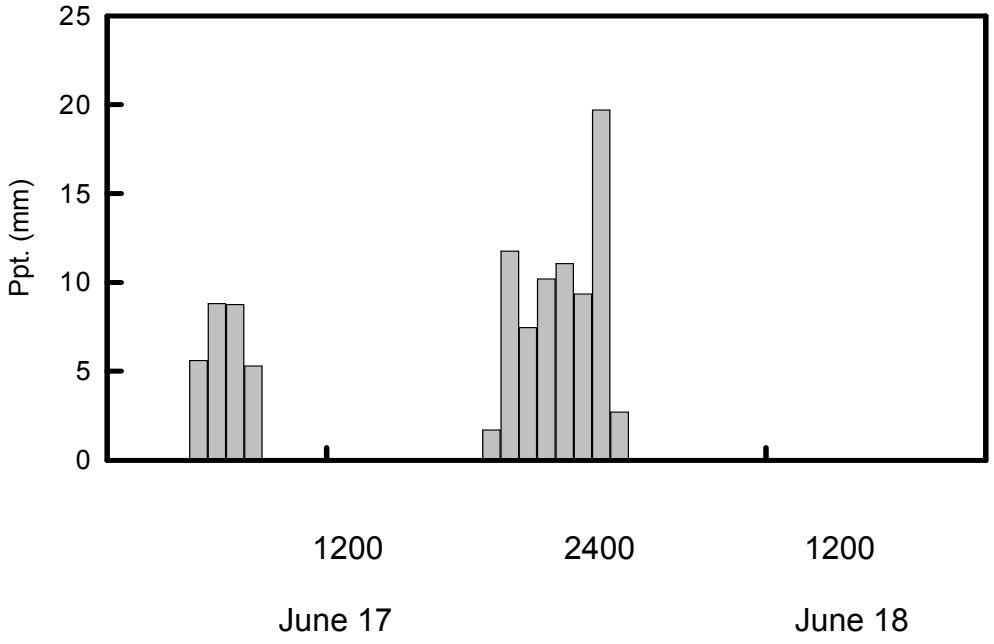

Figure 3.10. Hourly rainfall distribution from the intense rainfall event on June 17 – 18, 2005. 1200 in the horizontal axis indicates noon and 2400 indicates mid-night of June 17.

The 2005 growing season rainfall accumulation was dramatically higher than the 30 year average for the Saskatoon Airport (Figure 3.11) and the rainfall of June 17 – 18 was directly responsible. Ignoring this event makes the 2005 June accumulation approximately equal to the 30-year average. In comparison with other 2005 on-site

rainfalls, the next largest event occurred from September 10 – 12 (DOY 253 – 255) in a long low-rate precipitation event with a total accumulation of 57 mm. The 19.7 mm h^{-1} on June 18 is the greatest rate of rainfall for the site in 2005, with a seasonal average of 1.0 mm h^{-1}. Therefore, the rainfall event of June 17 – 18 was rare for the season and for the site in general.

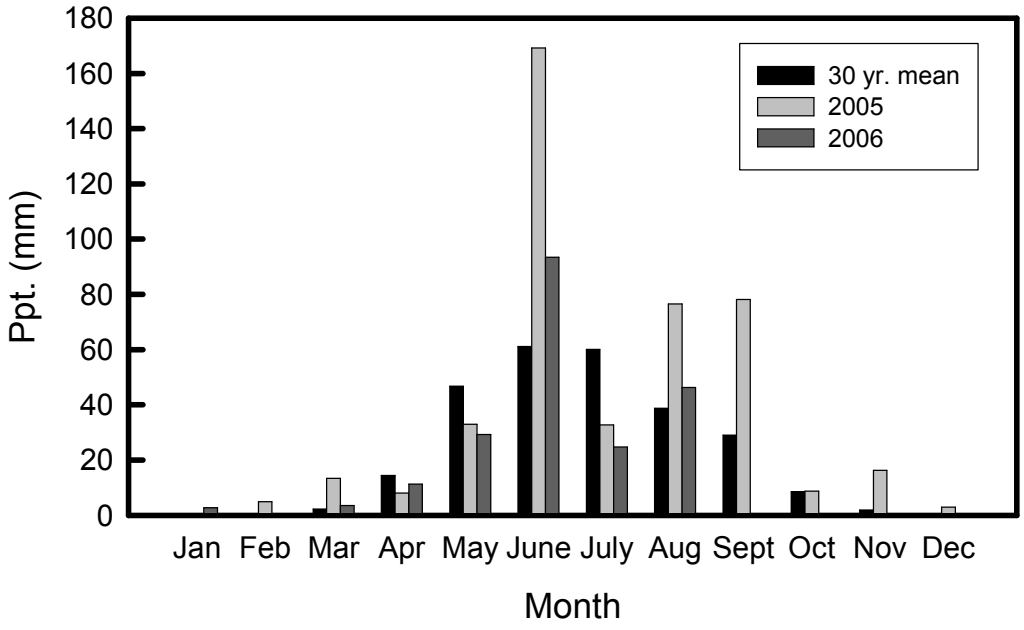

Figure 3.11. Monthly rainfall totals of 2005 and 2006 compared to the 30 year mean (1971 – 2000) measured at the Saskatoon Airport.

3.3.3.1 Pond Response

The rainfall of June 17 – 18 caused the second largest influx of water to S118 in 2005, with the spring snowmelt generating the greatest (Figure 3.12). Throughout the growing season, the pond level dropped from infiltration and evapotranspiration. The pond drained on June 3 (DOY 154), illustrated in Figure 3.12, and remained dry until the

rainfall of June 17 – 18, 2005. This rainfall caused a total rise of 0.50 m in pond level and took unit late fall to drain for the second time in 2005.

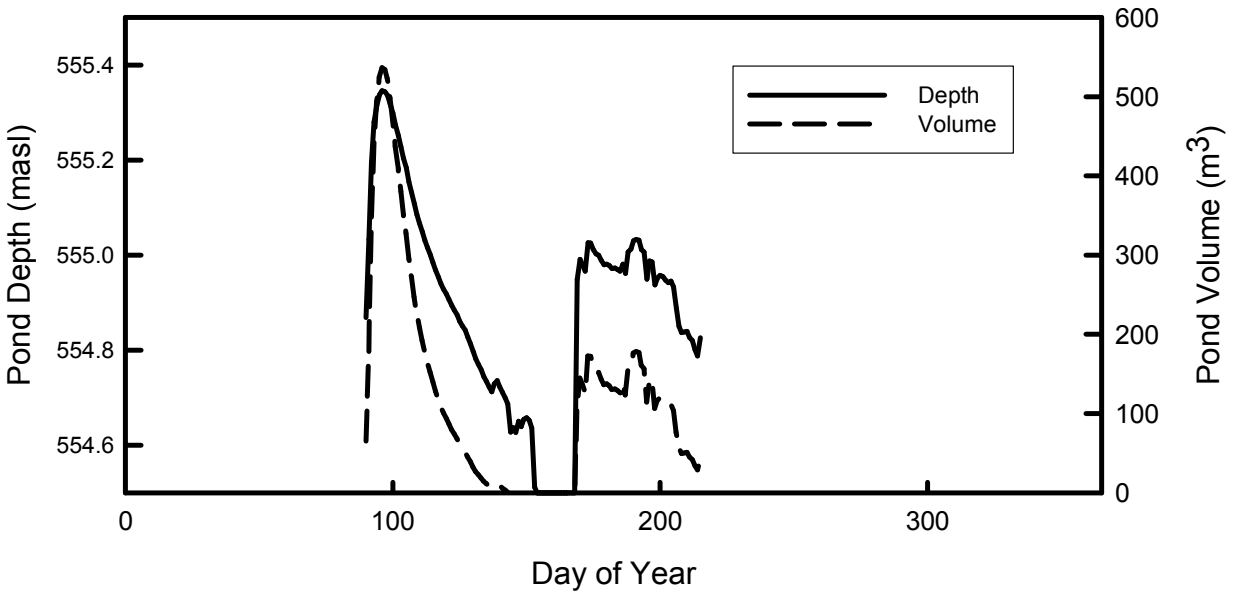

Figure 3.12. Pond 118 water depth, in meters above sea level (masl), and volume throughout the summer of 2005.

The pond remained unaffected by the event until 3:00 on June 18 (22 hours after onset of rainfall), the hour with the greatest rainfall rate, 19.7 mm. Within one hour, water levels increased by 0.322 m and a volume of 45 m^3. The rapid increase in the pond water level of 322 mm with only 19 mm of rainfall is indicative of the overland flow within the catchment. The maximum pond depth of 0.497 m (~ 150 m^3) was reached nine hours later, which is approximately five times the accumulated rainfall. This lag suggests that a large portion of pond water accumulation was a result of throughflow or spillover from the small basin located within the TR. Further evidence to the occurrence of throughflow is the increases in pond depth and volume on June 22 (DOY 173) and July 10 (DOY 191) without any corresponding rainfalls to account for the increases. These increases in pond depth and volume are illustrated in Figure 3.12. On June 22 pond depth rose to 0.526 m

and 172.9 m^3, while on July 10 a further increase to 0.533 m and 178.5 m^3 was recorded. Throughflow is expected as we have had a substantial increase in the water potential under the TR and the uplands because of the infiltrability of the concave uplands and low-lying areas

3.3.3.2 Vadose Zone Response

Analysis of the vadose zone response focuses on the real-time volumetric water content and matric potential of the CXU, CVU, and TR, as they experienced the greatest changes from the event. The cumulative infiltration at each location was calculated using Eqs. 3.3 and 3.4. Matric potential data confirmed the rate and depth of infiltration determined volumetrically by the Enviroscan sensors and provides evidence of flow directions.

Figure 3.13 describes the soil water condition to a depth of 0.5 m for the volumetric water content and 1.85 m for matric potential on the CXU site. Soil salinity affected the volumetric water content instrumentation at depths below 0.85 m from the soil surface. Therefore, water content below this depth was calculated using matric potential and the water retention curve. Prior to the rainfall, CXU soils were relatively dry, with the upper 0.5 m at or below 0.30 $m^3\ m^{-3}$ water content. The hydraulic gradient was upward above 1 m. Cumulative infiltration, determined using Eq. 3.3, into the upper 0.5 m during the first portion of the rainfall was ~28 mm, equal to the recorded rainfall. The dry antecedent conditions and the low rates of rainfall allowed the soil to absorb this portion of the event. As expected, the second portion of the rainfall had a greater influence on the soil water content and matric potential. Water contents reached their maximum in the upper 0.3 m of the profile at 3:00 on June 18 (22 hours after onset of rainfall), during the greatest rate of rainfall, coinciding with the time of pond refilling.

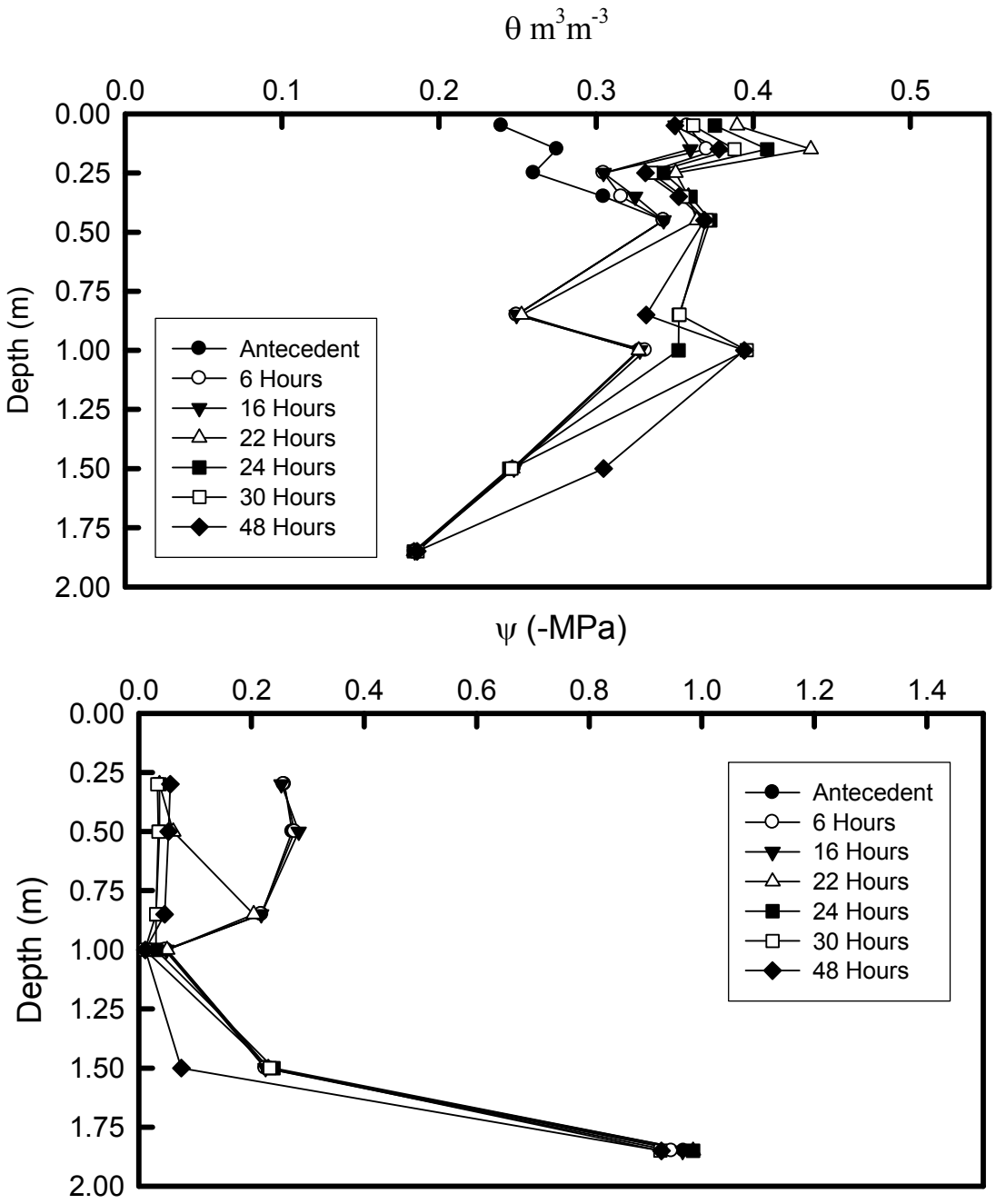

Figure 3.13. Convex Upland soil water dynamics following June 17 – 18, 2005 rainfall event. a) θ and b) ψ. All times are the hours following the initiation of the rainfall event.

Total infiltration of the second portion of rainfall was 44.8 mm, considerably less than the accumulated rainfall. The CXU infiltrated a total of 72.8 mm, accounting for approximately 71 % of the ~103 mm falling on the site. Overland flow was generated

from this convex landscape position. Historic overland flow from the north side of wetland S118 is recorded by Bedard-Haughn et al., (2006). These researchers identified erosional tongues from past events caused by overland flow adjacent to the CXU site. Furthermore, Stoof, (2004) in a modeling exercise determined that nearly all cultivated landscape elements on the study site would generate overland flow with a rainfall event of 19.8 mm hr^{-1}, equal to the greatest intensity experienced in this event.

At 3:00 on June 18 (22 hours after onset of rainfall), infiltration caused an increase in matric potential throughout the profile to 1 m depth, reversing the upper hydraulic gradient. Within twelve hours (data not shown) of rainfall ceasing water had drained through the soil zone to a depth of 1.5 m and the deepest sensor recording a small rise in matric potential. At 1.85 m, matric potential rose from -0.98 MPa at the end of the event to a high of -0.37 MPa six days later (data not shown). Soil water within the CXU profile is redistributed through the 1.85 m depth, but at a relatively slow rate. This slow rate of vertical redistribution provides plants and the atmosphere time to consume this moisture through evapotranspiration.

In contrast, soils of the CVU have a much higher infiltrability. The CVU response of volumetric water content, to a depth of 2.0 m, and matric potential, to 1.5 m, is shown in Figure 3.14. The upper antecedent water content ranged from 0.23 – 0.32 $m^3 m^{-3}$ with an upward gradient from 0.30 m. Again, using Eq. 3.3, approximately 30 mm of infiltration was measured to a depth of 0.30 m immediately following the initial portion of the rainfall. Approximately 74 mm fell in the second portion of the rainfall and the CVU had an accumulated infiltration of 73 mm. The concave CVU soil with high porosity, lower density, and well established root channels with adequate soil properties

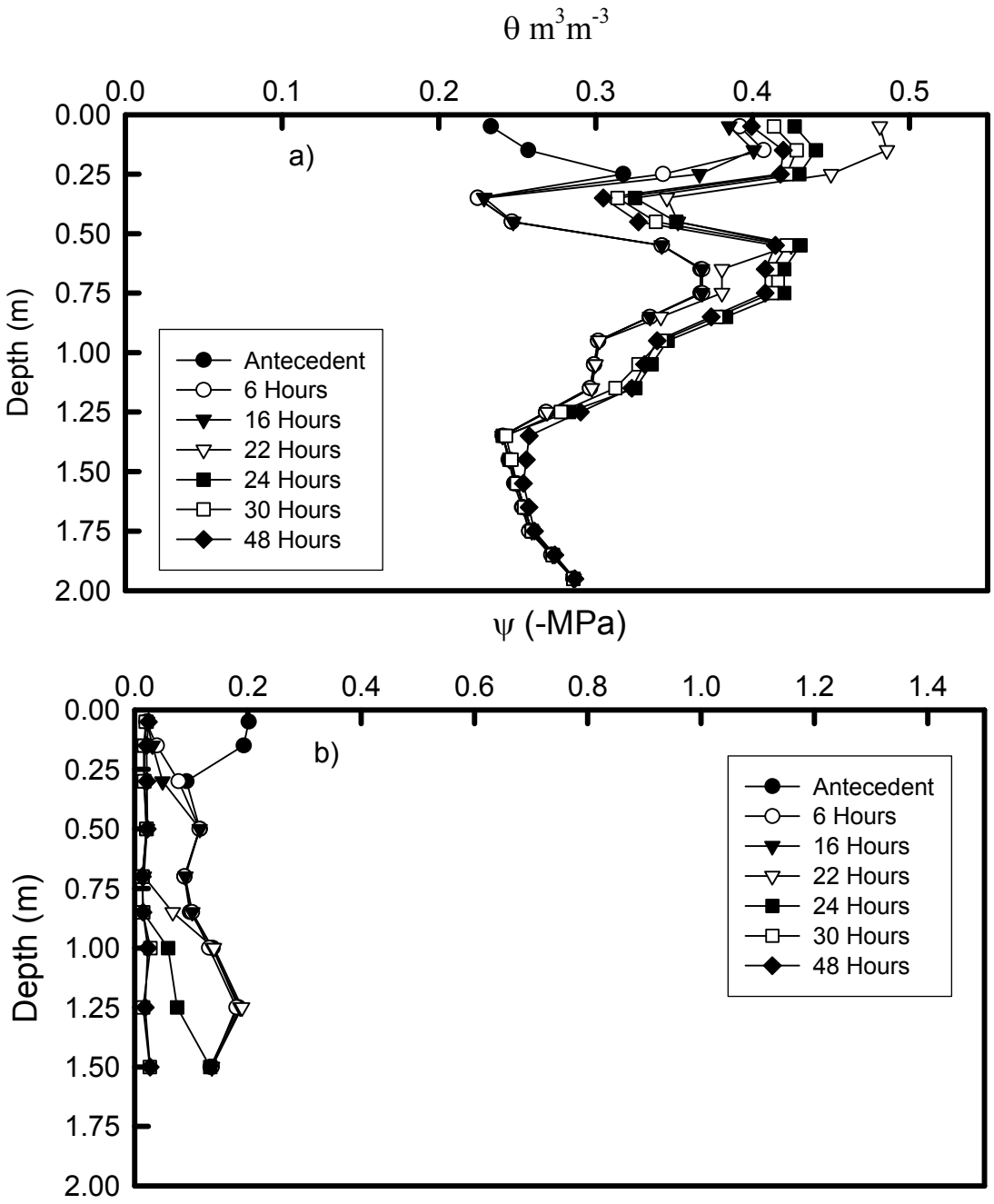

Figure 3.14. Concave Upland soil water dynamics following June 17 – 18, 2005 rainfall event. a) θ and b) ψ. Times are hours following the initiation of the rainfall event.

to infiltrate the entire event. According to Stoof, (2004) concave cultivated soils have thicker A-horizons, increased porosity, field saturated hydraulic conductivity, and plant residue than convex cultivated landscape elements.

CVU matric potential from the surface to 1.5 m depth rose to -0.02 MPa, Figure 3.14 b). This minimal gradient indicates the downward drainage of water through the soil profile driven by gravitational flow. Rainfall on the surface of the CVU moved quickly through the soil profile, potentially contributing directly to the upland groundwater. Within twelve hours of the rainfall event more than 10 mm of water drained through the soil zone below 1 m of the surface, Figure 3.14 a).

The TR contains the largest and most diverse vegetation. The land surface within the TR is 1.5 m lower than the CVU and approximately 0.5 m higher than the lowest point in the catchment. There is a second small isolated basin within the TR landscape element, which spills into the main pond of S118 (Figure 3.1). TR soil water content and matric potential are shown in Figure 3.15. The antecedent water conditions within the TR soil profile was relatively high compared to the upland soils. The upper 0.5 m of the soil ranged from 0.30 – 0.45 $m^3 m^{-3}$. The first portion of rainfall resulted in ~6 mm of infiltration within the TR soils. Leaf interception, water retention by the LFH horizon, and high antecedent water content reduced the initial infiltration. During the 74 mm, latter portion of the event, ~63 mm infiltrated the TR soils. Prior to the rainfall, the site had a slight upward gradient. Matric potential at 0.05 m preceding the event was -0.07 MPa and rose slightly to -0.02 MPa, indicating the obvious downward flow following the rainfall.

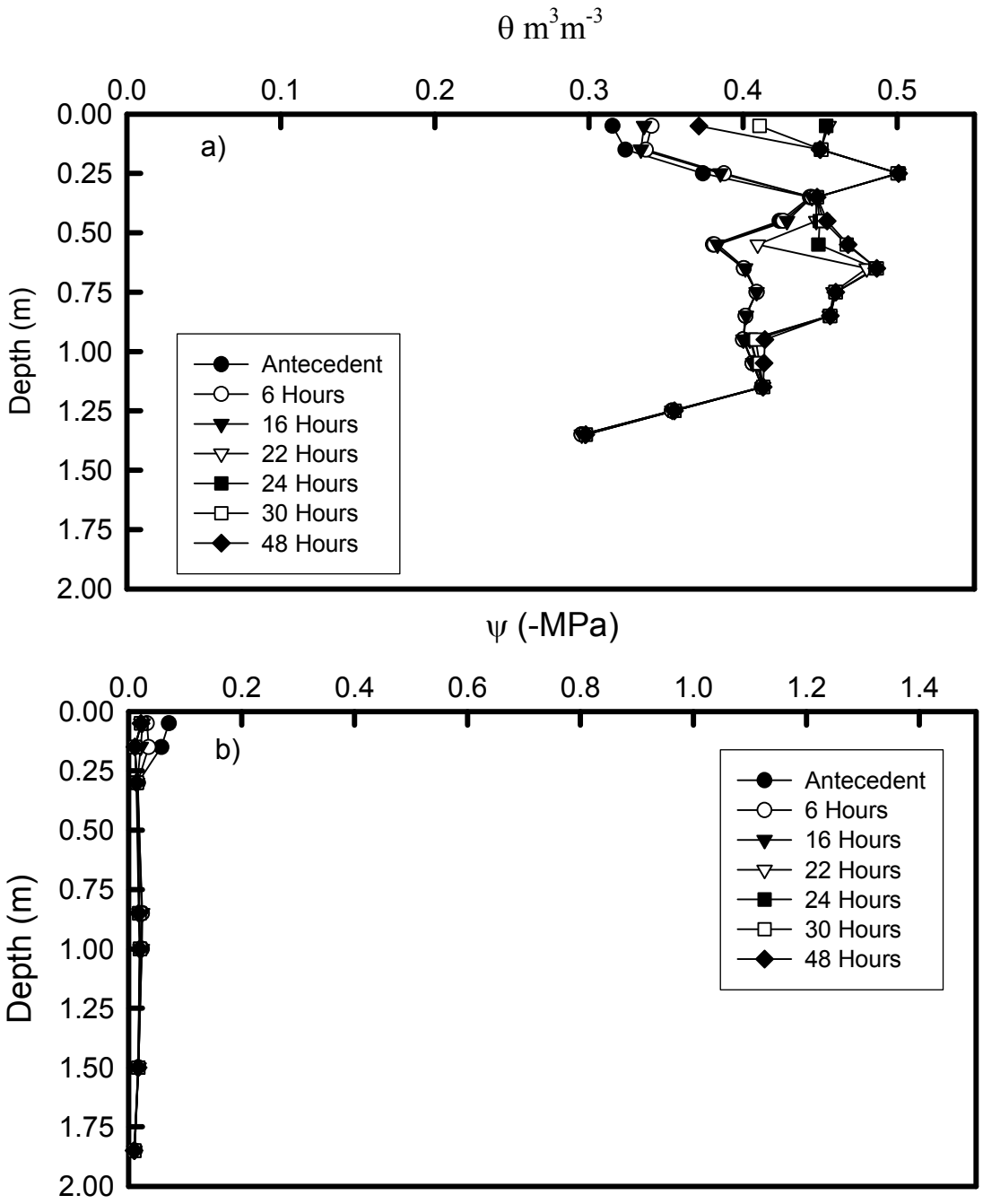

Figure 3.15. Tree Ring soil water dynamics following June 17 – 18, 2005 rainfall event. a) θ and b) ψ. All times are the hours following the initiation of the rainfall event.

Prior to the end of the rainfall ~25 mm of water had infiltrated below 0.5 m. Twelve hours following the rainfall, infiltration below this depth was limited to 5 mm. Infiltration and redistribution was limited by the high water table (1.2 m) under the TR.

The anomaly within the profile is at 0.30 – 0.40 m, which does not respond, but allows water to move through that layer. This is the location of the very dense Bt horizon. Bt soil horizons are often located under tree stands. These soil layers are finely textured, Table B1, Appendix B, and prone to the development of preferential flow paths. Infiltrated water likely by-passed this layer through a preferential flow path, causing the rapid response at depths below, while there was no measured response at 0.30 – 0.40 m.

3.3.3.3 Groundwater Response

At the time of this rainfall, piezometers were installed on the GE at a depth of 9 m, within the PC at depths of 4 and 8 m, and on the CVU at depths of 3, 6, and 9 m. GE and PC piezometers were receding after reaching their maximum values from the spring snowmelt. The spring snowmelt and mounded water table continued to influence the groundwater of the CVU. Therefore, the changes in the CVU instruments are not entirely because of the rainfall event of June 17 – 18, 2005, but the rates of recharge are significantly higher following the event, Figure 3.5. Prior to the event, rates of recharge to CVU-6 and CVU-9 were 6.25×10^{-3} and 1.5×10^{-2} m d^{-1}, respectively. Following the rainfall the rate of change increased an order of magnitude within CVU-6 and by five times in CVU-9. Prior to the rainfall, CVU-3 did not contain any water, following the event the groundwater reached the instrument and remained until the end of the year (Figure 3.5 c). The short-term groundwater response to the rainfall event is shown in Table 3.4.

Table 3.4. Groundwater response following June 17 – 18, 2005 rainfall event.

	Depth of piezometer (m)	June 15, 2005 (m)	July 5, 2005 (m)	~ Change (m)
Grassed Edge (GE)	9	553.26	554.00	0.74
Pond Center (PC)	4	554.30	555.05	0.74
	8	553.80	554.20	0.40
Concave Upland (CVU)	3	No Water	553.26	0.83
	6	553.12	554.44	1.32
	9	552.59	553.69	1.10

Prior to the rainfall event the groundwater instruments were measured on June 15 (DOY 166), the next measurements occurred more than two weeks later on July 5 (DOY 186). The CVU experienced the greatest increase in potential, with CVU-3, CVU-6, and CVU-9 increasing by 0.83, 1.32, and 1.10 m, respectively. The shallower instruments, 3.0 and 6.0 meter instruments, which are installed in the zone of oxidation, have low lag times (Table 3.1) and experience a rapid increase in potential. The piezometric surface within the wetland did not display this rapid increase in potential. GE-9, PC-4, and PC-8 increased by 0.74, 0.74, and 0.40 m, respectively (Table 3.3).

The spring snowmelt is generally considered the greatest contributor to subsurface flows. The rate of recharge following the spring snowmelt of 2005 was 3.72 $x10^{-2}$, 4.10 $x10^{-2}$, and 1.68 $x10^{-1}$ m d^{-1}, for GE-9, PC-4, and PC-8, respectively (calculated from measured groundwater level data shown in Fig. 3.5). Following the rainfall of June 17 – 18, rates of recharge do not change from the spring snowmelt for GE-9 and PC-4. While, PC-8 recharge rates are slightly lower, at 2.0 $x10^{-2}$ m d^{-1} (= change of groundwater level per unit time; Table 3.4). This indicates the movement of water and solutes through the

upper portions of the wetland is significant following an extreme rainfall event. These rates and volumes reaching the piezometric surface following the rainfall event indicate significant preferential flow and that a large rainfall event is equivalent to the spring snowmelt.

3.4 Summary of Vadose Zone Results

Due to the complex nature of the results provided throughout Section 3.3, a summary of the vadose zone responses to the three major events, snowmelts 2005 and 2006 and the rainfall on June 17 – 18, 2005, are provided in Table 3.5.

Typical rainfall events are not included as these provide supplementary data and are not the major focus of this research. The lowland, GE and PC, are not included in this summary. The hydrologic response of these land elements was consistent during all three of these events. They were inundated by water due to direct precipitation and overland flow from the surrounding uplands. The TR position, at a relatively low elevation, was also inundated during the three events. Although, volumetric water content instrumentation was present during the rainfall event, allowing for analysis of the vadose zone response to this event. The vadose zone of the TR cannot be included in the analysis of the snowmelts as the access tube for the volumetric water content instrumentation was flooded following both spring snowmelts. The upland, CVU and CXU, positions are the focus as they have the most robust data and they exhibit the greatest variability in hydrologic response to the three events.

Detailed descriptions on the methodology and results are provided in Sections 3.2 and 3.3. The redistribution of water on these uplands is a complex problem. Many variables can change in short and long time scales. Consider the change in the proportion of spring snowmelt infiltration from spring of 2005 to 2006, during the 2005 snowmelt the CVU

was a location of water collection and infiltration. CVU infiltrated 22.2 mm more water than was available according to the snow survey. In contrast, during the

Table 3.5. Summary of infiltration measured for snowmelts, 2005 and 2006, and rainfall on June 17 – 18, 2005. Snow depth and density measurements for determining water equivalence (WE) were made at EnviroScan instrument locations. EnviroScan measured changes in volumetric water content to determine change in storage.

Event/Landscape Position	Area (m^2)	Input – WE (mm)	Δ S - Infiltration (mm)	Out – Runoff (mm)	% Runoff
Snowmelt 2005					
Tree Ring (TR)	1553	87.1	--	--	--
Concave Upland (CVU)	3258	33.6	55.8	0	- 66 %
Convex Upland (CXU)	6146	65.2	47.1	18.1	28 %
Snowmelt 2006					
Tree Ring (TR)	1553	24.5	--	--	--
Concave Upland (CVU)	3258	116.0	41.3	74.7	64 %
Convex Upland (CXU)	6146	75.5	36.6	38.9	52 %
Rainfall: June 17 – 18, 2005					
Tree Ring (TR)	1553	103.0	69.2	34	33 %
Concave Upland (CVU)	3258	103.0	103.0	0	0
Convex Upland (CXU)	6146	103.0	72.8	30.2	29 %

snowmelt of 2006 only 36 % of available water was infiltrated into the soil, 64 % was available for runoff to lower landscape positions. The source of this change is likely a result of the antecedent water conditions prior to the spring snowmelt. Precipitation at the nearby Saskatoon Airport in the years leading up to the spring of 2005 (2001 – 159 mm; 2002 – 299 mm; 2003 – 233 mm; 2004 – 402 mm) were well below, with the exception of 2004, the 30 year average, 350 mm (Environment Canada, 2008). The decreased precipitation from 2001 to 2003 reduced soil water storage. This contributed

to the increase in soil infiltration at the CVU in the spring of 2005. Although 2004 was above average, it is unlikely that a single year's increase in precipitation would completely replenish the soil water. Instead, it appears that the high levels of precipitation through 2005, 523 mm, had a substantial affect on the response of this CVU landscape position (Environment Canada, 2008). A comparison of Figure 3.8 c), which describes the soil water content response to typical rainfalls in 2005, to Figure 3.9 c), which describes the same for 2006, indicates that CVU soil water contents were higher in 2006 than 2005.

Although, spring snowmelt response appears to be highly variable for the CVU, taking into account the response to the June 17 – 18, 2005 rainfall and previous research on the site, Stoof, (2004), CVU landscape positions can be locations of water collection and are consistently locations of high infiltrability. During the rainfall event, 103.0 mm of rainfall was recorded on the site over a two-day period. The change in storage on the CVU site indicates that the entire event was infiltrated into the soil, consistent with the soil response from the spring snowmelt in 2005. Additionally, Stoof, (2004), found that CVU cultivated elements were identified as having thick A-horizons, high porosity, field saturated hydraulic conductivity, and surface residue. This research indicates that CVU cultivated soils retain high volumes of water and are locations of water collection and infiltration.

The CXU position displays a different, but similar response to the changes in spring antecedent water conditions. CXUs are consistently locations of limited infiltration. During both spring snowmelts the CXU infiltrates a portion of the available water. The spring of 2005 proportion of water infiltrated is considerably greater than 2006, 76% in

2005 as compared to 34 % in 2006. Again, this is likely a result of the changes in seasonal precipitation and prolonged drought from 2001 – 2003. Regarding the rainfall event of 2005, the response of the CXU landscape elements is consistent with 29% of the available rainfall resulting in runoff. This is consistent with the longer-term analysis of Stoof, (2004) who found that CXU cultivated landscapes had a limited topsoil development, relatively low porosity, field saturated hydraulic conductivity, and surface residues.

The TR summary is somewhat limited as no vadose zone data from the spring snowmelts is available. This position was inundated with water for weeks following the spring snowmelt events. During the rainfall event, the piezometric surface was within 0.5 m of the soil surface, which limited the amount of water infiltrating into the TR vadose zone. Instead, the water that could not infiltrate into the vadose zone was likely stored within the highly porous LFH horizon and the leaf litter on the soil surface. Limited ponding in micro-depressions may have occurred. This would not have been measured by the single instrument in this landscape position.

3.5 Conclusion

The rainfall of June 17 – 18, 2005, and the hydrologic response of the pond, vadose zone, and groundwater of S118 and the surrounding uplands were examined. This rainfall overwhelmed the hydrologic system of S118, causing overland flow, throughflow, and the rapid filling of the dry wetland. The event occurred in two phases, the first ~28 mm, followed by the second in which ~74 mm fell. The CXU infiltrated ~72 mm, while the CVU accepted the entire rainfall. The CXU soils were overwhelmed at 3:00 on June 18 (22 hours after the onset of rainfall), when 19.7 mm fell generating overland flow that quickly replenished the pond. Stoof, (2004), found this intensity of

rainfall was more than adequate to generate overland flow on the majority of cultivated landscape elements on the study site. Within one hour water accumulated to a depth of 0.322 m and a volume of 165 m^3. The maximum depth of 0.497 m (> 323 m^3) was reached nine hours later. This lag was likely the result of throughflow from the TR. The accumulation of water under the TR led to the lateral movement of water from the TR to the pond during the later stages of the event.

CXU landscape elements were primarily responsible for overland flow. Analysis of the spring snowmelts of 2005 and 2006 indicate that 24 % and 66 % of the SWE ran off into the S118. Similarly, analysis of June 17 – 18, 2005 rainfall indicates that approximately 29 % of the precipitation falling on the site found its way to the pond center through overland flow. Consistent with the findings of Stoof, (2004), the convex CXU soils are poorly developed and lack sufficient preferential flow paths for sustained rapid infiltration. Alternatively, the concave CVU landscape soils are highly porous and allowed the entire rainfall event and spring snowmelts to enter the soil surface and advance through the vadose zone to the CVU water table. The relative topographic relief and shape of the landscape are significant contributors to the development of overland flow on the site. The CXU has a much greater slope and convex shape, leading to the generation of overland flow. The nearly flat topography and slight concavity of the CVU allowed the temporarily ponded water opportunity to infiltrate into the soil.

Regarding groundwater, both upland and lowland piezometers, experienced a rapid increase in potential following the rainfall event. This indicates that extreme rainfall events do significantly affect the groundwater recharge at all landscape positions. The

jointed nature of glacial till causes preferential flow and the rapid movement of rainfall water to depth.

The results of this study compliment the findings of Hayashi et al., (1998a; 1998b) who found that spring snowmelts have a substantially greater influence on PPR closed basin hydrology than rainfall events. This new research indicates that rare, but intense storms easily and rapidly overwhelm poorly developed soils, generating overland flow that refills wetland depressions and has a significant influence on the catchment hydrologic cycle.

The root cause of overland flow within S118 is the topographic relief of the CXU. Topography on this site has historically limited the development of the soil, surface pores, and preferential flow paths. In contrast, the CVU with a relatively flat landscape developed a thick A-horizon with ample water conducting macropores. This results in the rapid infiltration and redistribution of large volumes of water on the CVU site. The CXU soils were quickly saturated and lacked sufficient internal conductivity to remove the water build-up at the soil surface, resulting in the observed overland flow to the wetland basin.

Comparison of the rainfall of June 17 – 18, 2005 with the spring snowmelts of 2005 and 2006 indicates that the hydrologic consequences of these very different events are similar. Overland flow, substantial ponding in lowlands, and recharge of the groundwater occur in both cases. The source of overland flow and ponding from the rainfall event proved to be primarily the CXU, whereas ponding water from snowmelt is sourced throughout the catch basin, including snow trapped within the basin itself. Groundwater recharge in both cases is likely limited to the upper, seasonal zones of

saturation and in the long-term very little from either source seeps below the unoxidized till layer, recharging the permanent, regional groundwater. In conclusion, extreme rainfall events are hydrologically equivalent to the annual spring snowmelt, the major source of water for closed catchments in the PPR.

3.6 References

Bedard-Haughn, A., F. Jongbloed, J. Akkerman, A. Uijl, E. de Jong, T. Yates, and D. Pennock. 2006. The effects of erosional and management history on soil organic carbon stores in ephemeral wetlands of hummocky agricultural landscapes. Geoderma 135:296-306.

Berthold, S., L.R. Bentley, and M. Hayashi. 2004. Integrated hydrogeological and geophysical study of depression focused groundwater recharge in the Canadian prairies. Water Resources Research 40:W06505.

Bodhinayake, W., and B. Si. 2004. Near-saturated surface soil hydraulic properties under different land uses in the St. Denis National Wildlife Area, Saskatchewan, Canada. Hydrological Processes 18:2835 - 2850.

Dyck, M.F., R.G. Kachanoski, and E. de Jong. 2003. Long-term movement of a chloride tracer under transient, semi-arid conditions. Soil Science Society of America Journal 67:471-477.

Environment Canada. 2008. Canadian climate normals [Online] http://www.climate.weatheroffice.ec.gc.ca/climate_normals/index_e.html (Verified May 27 2008).

Geesing, D., M. Bachmaier, and U. Schmidhalter. 2004. Field calibration of soil water probe in heterogeneous fields. Australian Journal of Soil Research 42:289-299.

Gomez-Plaza, A., M. Martinez-Mena, J. Albaladejo, and V.M. Castillo. 2001. Factors regulating spatial distribution of soil water content in small semiarid catchments. Journal of Hydrology 253:211-226.

Hayashi, M., G. van der Kamp, and D.L. Rudolph. 1998a. Water and solute transfer between a prairie wetland and adjacent uplands, 1. Water balance. Journal of Hydrology 207:42-55.

Hayashi, M., G. van der Kamp, and D.L. Rudolph. 1998b. Water and solute transfer between a prairie wetland and adjacent uplands, 2. Chloride cycle. Journal of Hydrology 207:56-67.

Hayashi, M., G. van der Kamp, and R. Schmidt. 2003. Focused infiltration of snowmelt water in partially frozen soil under small depressions. Journal of Hydrology 270:214-229.

Hillel, D. 1998. Environmental Soil Physics Academic Press, London.

Gray, D.M. 1973. Handbook on the principles of hydrology Water Information Center Inc., New York.

Jackson, N.A., and J.S. Wallace. 1999. Analysis of soil water dynamics in an agroforestry system based on detailed soil water records from time-domain reflectometry. Hydrology & Earth System Sciences 3:517-527.

Meyboom, P. 1966. Unsteady groundwater flow near a willow ring in hummocky moraine. Journal of Hydrology 4:38-62.

Miller, J.J., D.F. Acton, and S.A. R.J. 1985. The effect of groundwater on soil formation in a morainal landscape in Saskatchewan. Canadian Journal of Soil Science 65:293-307.

Musters, P.A.D., and W. Bouten. 2000. A method for identifying optimum strategies of measuring soil water contents for calibrating a root water uptake model. Journal of Hydrology 227:273-286.

Paltineanu, I.C., and J.L. Starr. 1997. Real-time soil water dynamics using multisensor capacitance probes: laboratory calibration. Soil Science Society of America Journal 61:1576-1585.

Parsons, D.F., M. Hayashi, and G. van der Kamp. 2004. Infiltration and solute transport under seasonal wetland: bromide tracer experiments in Saskatoon, Canada. Hydrological Processes 18:2011-2027.

Pennock, D. 2006. pp. Personal communication.

Pomeroy, J.W., and D.M. Gray. 1995. Snow Accumulation, Relocation, and Management. National Hydrology Research Institute, Saskatoon.

Scott, H.D. 2000. Soil physics; agricultural and environmental applications Iowa State University Press, Ames.

Si, B., and R.G. Kachanoski. 2003. Measurement of local soil water flux during field solute transport experiment. Soil Science Society of America Journal 67:730-736.

Sloan, C.E. 1972. Ground-water hydrology of prairie potholes in North Dakota. Geological Survey Professional Paper 585-C.

Stahli, M., and D. Stadler. 1997. Measurement of water and solute dynamics in freezing soil columns with time domain reflectometry. Journal of Hydrology 195:352-369.

Starks, P.J. 1999. A general heat dissipation sensor calibration equation and estimation of soil water content. Soil Science 164:655-661.

Stoof, C. 2004. Soil hydraulic properties of landscape elements in a cultivated hummocky till in Southern Saskatchewan, Canada, Wageningen University, Wageningen.

van der Kamp, G., M. Hayashi, and D. Gallen. 2003. Comparing the hydrology of grassed and cultivated catchments inthe semi-arid Canadian prairies. Hydrological Processes 17:559-575.

van Wesenbeeck, I.J., and R.G. Kachanoski. 1988. Spatial and temporal distribution of soil water in the tilled layer under a corn crop. Soil Science Society of America Journal 52:363-368.

CHAPTER 4.0
SUMMARY AND CONCLUSION

Isolated catchments found throughout the PPR are the major location of infiltration across the prairies. Consequently, ponding is a significant factor in determining the amount of annual infiltration and contribution to the local and regional groundwater. Estimates of annual groundwater deep recharge range from 1 to 12 mm yr^{-1} (Hayashi et al., 1998a; Hayashi et al., 1998b; Dyck et al, 2003, Si and de Jong, 2007). This estimate assumes a single spring melt, but intense rainfall events are nearly as hydrologically significant. Additionally, these catchments contain different vegetation or ecological units, such as the grassed edge, tree ring, and uplands. The ecohydrological functions of these land units is not well understood. The research described in this dissertation was designed to answer some of the essential questions contributing to understanding soil water dynamics in different land units of a typical slough in the Prairies. The specific objective was to examine how these different landscape/ecological elements respond to snowmelt and extreme rainfall events, in particular one that occurred on June 17 – 18, 2005. To achieve this objective, a closed recharge wetland at the St. Denis National Wildlife Area (NWA) Saskatchewan, Canada (106°06'W, 52°02'N) was selected for installation of instrumentation to measure the hydrologic response of each landscape/ecological element. Instruments consisted of real-time meteorological, soil water, and groundwater sensors. These sensors, manual measurements, and field observations were used to provide a unique dataset that captured relevant hydrologic measurements for the rainfalls and the spring snowmelts of 2005 and 2006.

The hydrologic analysis of the June 17 – 18, 2005 rainfall event at the St. Denis NWA concluded that an intense rainfall resulted in overland flow, ponding, and rapid groundwater

response. The analysis of this rainfall event compliments previous research on the wetland water dynamics in the PPR. Previously, spring snowmelts were thought to have a substantially greater influence on PPR closed basin hydrology than rainfall events. Following the analysis of this rainfall event it is apparent that intense storms easily and rapidly overwhelm poorly developed soils, generating overland flow that refills wetland depressions. This ponding, which is in addition to the spring freshet, has a substantial influence on the catchment hydrologic cycle, including the surface, soil, and groundwater.

Overland flow is governed by the relative topographic relief and the soil hydraulic properties. Sites with relatively high slopes and convex shapes are more susceptible to the generation of overland flow, such as the convex upland (CXU) studied at the St. Denis NWA. These locations have restricted water retention, limiting soil development. Conversely, landscape positions with relatively flat or slightly concave topography develop rich soils with thick A-horizons, substantial rooting channels and preferential flow paths. These soil properties significantly increase infiltrability and internal redistribution capabilities. Therefore, these flatter landscape positions are less likely to generate overland flow and secondary lowland ponding during extreme summer rainfall events. Groundwater recharge is likely limited to the upper, seasonal zones of saturation and in the long-term very little seeps below the unoxidized till layer, recharging the permanent, regional groundwater.

The findings from this thesis have significant implications understanding the hydrological functions of different land forms and their response to snowmelt and extreme rainfall. The infiltration rate is much faster than expected in the concave upland (CVU), where rainfall water exceeded 1.25 m depth within two hours of the most intense rainfall, 19.7 $mmhr^{-1}$. In the prairies, deep drainage rate is estimated to be between 1 to 12 mm yr^{-1} (Hayashi et al., 1998a;

Hayashi et al., 1998b; Dyck et al, 2003, Si and de Jong, 2007). This assumes water flow below the active root zone is in steady-state. However, the response of the soil to extreme rainfall events suggests that the deep drainage rate could be episodic, dominated by extreme rainfalls, which occur only once in several years. Therefore, drainage below the active root zone may happen once in several years.

Although a unique dataset was collected during research there are limitations with this type of intensive field study. The study was conducted during two extremely wet years. Therefore, the results from this study represent only the response of different land forms to extreme rainfall in wet years. In dry years, the chance of extreme rainfalls is reduced and soil water storage is generally low, thus runoff generation in dry years is unlikely. Further, only two upland positions were instrumented. Generalizing the upland results to the whole watershed (or basin) could be misleading, as a single CVU and CXU position may not be representative of all of these unique landscape positions. Finally, upland soils in the prairies have high salt content, eliminating the popular electromagnetic wave methods for measurement of soil water content. In this study, the CXU soil water content could not be directly measured below 0.5 meters depth. An indirect, water retention curve method was used to determine volumetric water content below this depth. As instrumentation improves, techniques such as the heat pulse probe methods may be used in the future, eliminating the need for indirect methodologies.

Into the future, research should examine the role of vegetation in the water balance of different land forms. For example, vegetation of uplands, tree ring and the grassed edge not only affected rainfall infiltration during extremely rainfall, but they are also unique in how they take up water from soil, affecting the soil water balance for that location and the whole watershed. In addition, observational studies, as showed in this research, provide important understanding on

the hydrological role of different land forms. However, complete instrumentation of all different landforms is not possible, whereas models to capture the main mechanisms of soil water balance of the watershed should be established. These models will provide guidance in the selection of monitoring sites, reconstructed watershed design, and response of a watershed to changes in management practices and climate change.

References

Dyck, M.F., R.G. Kachanoski, and E. de Jong. 2003. Long-term movement of a chloride tracer under transient, semi-arid conditions. Soil Science Society of America Journal 67:471-477.

Hayashi, M., G. van der Kamp, and D.L. Rudolph. 1998a. Water and solute transfer between a prairie wetland and adjacent uplands, 1. Water balance. Journal of Hydrology 207:42-55.

Hayashi, M., G. van der Kamp, and D.L. Rudolph. 1998b. Water and solute transfer between a prairie wetland and adjacent uplands, 2. Chloride cycle. Journal of Hydrology 207:56-67.

Si, B.C. and E. de Jong. 2007. Determining long-term (Decadal) deep drainage rate using multiple tracers. Journal of Environmental Quality 36:1686-1694.

APPENDIX A
COILED TDR MATRIC POTENTIAL SENSOR

1. Introduction

Soil water is the primary limiting factor to agricultural production in semi-arid environments. A good understanding of soil water dynamics is critical for researchers, legislators, and producers to make regulatory and productivity decisions. One component of soil water dynamics is matric potential. Matric potential is a measure of the combined capillary and adsorptive forces of soil particles and is imperative in determining both the direction and magnitude of water flow in unsaturated soils. The measurement of soil matric potential has been a challenge in semi-arid environments, where matric potential varies over a wide range from 0 MPa, at saturation, to -1.5 MPa, the permanent wilting point of agronomic crops (Hillel, 1998; Kutilek and Nielsen, 1994).

A variety of methods are available for measuring soil matric potential. The most common methods include tensiometers, electrical resistance, psychrometer, and heat dissipation sensors (Reece, 1996; Scanlon et al., 2002). All of these methods have limited capability (Carlos et al., 2002; Flint et al., 2002; Phene et al., 1971; Reece, 1996; Si et al., 1999). Tensiometers operate through approximately six percent of the entire matric potential range in semi-arid environments (0 to -0.09 MPa) and are limited to the wet end of the spectrum (Reece, 1996). The electrical resistance method uses two electrodes embedded in a porous block. The sensor equilibrates with the soil water solution to measure the electrical conductivity between the two electrodes. These sensors are exceptionally sensitive to soil salinity and require gypsum to counteract the salinity. These gypsum blocks degrade over time, significantly changing the physical characteristics of the instrument, nullifying the laboratory calibration (Jovanovic and Annandale, 1997). In

addition, the range of measurement is limited to -0.09 to -0.5 MPa. Thermocouple psychrometers are suited to very dry soils and do not operate in wet conditions. Measurements made with psychrometers are only valid from -0.1 MPa to -8 MPa (Agus and Schanz, 2005). These sensors measure the humidity of a porous chamber in equilibrium with the water vapor phase of the surrounding soil. Thermocouple psychrometers measure the total water potential, therefore the matric and osmotic potentials must be separated through a number of rough estimations of soil water solute concentrations (Andraski and Scanlon, 2002). Finally, heat dissipation sensors relate the water content of a porous ceramic cup to matric potential through a laboratory generated calibration curve. The CS-229, a commercially available sensor, has a hypodermic needle, encasing a heating element and thermocouple that is inserted into a porous block. The porous block equilibrates with the surrounding soil water and based on the water content and the high thermal diffusivity of water compared to air, the change in temperature over a set amount of time is directly related to the water content of the sensor body and indirectly to the soil matric potential (Fredlund, 1992; Phene et al., 1971). Again heat dissipation sensors are limited in their range, with the CS-229 sensor detecting matric potentials from -0.01 MPa to -1 MPa (Reece, 1996). The above sensors are incapable of meeting the needs of researchers working in semi-arid environments.

Recently proposed methods have had limited success. New methods have included several modifications of TDR probes. To reduce the size and increase sensitivity, Nissen et al., (1998) were the first to present and test a coiled TDR design and Or and Wraith, (1999) were the first to combine TDR technology with a porous medium. In the latter case, prototypes were built in two forms. The first with a 0.1 MPa bubbling pressure ceramic cylinder enclosed in a coaxial cage. The second prototype used a variety of porous disks, ranging from 120 μm (0.0025 MPa) to 0.6

μm (0.5 MPa). The coaxial cage is a series of inner and outer conductors, serving to measure the dielectric constant of the porous disks or cylinder. Their design does not address the limited range issue, as the first prototype functions from 0 to -0.5 MPa, and the second must be customized for different soil textures. Inspired by this work, Vaz et al., (2002) coiled two copper wires around the porous base of a tensiometer to simultaneously measure volumetric water content and matric potential. Unfortunately, this design's ability to measure matric potential is limited by the range of the tensiometer and does not address the need for a wide-ranging instrument. Persson et al. (2006) took the design further and coiled two copper wires around a metal rod, which was then embedded into a cylindrical gypsum core. The design is promising, but the use of gypsum, as previously discussed is undesirable. Gypsum degrades quickly in the soil solution, changing the physical characteristics of the instrument (Jovanovic and Annandale, 1997). The same is true of the development by Noborio et al., (1999). These researchers propose a probe capable of measuring soil volumetric water content and matric potential simultaneously by coating a portion of a traditional TDR rod design with gypsum. The gypsum coated portion measures matric potential, while the uncoated sections of rods measures volumetric water content. Again, the gypsum degrades overtime and matric potential portion of the instrument no longer functions. Recognizing this constraint, Whalley et al. (2001), studied a large variety of ceramics to determine the best option for the development of their sensor. Unfortunately, these researches limited their sensor development between 0 and -0.06 MPa and have not addressed the limited range issue presented in all sensors.

Given the limitation of available methods, the objective of this research is to develop a soil matric potential sensor capable of functioning through the full spectrum of potentials present in semi-arid environments, 0 MPa to -1.5 MPa

2. Materials and Methods

2.1. Design

The proposed coiled TDR probe (Fig. A1) uses two copper TDR rods, 15 cm long and 0.5 mm diameter, wrapped around a dually threaded 5 mm diameter Plexiglas core. Plexiglas is an ideal material as it is nonconductive, does not absorb water, and has a dielectric constant of about 3 (Persson and Wraith, 2002). The wrapped core is inserted into a 1.4 cm diameter and 2.6 cm long porous ceramic tube with a 5 mm hole drilled through the center. Good contact between the wrapped core and ceramic tube was obtained through a tight fit of the core in the ceramic tube. The ceramic is manufactured by Campbell Scientific for use with their CS-229 heat dissipation sensors. This material is ideal, as it is highly porous, has a wide ranging pore size distribution, and is robust, as it is difficult to break during installation and does not degrade substantially over time. Care was taken during production to ensure maximum contact between the ceramic core and the coiled TDR rods. The center core was fixed in place with a small amount of epoxy at the end of the probe. The top of the TDR rods were soldered to RG58 50 ohm coaxial cable for measurement of waveforms using a Tektronix 1502 B cable tester.

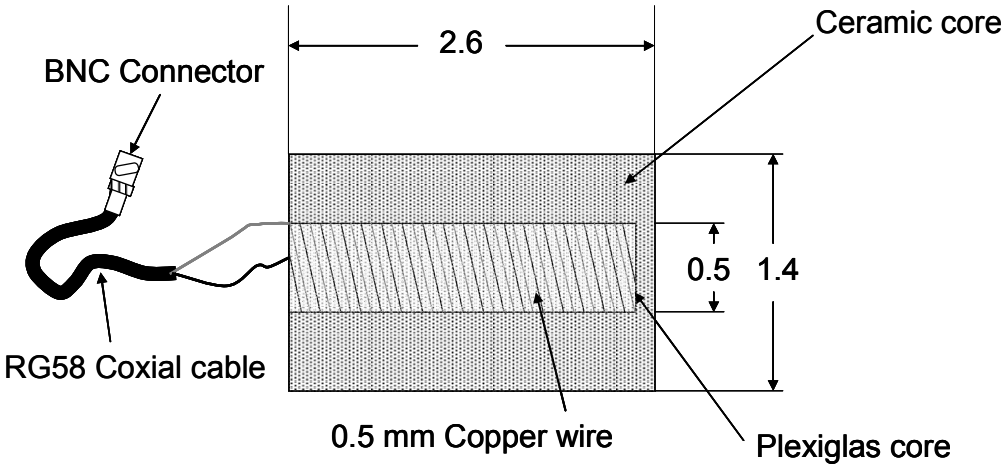

Figure A1. Diagram of Coiled TDR matric Potential Sensor. Measurements are in cm, unless stated otherwise.

2.2. Calibration

The calibration of the probe involved the use of a tension table and pressure plate apparatus. The probe was packed into an 80 cm3 soil core with a bulk density of about 1.25 g cm-3 and soil used in packing was silty loam Typic Haploborolls from the Goodale Research Farm, east of Saskatoon, Saskatchewan. The dielectric constant was measured at the following tensions: 0, -0.002, -0.003, -0.005, -0.007, -0.008, -0.0085, -0.01, -0.3, -0.5, -0.8, and -1.5 MPa. The dielectric constant was monitored during the course of the measurement in the pressure plate and equilibrium conditions was considered reached when there was no noticeable difference in the dielectric constant for two consecutive measurements. At high pressures, the equilibrium time is as long as 6 weeks. This calibration was similar to that performed by Flint et al. (2002), who generated a general calibration curve for the CS-229 heat dissipation sensor using the van Genuchten (1980) water retention equation. In our case a modified van Genuchten water retention equation was used to describe the relationship between matric potential and dielectric constant and is shown in Eq. [1].

$$\psi = \psi_o \left[\left(\frac{Dc}{12.5} \right)^{-\frac{1}{m}} - 1 \right]^{\frac{1}{n}} \qquad [1]$$

Where, ψ is the matric potential (MPa), ψ_o is the air entry value of the ceramic (MPa), *Dc* is the dielectric constant, and *m* and *n* are dimensionless fitting parameters. The *Dc* in this case is divided by 12.5, the maximum recorded *Dc* during the calibration procedure.

3. Results and Discussion

The measured dielectric constant and the corresponding applied pressures are shown in Fig. A2. The data was fit using the modified van Genuchten model. The dielectric constant is

positively related to matric potential, as matric potential decreases so does the measured dielectric constant. This is expected, as water content within the porous block decreases, matric potential also decreases. The reduced water content limits the conductivity of the electromagnetic pulse, resulting in a decrease in dielectric constant. The sensitivity (partial derivative of dielectric constant with respect to matric potential) decreases at the very wet ends of the spectrum. The steep nature of those portions of the curve, where the dielectric constants are above 10, is indicative of the nonlinear response of dielectric constant to matric potential. In the middle portions of the spectrum, where dielectric constants range from 2 to 10, a linear relationship exists. Slope throughout this portion of the calibration is adequate to easily discern variations in matric potential. The model does a good job of fitting the data with a coefficient of determination of 0.84, providing an equation capable of predicting matric potential from measured dielectric constant of an unknown sample. The fitted parameters = 0.5937 MPa, m = 3.358, and n = 0.525. This finding is significant as the model describes the relationship between dielectric constant and matric potential through the entire range of values.

In comparison with other researcher's work and conventional instrumentation, the proposed sensor is able to measure a wide range of matric potentials. Therefore, the proposed sensor is a superior instrument for measuring matric potential in the vadose zone of semi-arid and arid environments, although cost estimation is uncertain at this point.

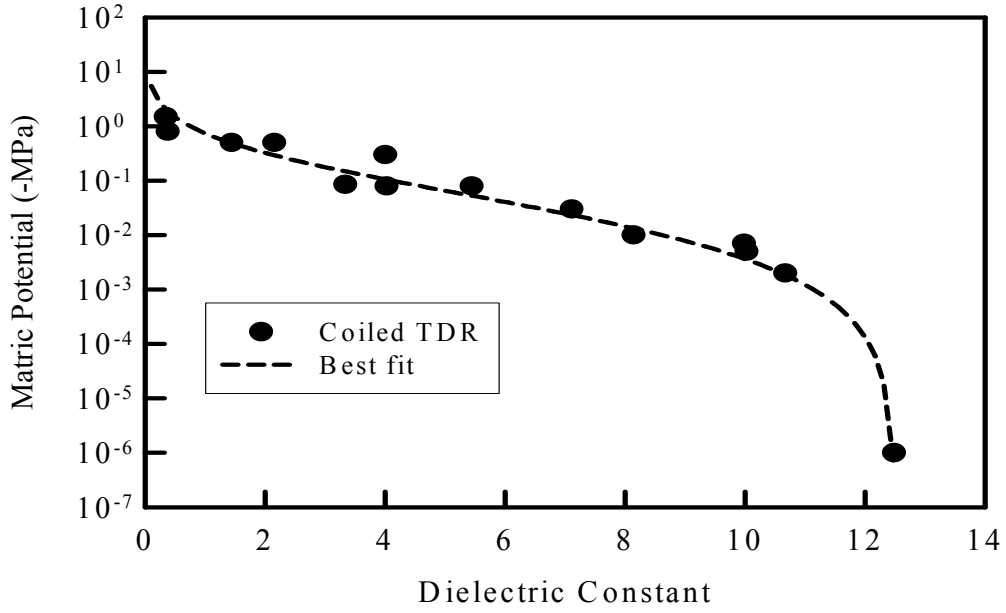

Figure A2. Curve fit of coiled TDR calibration data.

4. Conclusion

There is a need for a single sensor capable of measuring soil matric potential from saturation to the permanent wilting point. The proposed Coiled TDR sensor can measure soil matric potential from 0 MPa to -1.5 MPa. The van Genuchten model was successful in describing the relationship between the measured dielectric constant and matric potential, providing a simple and effective means of relating dielectric constant back to matric potential. The results presented are preliminary and require further field verification.

5. References

Agus, S.S., and T. Schanz. 2005. Comparison of four methods for measuring total suction. Vadose Zone Journal 4:1087-1095.

Andraski, B.J., and B.R. Scanlon. 2002. Thermocouple Psychrometry, p. 609-642, In J. H. Dane and G. C. Topp, eds. Methods of Soil Analysis, Part 4, Physical Methods, Vol. SSSA Book Ser. 5. SSSA, Madison, WI.

Carlos, M.P., J.W. Hopmans, A. Macedo, L.H. Bassoi, and D. Wildenschild. 2002. Soil water retention measurements using a combined tensiometer-coiled time domain reflectometry probe. Soil Science Society of America Journal 66:1752-1759.

Flint, A.L., G.S. Campbell, K.M. Ellett, and C. Calissendorff. 2002. Calibration and temperature correction of heat dissipation matric potential sensors. Soil Science Society of America Journal 66:1439-1445.

Fredlund, D.G. 1992. Background, theory, and research related to the use of thermal conductivity sensors for matric suction measurement. Soil Science Society of America Journal SSSA Special Publication Number 30:249-261.

Hillel, D. 1998. Environmental Soil Physics Academic Press, London.

Jovanovic, N.Z., and J.G. Annandale. 1997. A laboratory evaluation of Watermark electrical resistance and Campbell Scientific 229 heat dissipation matric potential sensors. Water SA 23:227-232.

Kutilek, M., and D.R. Nielsen. 1994. Soil Hydrology Catena Verlag, Cremlingen-Destedt.

Nissen, H.H., P. Moldrup, and K. Henrikson. 1998. High-resolution time domain reflectometry coil probe for measuring soil water content. Soil Science Society of America Journal 62:1203-1211.

Noborio, K., R. Horton, and C.S. Tan. 1999. Time domain reflectometry probe for simultaneous measurement of soil matric potential and water content. Soil Science Society of America Journal 63:1500-1505.

Or, D., and J.M. Wraith. 1999. A new soil matric potential sensor based on time domain reflectometry. Water Resources Research 35:3399-3407.

Persson, M., and J.M. Wraith. 2002. Shaft-mounted time domain reflectometry prob for water content and electrical conductivity measurements. Vadose Zone Journal 1:316-319.

Persson, M., J.M. Wraith, and T. Dahlin. 2006. A small-scale matric potential sensor based on time domain reflectometry. Soil Science Society of America Journal 70:533-536.

Phene, C.J., G.J. Hoffman, and S.L. Rawlins. 1971. Measuring soil matric potential in situ by sensing heat dissipation within a porous body: I. theory and sensor construction. Soil Science Society of America Proc 35:27-32.

Reece, C.F. 1996. Evaluation of a line heat dissipation sensor for measuring soil matric potential. Soil Science Society of America Journal 60:1022-1028.

Scanlon, B.R., B.J. Andraski, and J. Bilskie. 2002. Miscellaneous methods for measuring matric or water potential, p. 643-670, In J. H. Dane and G. C. Topp, eds. Methods of soil analysis, Part 4, Physical Methods, Vol. SSSA Book Ser. 5. SSSA, Madison, WI.

Si, B., R.G. Kachanoski, F. Zhang, G.W. Parkin, and D.E. Elrick. 1999. Measurement of hydraulic properties during constant flux infiltration: field average. Soil Science Society of America Journal 63:793-799.

Vaz, C.M.P., J.W. Hopmans, A. Macedo, L.H. Bassoi, and D. Wildenschild. 2002. Soil water retention measurements using a combined tensiometer-coiled time domain reflectometry probe. Soil Science Society of America Journal 66:1752-1759.

Whalley, W.R., C.W. Watts, M.A. Hilhorst, N.R.A. Bird, J. Balendonck, and D.J. Longstaff. 2001. The design of porous material sensors to measure the matric potential of water in soil. European Journal of Soil Science 52:511-519.

APPENDIX B
S118 SOIL CLASSIFICATION AND TEXTURE

Table B1. S118 landscape element soil classification.

Position	**Classification**	**Parent Material**	**Horizons**	**Depths (m)**
Convex Upland	Orthic Regosol	N/A	Apk	0.0-0.05
			Ck I	0.05-0.65
			Ck II	0.65-1.00
			Ck III	1.00-1.50
			Ck IV	1.50-2.50
Grassed Edge	Humic Luvic Gleysol	Glaciolacustrine	Ah	0.0-0.40
			Ahb	0.40-0.50
			Aeg	0.50-0.65
			Btg	0.65-1.20
			C I	1.20-1.25
			C II	1.25-2.50
Pond Center	Orthic Humic Gleysol	Glaciolacustrine	Ah	0.0-0.50
			Bg	0.50-1.25
			C I	1.25-1.35
			C II	1.35-2.50
Tree Ring	Orthic Dark Grey Chernozem	Glaciolacustrine	L	0.03-0.0
			Ah	0.0-0.20
			Ae	0.20-0.28
			Bnt	0.28-0.85
			Cca	0.85-1.00
			Ck	1.00-1.50

Concave Upland	Gleyed Calcareous Dark Brown Chernozem	Silty Lacustrine	Apk	0.0-0.20
			ABk	0.20-0.25
			Bkgj	0.25-0.35
			Ckgj	0.35-1.50

Table B2. S118 landscape element soil texture. Determined using Standard Hydrometer Methodology.

Convex Upland				Grassed edge				Pond Center			Tree Ring			Concave Upland		
Depth (m)	Clay	Sand	Silt	Depth (m)	Clay	Sand	Silt	Clay	Sand	Silt	Clay	Sand	Silt	Clay	Sand	Silt
0-0.1	10.2	38.8	51.0	0-0.10	4.1	61.5	34.4	24.9	35.5	39.7	15.9	29.8	54.3	10.2	24.6	65.2
0.15-0.25	17.8	32.6	49.5	0.10-0.20	9.7	52.0	38.4	36.3	19.2	44.5	13.9	27.6	58.6	12.7	30.8	56.4
0.25-0.35	17.3	33.4	49.4	0.20-0.30	10.2	44.0	45.7	35.6	19.8	44.5	17.6	20.5	61.9	31.8	28.0	40.2
0.35-0.45	17.8	33.9	48.3	0.30-0.40	10.2	44.4	45.4	25.5	28.9	45.7	44.0	12.2	43.8	26.7	32.7	40.7
0.45-0.55	13.6	58.3	28.1	0.40-0.50	5.1	52.5	42.4	25.5	32.5	42.1	44.0	12.0	44.0	26.1	24.4	49.5
0.55-0.65	11.6	49.5	38.8	0.50-0.60	5.1	55.0	39.9	28.0	40.0	32.0	44.0	13.6	42.5	23.5	22.8	53.7
0.65-0.75	17.3	35.3	47.5	0.60-0.70	21.0	33.8	45.3	49.1	26.9	24.0	41.4	11.7	46.9	18.4	25.6	56.0
0.75-0.85	11.1	44.5	44.4	0.70-0.80	27.4	36.3	36.3	52.4	11.5	36.2	41.4	10.3	48.2	17.3	38.7	44.0
0.85-0.95	9.7	38.4	51.9	0.80-0.90	22.9	40.3	36.7	52.8	12.3	34.9	39.5	17.4	43.0	14.7	37.2	48.1
0.95-1.05	9.7	40.6	49.8	0.90-1.00	27.4	30.1	42.5	50.9	12.1	37.0	32.4	11.7	55.8	11.6	56.6	31.7
1.05-1.15	12.7	32.0	55.3	1.00-1.10	34.4	31.5	34.1	50.2	11.1	38.6	23.5	7.1	69.4	11.6	58.1	30.3
				1.10-1.20	42.1	17.0	40.9	56.8	9.0	34.3	26.1	10.3	63.7	11.6	49.2	39.2
				1.20-1.30	22.9	54.7	22.4	42.6	44.6	12.8	19.4	16.5	64.1	31.3	61.6	7.1
				1.30-1.40	13.6	59.2	27.2	34.4	62.6	3.0	22.0	19.8	58.2	28.3	60.9	10.8
				1.40-1.50	13.0	69.9	17.1	36.9	58.2	4.9	17.0	32.3	50.7	23.3	53.9	22.8
				1.50-1.60	29.2	32.5	38.3	42.7	15.0	42.3	15.9	40.4	43.8	26.6	67.6	5.8